

# **Monitoring Procedures for Wellsite, In-Situ Oil Sands and Coal Mine Reclamation in Alberta (MOPRA) – December 2014 Update**

Nadia Rochdi, Jinkai Zhang, Karl Staenz, Xiaohui Yang, Rolfson David, James Banting,  
Chelsea King, and R. Doherty

Alberta Terrestrial Imaging Centre, University of Lethbridge

December 2014



## Oil Sands Research and Information Network

The Oil Sands Research and Information Network (OSRIN) is a university-based, independent organization that compiles, interprets and analyses available knowledge about managing the environmental impacts to landscapes and water impacted by oil sands mining and gets that knowledge into the hands of those who can use it to drive breakthrough improvements in regulations and practices. OSRIN is a project of the University of Alberta's School of Energy and the Environment (SEE). OSRIN was launched with a start-up grant of \$4.5 million from Alberta Environment and a \$250,000 grant from the Canada School of Energy and Environment Ltd.

OSRIN provides:

- **Governments** with the independent, objective, and credible information and analysis required to put appropriate regulatory and policy frameworks in place
- **Media, opinion leaders and the general public** with the facts about oil sands development, its environmental and social impacts, and landscape/water reclamation activities – so that public dialogue and policy is informed by solid evidence
- **Industry** with ready access to an integrated view of research that will help them make and execute environmental management plans – a view that crosses disciplines and organizational boundaries

OSRIN recognizes that much research has been done in these areas by a variety of players over 40 years of oil sands development. OSRIN synthesizes this collective knowledge and presents it in a form that allows others to use it to solve pressing problems.

## Citation

This report may be cited as:

Rochdi, N., J. Zhang, K. Staenz, X. Yang, D. Rolfson, J. Banting, C. King and R. Doherty, 2014. Monitoring Procedures for Wellsite, In-Situ Oil Sands and Coal Mine Reclamation in Alberta (MOPRA) – December 2014 Update. Oil Sands Research and Information Network, University of Alberta, School of Energy and the Environment, Edmonton, Alberta. OSRIN Report No. TR-47. 167 pp.

Copies of this report may be obtained from OSRIN at [osrin@ualberta.ca](mailto:osrin@ualberta.ca) or through the OSRIN website at <http://www.osrin.ualberta.ca/en/OSRINPublications.aspx> or directly from the University of Alberta's Education & Research Archive at <http://hdl.handle.net/10402/era.17507>.

## Table of Contents

LIST OF TABLES .....	iv
LIST OF FIGURES .....	iv
REPORT SUMMARY .....	viii
DECEMBER 2014 UPDATE .....	ix
ACKNOWLEDGEMENTS .....	x
1 INTRODUCTION .....	1
1.1 Wellsites and Associated Facilities .....	1
1.2 Other Specified Lands .....	1
1.3 Need for a Supplemental Assessment Tool .....	1
2 REMOTE SENSING (RS) DATA .....	3
2.1 Spaceborne Multi-/Hyperspectral Data .....	4
2.2 Airborne Hyperspectral/LiDAR Data .....	10
2.2.1 Cold Lake – Forested Area (Cold_Lake_FW) .....	12
2.2.2 Cold Lake – Agricultural Area (Cold_Lake_AG) .....	12
3 FIELD CAMPAIGNS .....	15
3.1 Cold Lake Field Campaign .....	15
3.1.1 Study Areas .....	15
3.1.2 Test Plots .....	16
3.2 Coal Valley Field Campaign .....	23
3.3 Mattheis Ranch Field Campaign .....	26
3.4 Ground Measurements Analysis .....	28
3.4.1 Forest Above-Ground Biomass, Volume and Stem Density .....	28
3.4.2 Canopy Leaf Area Index (LAI) .....	31
3.4.3 Leaf Chlorophyll Content .....	34
4 METHODOLOGY – INFORMATION EXTRACTION .....	36
4.1 Baseline Land-Cover Mapping .....	36
4.2 Monitoring Change Using Multispectral Satellite Imagery .....	39
4.3 Assessment of Multi-Temporal Satellite Multispectral Imagery for Monitoring Reclamation Trend .....	45

4.4	Mapping Canopy Structure Using LiDAR .....	52
4.5	Assessment of Canopy Structure within Reclaimed Wellsites in the Cold Lake Study Area Using LiDAR Data .....	54
4.6	Mapping Tree Species Using Multi-/Hyperspectral and LiDAR Data .....	58
4.6.1	Assessment of RapidEye and LiDAR Data in the Cold Lake Study Area.....	58
4.6.2	Assessment of SPOT-5 and LiDAR Data in the Cold Lake Study Area ...	64
4.6.3	Assessment of Hyperspectral CHRIS and LiDAR Data for Mapping Tree Species in the Cold Lake Study Area .....	66
4.7	Mapping Leaf Area Index in Cold Lake .....	68
5	MOPRA MONITORING SYSTEM DEVELOPMENT .....	70
5.1	MOPRA Remote Sensing Data Processing Toolbox.....	70
5.2	MOPRA Stand-Alone Assessment Tool.....	70
6	CONCLUSIONS.....	71
7	KEY REMARKS AND RECOMMENDATIONS.....	73
8	REFERENCES .....	74
9	GLOSSARY .....	75
9.1	Terms .....	75
9.2	Acronyms .....	77
	APPENDIX 1: Examples of Spatial High-Resolution Sensors Characteristics and Data Costs ..	79
	APPENDIX 2: MOPRA Field Plan – Cold Lake Study Area .....	80
	APPENDIX 3: Remote Sensing Data Processing Toolbox: ENVI-Plug in.....	88
	APPENDIX 4: Stand-Alone Reclamation Assessment Tool.....	121
	APPENDIX 5: Assessment of Reclaimed Areas near Cold Lake Using Hyperspectral Data ....	152
	LIST OF OSRIN REPORTS .....	161

## LIST OF TABLES

Table 1.	Spectral and spatial characteristics of satellite imagery acquired within MOPRA.	5
Table 2.	The satellite multi-/hyperspectral imagery acquired within MOPRA at the specific study areas.....	6
Table 3.	Agricultural and forested wellsites sampled during the 2012 Cold Lake field campaign. ....	18
Table 4.	Species-specific parameters used in biomass (equation 1) and volume (equation 2) models. ....	29
Table 5.	The certification and disturbance dates for the selected certified wellsites and non-oil-and-gas disturbances.....	56
Table 6.	The classification hierarchy used for tree species mapping.....	59
Table 7.	Accuracy assessment of species classification using RF for both RapidEye and 2012 LiDAR/RapidEye data. ....	61
Table 8.	Accuracy assessments using 2012 LiDAR/RapidEye data for SVM and RF classifiers.....	62
Table 9.	Accuracy assessments using the RF classifier for 2006 and 2012 LiDAR combined with RapidEye imagery.....	63
Table 10.	Accuracy assessment results using the RF classifier for 2012 LiDAR/SPOT-5. .	65
Table 11.	Accuracy assessment results using the SVM classifier for CHRIS (top) and 2012 LiDAR/CHRIS data (bottom). ....	67

## LIST OF FIGURES

Figure 1.	Locations of the four study areas adopted in the MOPRA project including the Cold Lake, Coal Valley, Lacombe and Mattheis Ranch areas. ....	3
Figure 2.	A subset of the Landsat ETM+ false-colour composite acquired in 2001 over the Coal Valley study area. ....	7
Figure 3.	A subset of the Landsat TM 5 false-colour composite acquired in 1998 over the Cold Lake study area. ....	8
Figure 4.	A subset of the Landsat TM 5 false-colour composite acquired in 2001 over the Lacombe study area. ....	9
Figure 5.	The Cold_Lake_FW (red box) and Cold_Lake_AG (blue box) study areas located west of the Town of Cold Lake.....	11

Figure 6.	The 2012 AISA/LiDAR coverage over the Cold_Lake_FW (left) and Cold_Lake_AG (right) areas highlighted in white. ....	13
Figure 7.	Example of AISA flight lines acquired over the Cold_Lake_FW and zoomed-in subsets. ....	14
Figure 8.	Examples of surface reflectance spectra derived from AISA data over coniferous forest (blue), deciduous forest (red) and a bare-ground area (green). ....	14
Figure 9.	The wellsites sampled in the FW_CL (left) and AG_CL (right) study sites. ....	16
Figure 10.	The sampling protocol used for collecting indirect measurements of leaf area index (LAI) using hemispherical photographs. ....	17
Figure 11.	Photographs of land cover in the well (F20088253) and reference (RF20088253) sites. ....	19
Figure 12.	Land cover of the well (AG0164151) and reference pasture sites (RAG0164151). ....	20
Figure 13.	Downward and upward hemispherical photographs of the reference site RF20088253. ....	21
Figure 14.	Downward facing hemispherical photograph of the reference site RAG0164151 (pasture). ....	22
Figure 15.	Test plots characterized in the Coal Valley study area in summer of 2013. ....	24
Figure 16.	Photographs of land cover in the mine and reference areas for the Pit 14/15_2 test plot. ....	25
Figure 17.	Test plots characterized in the Mattheis Ranch study area (red line) in July 2013. ....	26
Figure 18.	Photographs of land cover in well (top) and reference (bottom) areas as observed during the Mattheis Ranch field campaign in July 2013. ....	27
Figure 19.	Above-ground biomass in forested well and reference sites for the FW_CL study site. ....	29
Figure 20.	Canopy volume in well and reference sites for the FW_CL study site. ....	30
Figure 21.	Stem density in forested well and reference sites for the FW_CL study site. ....	30
Figure 22.	Downward looking hemispherical photographs (a) and classified images (b) derived using the CanEye software for the F10182632 test plot in the FW_CL study site. ....	31
Figure 23.	Upward looking hemispherical photographs (a) and classified images (b) derived using the CanEye software for the RF10182632 test plot in the FW_CL study site. ....	32

Figure 24.	Canopy LAI as derived from hemispherical photographs in well and reference test plots for the FW_CL study site. ....	34
Figure 25.	Averaged relative chlorophyll content of forbs (top) and grass (bottom) for all well and reference test plots within the AG_CL study site. ....	35
Figure 26.	30 m land-cover map of the Lacombe study area using Landsat imagery acquired in 2001. ....	37
Figure 27.	30 m land-cover maps over the Cold Lake (top) and Coal Valley study (bottom) areas using Landsat imagery acquired in 1998 and 2002, respectively. ....	38
Figure 28.	Landsat colour composites over the Coal Valley study area acquired in 2001 (top) and 2009 (bottom). ....	40
Figure 29.	Landsat colour composites over the Cold Lake study area acquired in 1998 (top) and 2011 (bottom). ....	41
Figure 30.	Change detection maps showing the areas that have been cleared (left) or revegetated (right) between 1998 and 2011 in the Cold Lake study site. ....	42
Figure 31.	Change detection maps showing the areas in the Coal Valley study site that have been cleared (top) or re-vegetated (bottom) between 2001 and 2009. ....	43
Figure 32.	Examples of areas that were cleared or revegetated in the Cold Lake study area after 1998. ....	44
Figure 33.	Examples of areas that were cleared or revegetated in the Coal Valley study area between 2001 (top) and 2009 (middle). ....	46
Figure 34.	The control area delineation scheme used for lease area assessment. ....	48
Figure 35.	Examples of NDVI temporal trend plots for three different certified wellsites in the Cold Lake study area. ....	50
Figure 36.	Temporal trend plots for three different VIs including SR, NDVI and ISR for a certified wellsite in the Cold Lake study area. ....	51
Figure 37.	Canopy height (top) and canopy fractional cover (bottom) derived using the ESRD 2006 LiDAR data over the Coal Valley study area. ....	52
Figure 38.	Canopy height (top) and canopy fractional cover (bottom) derived using the ESRD 2006 LiDAR data over the Cold Lake study area. ....	53
Figure 39.	Canopy height (left) and canopy fractional cover (right) derived using the 2012 LiDAR data over the Cold Lake study area. ....	54
Figure 40.	Certified wellsites (red) and non-oil-and-gas related disturbed areas (green) as extracted from the AVI data and overlaid on top of the LiDAR canopy height map. ....	55
Figure 41.	Differences in canopy height (top) and fractional cover (bottom) averages between certified wellsites and non-oil-and-gas disturbed sites. ....	57

Figure 42.	The 2012 RapidEye image acquired over the Cold Lake study area (left) and the corresponding Level-1 classification map (right). ....	60
Figure 43.	5 m species map using the RF classifier and the 2012 LiDAR/RapidEye data over the Cold Lake study area.....	61
Figure 44.	5 m species maps using RF classifier together with the 2012 LiDAR/ RapidEye (top) and RapidEye (bottom) data.....	63
Figure 45.	10 m tree species map of the Cold Lake study area using the RF classifier together with the 2012 LiDAR/SPOT-5 data.....	65
Figure 46.	34 m tree species map of the Cold Lake study area using the CHRIS data and SVM classifier. ....	66
Figure 47.	20 m leaf area index map of the Cold Lake study area produced using LAI-VI empirical models and SPOT-5 data. ....	68
Figure 48.	LAI-VI empirical models developed using VIs derived from SPOT-5 data and ground measurements collected in July 2012 at the Cold Lake study area. ....	69

## REPORT SUMMARY

The scope of the *Monitoring Procedure for Reclamation in Alberta (MOPRA)* project is to develop a geomatics-based monitoring system to support the Government of Alberta's efforts for monitoring reclamation success. This software will support the decision making process to screen almost all oil and gas wellsites and prioritize those that require immediate intervention allowing an efficient allocation of government resources.

Using remote sensing technologies, the following three types of information were pursued:

- Baseline maps of the pre-disturbance condition of sites,
- Vegetation condition related to species, and canopy structure, and vegetation productivity, and
- Temporal change of land condition in reclaimed areas.

The project provided the opportunity to assess remote sensing technologies including optical multispectral, hyperspectral and LiDAR, for monitoring vegetation condition in reclaimed wellsites and mine areas. Three study areas were assessed, sampling both wellsites and a coal mine areas, which cover different landscapes including forested, and agricultural areas.

A set of land products were developed within this project, including baseline land cover, land-cover change, canopy height, fractional cover, tree species and canopy leaf area index (LAI). In addition, multi-year profiles of vegetation index data were examined to assess vegetation regrowth in wellsites in comparison to undisturbed reference areas. Canopy structure attributes, derived from LiDAR data such as canopy height and fractional cover, were also examined to assess differences in vegetation structure between reclaimed wellsites and regenerated burnt/clear-cut areas. In addition, a reclamation monitoring system, composed of a *Remote Sensing Data Processing Toolbox* and *A Stand- Alone Assessment Tool*, was developed.

The land products derived from remote sensing data provide information related to some of the landscape and vegetation assessment parameters adopted within the 2010 reclamation criteria document (Alberta Environment and Sustainable Resource Development 2013), such as bare areas, vegetation species, land-use change, canopy height, percent canopy cover and vegetation quantity/quality.

The achievements of the MOPRA project have highlighted the benefits that remote sensing technologies can provide in support of reclamation monitoring efforts. Having access to a synoptic view of reclaimed lands at the landscape and regional level is of value for assessing land-use cumulative effects and making decisions in line with an integrated resource management system.

While the MOPRA outcomes have shown promise in this direction, there is still a need to test and validate the information extraction approaches adopted as well as the monitoring system developed on various landscapes, such as wetlands, rangelands, agriculture and forested areas. Although, this project has focused on reclaimed wellsites and reclaimed areas within coal mines, the work undertaken can be applicable to natural areas as well as reclaimed lands that have been

disturbed by other activities, such as transportation corridors, wind energy, sand and gravel operations, oil sands mines as well as pipelines.

To move towards an integration of remote sensing technologies as an operational monitoring tool, the MOPRA monitoring system would require further testing, involving consultants, industry (e.g., oil and gas, coal mine, wind energy farms), and monitoring organizations (Alberta Environmental Monitoring, Evaluation and Reporting Agency – AEMERA) and regulatory agencies (e.g., Alberta Energy Regulator, ESRD).

### **DECEMBER 2014 UPDATE**

AISA airborne hyperspectral and ground-reference data collected in the Cold Lake study area within the MOPRA framework were used to map tree species (trembling aspen, balsam poplar, white spruce, black spruce, tamarack, and jack pine) composition.

Sixteen AISA flight lines covering the south part of the study area were processed using the ENVI Effort Polishing module to remove the presence of spikes in the spectral profile. The Minimum Noise fraction (MNF) transformation was applied to the AISA mosaic to reduce the spectral dimensionality and innate spectral noise. In general, the classification maps based on hyperspectral data lacked well-defined spatial patterns associated with the type of tree species. Introducing the structural information derived from the LiDAR data reduced considerably the “salt and pepper” appearance in the hyperspectral-based classification maps and introduced spatial patterns where tree species tends to be grouped into distinct clusters. This improvement was visually more pronounced when combining LiDAR with the nine MNF components. However, accuracies are low to moderate for both the noise-reduced and the 9-MNF data. Although improvement was observed when adding the LiDAR-based information, accuracy values overall remain moderate.

The new information is in [Appendix 5](#).

## **ACKNOWLEDGEMENTS**

The Oil Sands Research and Information Network (OSRIN), School of Energy and the Environment (SEE), University of Alberta provided funding for this project.

The authors also thank Tecterra Inc. and Alberta Environment and Sustainable Resources Development for funding this project.

The authors also would like to thank Professor Edward Bork of the University of Alberta for providing access to the Mattheis Research Ranch test site.

## **1 INTRODUCTION**

One of the issues related to a successful implementation of a cumulative effects management system in Alberta is land reclamation. Based on Alberta's *Conservation and Reclamation Regulation*, "the objective of reclamation of specified land is to return the land to an equivalent land capability (ELC)" where ELC means that the ability of the reclaimed land to support various land uses is similar to the land ability prior to exploitation activities, but without being necessarily identical.

Up to March 2014, Alberta Environment and Sustainable Resources Development (ESRD) has been the Regulatory Authority responsible for reclamation certification of specified lands, including those lands that have been subject to different types of energy related activities, such as oil and gas wellsites, in-situ oil sands sites, and coal and oil sands mines. There are two separate reclamation certification processes that apply to specified lands, including one which is applied to wellsites and associated facilities, the second to all other specified lands.

### **1.1 Wellsites and Associated Facilities**

Once a Reclamation Certificate has been issued for a wellsite, the site can be selected for a field audit through a random selection process. These field audits are completed by compliance staff (historically from Environment and Sustainable Resource Development, now from the Alberta Energy Regulator). Between 10% and 15% of the Reclamation Certificates issued undergo an audit. Afterwards, these sites have 25-years of reclamation liability and a lifetime contamination liability.

### **1.2 Other Specified Lands**

For all other specified lands, all sites which have had reclamation certificate applications will undergo a field inquiry by the compliance staff, followed by a decision about issuing a reclamation certificate if reclamation was found successful. In this case, after the reclamation certificate has been issued, reclamation liability is transferred back to the Government of Alberta after a period of time specified in the *Conservation and Reclamation Regulation* (from 0 years to 25 years, depending on the type of activity and whether or not an approval had been issued for the activity), while remediation liability remains with the company for life.

### **1.3 Need for a Supplemental Assessment Tool**

In addition to the 213,000 active wellsites and about the 15,000 being drilled each year<sup>1</sup>, there is a large number of coal mines, oil sands mines, quarries, and sand and gravel pits in Alberta of varying sizes, ranging between few to hundreds of hectares that will require a reclamation certificate once closed. Moreover, further certification will be required for the 450,000 km of pipelines which is expected to double within the next 25 years. A significant backlog in the

---

<sup>1</sup> See <http://environment.alberta.ca/02484.html>

reclamation certification process with regards to the rate of site abandonment has been observed, which resulted in approximately 52,831 uncertified wellsites at the end of 2012<sup>2</sup>.

Relying exclusively on audit and/or inquiry assessments at all these sites is unrealistic and extremely costly due to the amount of time as well as human and economic resources that such endeavor would require. This is even more unsustainable if multi-temporal visits are required during the reclamation certification process.

In an attempt to mitigate this issue, remote sensing technologies have been identified as a possible means to enhance and augment field assessment of reclaimed lands. This has been motivated by the wide spatial coverage that these technologies offer in addition to their temporal frequency, which makes them suitable for long-term monitoring.

The scope of the *Monitoring Procedure for Reclamation in Alberta (MOPRA)* project is to develop a Geomatics-based monitoring system to support the Government of Alberta efforts for monitoring reclamation success. This software will support the decision making process to screen almost all sites and prioritize those that require immediate intervention, allowing an efficient allocation of government resources.

The Geomatics-based monitoring system makes use of remote sensing technologies to provide the following three types of information:

- Baseline mapping of the pre-disturbance condition of sites;
- Information about vegetation condition related to species, canopy structure, and vegetation productivity; and
- Information about the temporal change of land condition in reclaimed lands.

This project was organized in three major components:

- Ground characterization of reclaimed and undisturbed lands through the organization of field campaigns;
- Methodology development to extract information related to land condition using remote sensing technologies; this includes the assessment of various types of remote sensing data as well as different methods; and
- Software development to incorporate the approaches adopted in the methodology development section into an automated process.

This project has been conducted using four study areas, sampling both wellsites<sup>3</sup> and a coal mine area (Figure 1), which cover different landscapes including forest, agriculture, and rangeland.

---

<sup>2</sup> See <http://esrd.alberta.ca/focus/state-of-the-environment/land/response-indicators/oil-and-gas-wells-reclamation.aspx>

<sup>3</sup> In this report, unless otherwise specified, the term *wellsite* is used to mean both conventional upstream oil and gas sites and in-situ oil sands sites.

Four different eco-regions were sampled through these study areas, including: aspen parkland, boreal mixed wood, western Alberta uplands and moist mixed grasslands.

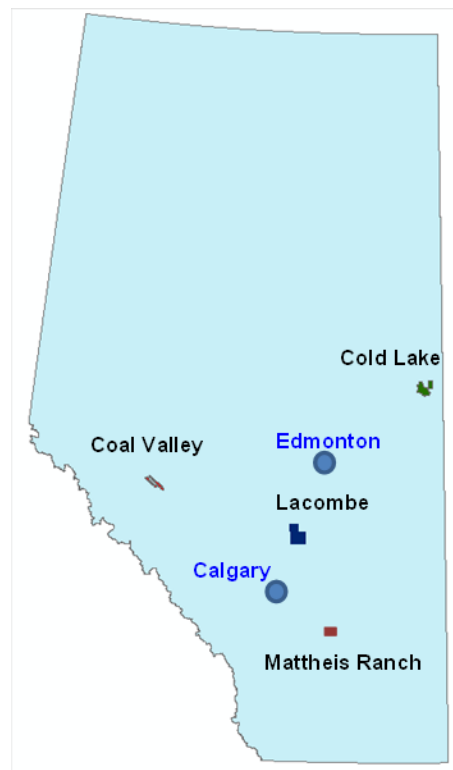


Figure 1. Locations of the four study areas adopted in the MOPRA project including the Cold Lake, Coal Valley, Lacombe and Mattheis Ranch areas.

The next sections in this report provide a detailed description of the major steps undertaken in the MOPRA project, including: remote sensing data acquisition ([section 2](#)), field campaigns ([section 3](#)), methodology development ([section 4](#)) and the MOPRA monitoring system development ([section 5](#)). The major conclusions and recommendations resulting from this project are addressed in sections 6 and 7, respectively.

## 2 REMOTE SENSING (RS) DATA

The methodology development phase of the MOPRA project required the acquisition of a set of remote sensing image data to assess their performances in retrieving information about condition of reclaimed areas. The choice of these data was mostly governed by the spatial resolution of available remote sensors due to the small size of wellsites which cover about a 100 m x 100 m area. In addition, the imagery cost was considered in the selection process ([Appendix 1](#)).

Multispectral optical remote sensors available for operational use, such as the French SPOT<sup>4</sup> (Satellite Pour l'Observation de la Terre “Satellite for Earth Observation”), American Landsat<sup>5</sup> and German/Canadian RapidEye<sup>6</sup> space missions, were considered in addition to airborne and current spaceborne hyperspectral sensors. Although these two latter categories are not suitable for operational monitoring due to the limited temporal frequency they offer, assessing the large number of spectral bands associated with this type of sensors is relevant for the future hyperspectral space missions that are planned for the next 10 years. In addition, Light Detection and Ranging (LiDAR) data were also acquired to be assessed within this project.

## 2.1 Spaceborne Multi-/Hyperspectral Data

During the MOPRA project, a number of new remote sensing data were acquired, as well as existing data were downloaded from historical data archives.

A series of high-resolution multi-spectral optical sensors (Table 1), characterized by a spatial resolution ranging between 5 m and 30 m, were selected as follows:

- SPOT HRV/HRVIR (High Resolution Visible/ High Resolution Visible InfraRed),
- Landsat TM/ETM (Transverse Mercator/ Enhanced Transverse Mercator), and
- RapidEye.

These sensors are also characterized by a number of spectral bands, which sample different locations of the visible (VIS), Near-Infrared (NIR), and Short-Wave-Infrared (SWIR) spectral regions. Data archives for the above mentioned sensors were examined to determine the imagery that has been acquired within the last 20 years. Imagery selection was defined considering the following three main criteria:

- Imagery cloud coverage does not exceed 20%;
- Imagery acquisition time constrained between mid-July and mid-August so that it is close to the maximum growing season – in the absence of imagery, the temporal window was then increased to include imagery from early July to late September; and
- Imagery viewing-acquisition geometry is close to nadir direction to minimize the directionality effect on the sensor signal.

In addition to multispectral sensors, the European hyperspectral Compact High Resolution Imaging Spectrometer (CHRIS) onboard the Proba-1 platform was also considered. This sensor is characterized by a larger number of spectral bands providing a higher sampling of the Visible and Near Infrared (VNIR) spectral region. While multispectral sensors can be used for

---

<sup>4</sup> See [http://en.wikipedia.org/wiki/SPOT\\_\(satellite\)](http://en.wikipedia.org/wiki/SPOT_(satellite))

<sup>5</sup> See <http://landsat.usgs.gov/>

<sup>6</sup> See <http://en.wikipedia.org/wiki/RapidEye>

operational monitoring due to their frequent temporal acquisition, the CHRIS hyperspectral sensor is a technology demonstrator that has been used in this project to assess its performance and prepare for future operational hyperspectral sensors planned to be launched after 2017.

Table 1. Spectral and spatial characteristics of satellite imagery acquired within MOPRA.

Satellite	Spectral Bands ( $\mu\text{m}$ )	Spatial Resolution (m)	Coverage ( $\text{km}^2$ )
SPOT 2	<b>B1:</b> 0.50-0.59 <b>B2:</b> 0.61-0.68 <b>B3:</b> 0.78-0.89	20	$60 \times 60$
SPOT 4	<b>B1:</b> 0.50-0.59 <b>B2:</b> 0.61-0.68 <b>B3:</b> 0.78-0.89 <b>B4:</b> 1.58-1.75	20	$60 \times 60$
SPOT 5	<b>B1:</b> 0.50-0.59 <b>B2:</b> 0.61-0.68 <b>B3:</b> 0.78-0.89 <b>B4:</b> 1.58-1.75	10	$60 \times 60$
Landsat TM	<b>B1:</b> 0.45-0.52 <b>B2:</b> 0.52-0.60 <b>B3:</b> 0.63-0.69 <b>B4:</b> 0.76-0.90 <b>B5:</b> 1.55-1.75 <b>B7:</b> 2.08-2.35	30	$185 \text{ EW} \times 172 \text{ NS}$
Landsat ETM+	<b>B1:</b> 0.45-0.515 <b>B2:</b> 0.525-0.605 <b>B3:</b> 0.63-0.69 <b>B4:</b> 0.75-0.90 <b>B5:</b> 1.55-1.75 <b>B7:</b> 2.09-2.35	30	$183 \text{ EW} \times 170 \text{ NS}$
Landsat 8	<b>B1:</b> 0.433-0.453 <b>B2:</b> 0.450-0.515 <b>B3:</b> 0.525-0.600 <b>B4:</b> 0.630-0.680 <b>B5:</b> 0.845-0.885 <b>B6:</b> 1.560-1.660 <b>B7:</b> 2.100-2.300 <b>B8:</b> 0.500-0.680 <b>B9:</b> 1.360-1.390	30	$185 \text{ EW} \times 180 \text{ NS}$
RapidEye	<b>B1:</b> 0.44-0.51 <b>B2:</b> 0.52-0.59 <b>B3:</b> 0.63-0.68 <b>B4:</b> 0.69-0.73 <b>B5:</b> 0.76-0.85	6.5	$50 \text{ NS} \times 77 \text{ EW}$ $300 \text{ NS} \times 77 \text{ EW}$
CHRIS/Proba	<b>61 bands</b> (0.415 to 1.1050)	34	$13 \times 13$

A list of the satellite imagery acquired during the project is summarized in Table 2. Examples of the multi-/hyperspectral imagery acquired over the study areas selected within the MOPRA project are illustrated in Figures 2 to 4.

Table 2. The satellite multi-/hyperspectral imagery acquired within MOPRA at the specific study areas.

Sensor	Cold Lake	Lacombe	Coal Valley	Mattheis Ranch
<b>SPOT</b>	<b>4</b> 06-08-22 <sup>1</sup> <b>5</b> 08-07-12 <b>5</b> 12-07-07 <b>5</b> 13-09-02 <b>5</b> 13-09-13	<b>2</b> 05-07-29 <b>4</b> 06-07-16 <b>4</b> 07-07-15 <b>4</b> 08-08-08	<b>4</b> 01-08-16 <b>4</b> 03-07-30 <b>2</b> 06-08-27 <b>5</b> 08-08-06 <b>4</b> 12-08-10 <b>5</b> 13-09-10	—
<b>Landsat</b>	<b>LT5</b> 98-08-17 <b>LT5</b> 01-08-25 <b>LT5</b> 03-07-30 <b>LT5</b> 09-08-31 <b>LT5</b> 11-08-05 <b>LT8</b> 13-06-29 <b>LT8</b> 13-08-10 <b>LT8</b> 13-09-02	<b>LT5</b> 01-07-06 <b>LT5</b> 03-07-28 <b>LT5</b> 06-07-04	<b>LE7</b> 01-09-14 <b>LT5</b> 02-08-08 <b>LT5</b> 09-09-12	—
<b>RapidEye</b>	<b>RE3</b> 12-08-05	<b>RE3</b> 11-07-30	<b>RE3</b> 13-08-03 <b>RE3</b> 13-08-11	<b>RE3</b> 10-07-08 <b>RE3</b> 10-08-07 <b>RE3</b> 11-07-17 <b>RE3</b> 11-08-21 <b>RE3</b> 12-07-12 <b>RE3</b> 12-08-20 <b>RE3</b> 13-08-09
<b>CHRIS</b>	<b>CHRIS</b> 12-07-20 <b>CHRIS</b> 13-07-13 <b>CHRIS</b> 13-08-01	—	—	—

<sup>1</sup>The images are specified by acquired date suffixed with the satellite sensor. For example, 4 06-08-22 means that 4 indicates SPOT 4 satellite and 06-08-22 denotes that the image was acquired on August 22, 2006.



Figure 2. A subset of the Landsat ETM+ false-colour composite acquired in 2001 over the Coal Valley study area. The shortwave infrared, near-infrared, and red bands are displayed in red, green and blue colours, respectively.

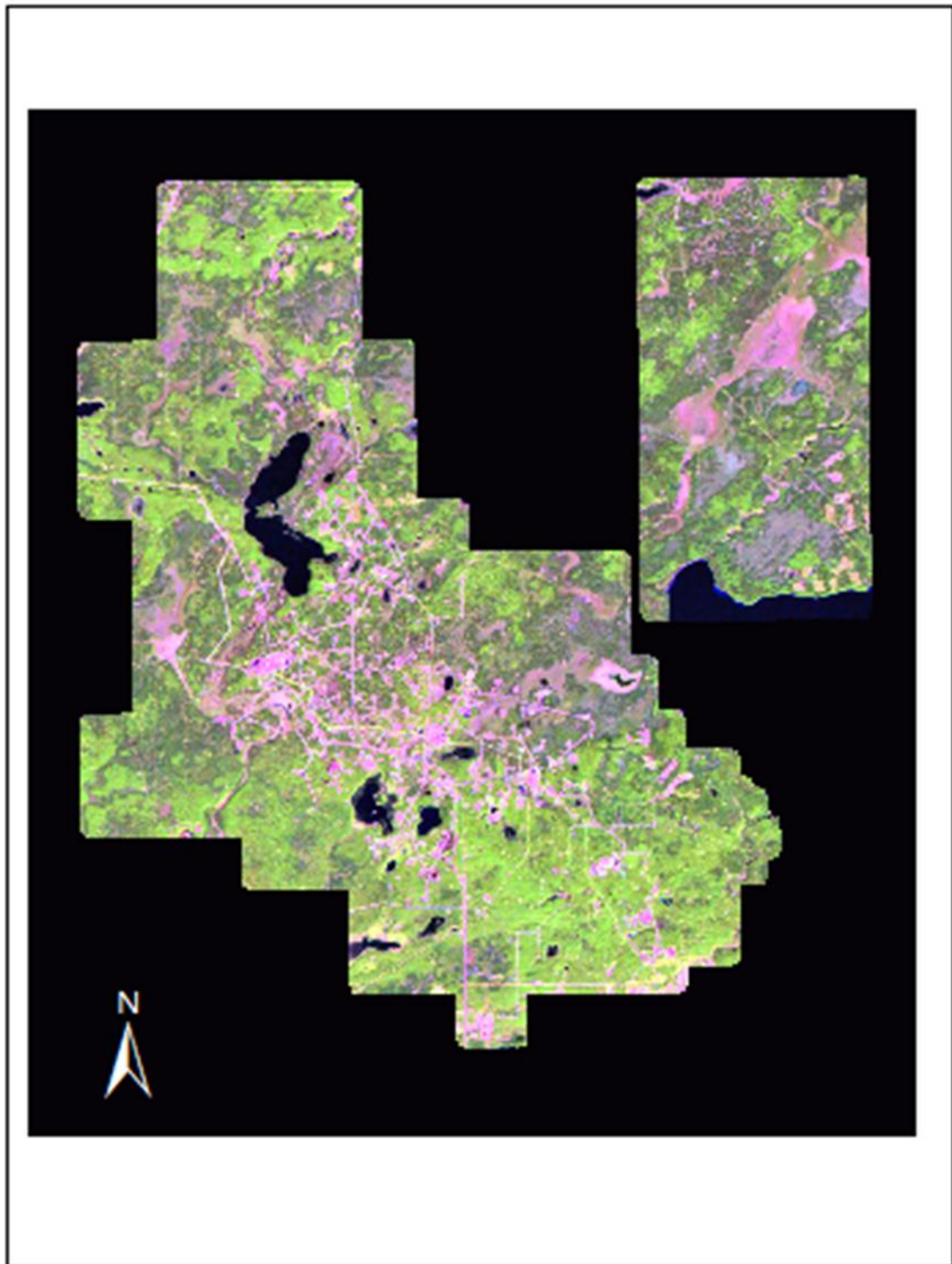


Figure 3. A subset of the Landsat TM 5 false-colour composite acquired in 1998 over the Cold Lake study area. The short-wave infrared, near-infrared, and red bands are displayed in red, green and blue colours, respectively.



Figure 4. A subset of the Landsat TM 5 false-colour composite acquired in 2001 over the Lacombe study area. The short-wave infrared, near-infrared, and red bands are displayed in red, green and blue colours, respectively.

Image data pre-processing was carried out to remove any sensor artifacts due to impacts from sensor malfunctions, atmosphere, and topography. Multispectral data were atmospherically, and geometrically corrected using the Atmospheric and Topographic Correction (ATCOR3) and OrthoEngine modules provided in the PCI Geomatics software<sup>7</sup>. The Fast Line-of-sight Atmospheric Analysis of Spectral Hypercubes (FLAASH) atmospheric module, embedded in the ENVI image processing software<sup>8</sup>, was also used to atmospherically correct multispectral data.

The raw CHRIS hyperspectral data were processed using the CHRIS/Proba-1 toolbox in the BEAM software developed by the European Space Agency (ESA) and Brockmann Consult<sup>9</sup>. Firstly, a noise reduction was applied to the data to correct for pixel drop-outs and vertical striping. A cloud screening tool was then used to identify and mask pixels based on a probabilistic map, which identifies cloud abundances per pixel. An atmospheric correction was then applied to the noise-removed and cloud-masked image data to convert at-sensor radiance to surface reflectance. The atmospheric correction adopted in the CHRIS/Proba-1 toolbox<sup>10</sup> uses the MODTRAN4 atmospheric model (Berk et al. 1999). Finally, an image-to-image geometric correction based on a previously geo-rectified image was applied to the atmospherically corrected CHRIS image data using the ENVI image processing software.

## **2.2 Airborne Hyperspectral/LiDAR Data**

The AISA airborne imaging hyperspectral systems<sup>11</sup> and LiDAR data acquired by Terra Remote Sensing Inc. over the Cold Lake study area in July 2012 were delivered atmospherically and geometrically corrected to ATIC by the University of Victoria in the summer of 2013. The hyperspectral data were orthorectified based on the LiDAR digital elevation model and atmospherically corrected using the atmospheric radiative transfer model (MODTRAN4) to derive surface reflectance data. Analysis of AISA data only focused on the forested study area because of the lack of coverage over the agricultural study area and the limited number of wellsites sampled due to the lack of access, ongoing field harvest or oil and gas operations. LiDAR data were acquired with an average point density of 1 point/m<sup>2</sup> per flight line. However with most flight lines being overlapped the average density was close to 2 points/m<sup>2</sup>. Two study sites in the Cold Lake area were planned as part of MOPRA so that both forested and agricultural sites are sampled (Figure 5).

---

<sup>7</sup> See <http://www.pcigeomatics.com/>

<sup>8</sup> See <http://www.exelisvis.com/ProductsServices/ENVI/ENVI.aspx>

<sup>9</sup> See <http://www.brockmann-consult.de/cms/web/beam/>

<sup>10</sup> See <https://earth.esa.int/web/guest/missions/esa-operational-eo-missions/proba>

<sup>11</sup> See <http://www.spectralcameras.com/aisa>

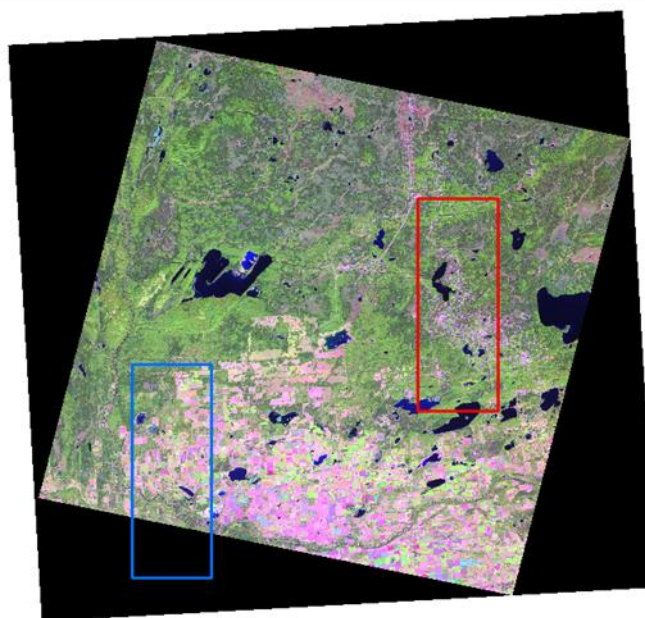


Figure 5. The Cold\_Lake\_FW (red box) and Cold\_Lake\_AG (blue box) study areas located west of the Town of Cold Lake.

### **2.2.1 Cold Lake – Forested Area (Cold\_Lake\_FW)**

The forested study site had to be adjusted because of no-fly restrictions in the Cold Lake Air Weapons Range, located north of this area. Data were acquired by the AISA/LiDAR system using a total of 26 flight lines covering an area of  $\sim 270 \text{ km}^2$  (Figure 6). The forested study area was flown using the Eagle AISA system at 1,150 m altitude resulting in a spatial resolution of 1.3 m and 138 spectral bands located in the VNIR spectral domain.

### **2.2.2 Cold Lake – Agricultural Area (Cold\_Lake\_AG)**

The agricultural study area was located to the southwest of the forested study area. Data were acquired by the AISA/LiDAR system using a total of 12 flight lines covering an area of  $\sim 135 \text{ km}^2$  (Figure 6). Coverage for this area was limited mostly due to the lack of clear-sky conditions. The acquisition over the agricultural study area was undertaken using the AISA Dual System at a 1,500 m flying altitude. The data over this area were acquired at a 2 m spatial resolution and in 497 spectral bands covering in addition to the VNIR the Short-Wave Infra-Red (SWIR) domain.

An example of AISA flight lines is shown in Figure 7. The spectral signatures of different targets on the ground (Figure 8) were examined to assess the quality of the data. Overall the spectral profile looks reasonable except in the 900-nm region where a sharp decrease in surface reflectance was noticed. This behaviour is likely due to the limitations in the atmospheric correction method that was applied to the at-sensor data.

In addition to the 2012 LiDAR data, the ESRD 2006 LiDAR data archive was also available through this project over the Cold Lake and Coal Valley study areas. These data were acquired in November, December and January of 2006 with an average point density of  $1.6 \text{ points/m}^2$ .



Figure 6. The 2012 AISA/LiDAR coverage over the Cold\_Lake\_FW (left) and Cold\_Lake\_AG (right) areas highlighted in white.

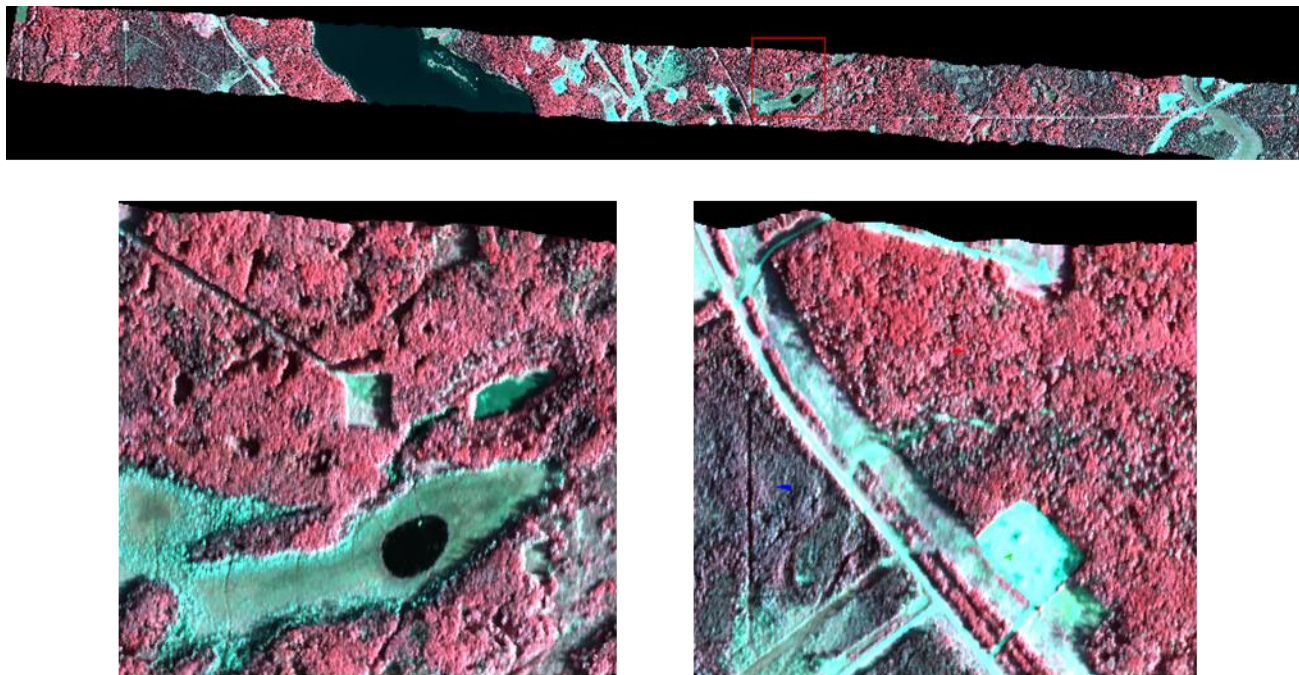


Figure 7. Example of AISA flight lines acquired over the Cold\_Lake\_FW and zoomed-in subsets.

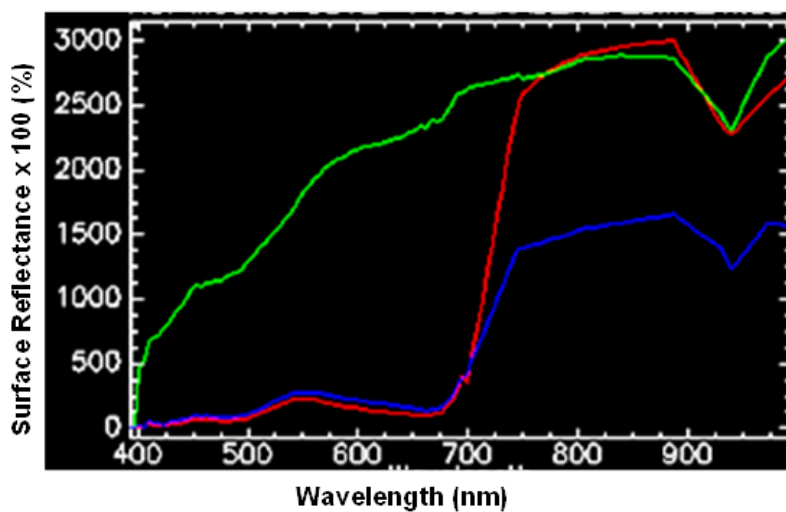


Figure 8. Examples of surface reflectance spectra derived from AISA data over coniferous forest (blue), deciduous forest (red) and a bare-ground area (green).

### **3 FIELD CAMPAIGNS**

Three field campaigns were undertaken over three study areas. The Cold Lake study area was visited in July 2012, while the Coal Valley and Mattheis Ranch areas were visited in July/August 2013. The next three sections address the field protocol adopted for these areas. The main scope of these field campaigns was the characterization of vegetation condition in reclaimed lease areas and adjacent undisturbed areas.

#### **3.1 Cold Lake Field Campaign**

##### **3.1.1 *Study Areas***

Two study sites were characterized on the ground from July 20 to August 3, 2012. The first one located North East of the City of Cold Lake is mostly dominated by forest and wetland areas (FW\_CL). The second site located North East of the City of Bonnyville is dominated by agricultural and forested areas (AG\_CL). Ground characterization was focused on the cultivated areas within this site (Figure 9).

The sampling scheme was governed by the location of certified reclaimed wells in both the FW\_CL and AG\_CL study sites. Access to the reclaimed wells in both of these sites was also a consideration. To sample the spatial variability of vegetation regrowth in wellsites the well's reclamation certificate issue date and the temporal NDVI derived from Landsat TM/ETM+ between 1998 and 2011 were used in the wellsite selection procedure. Alberta Vegetation Inventory data were used to sample wellsites in the FW\_CL study site that had different forest characteristics (e.g., species, crown closure).

Because forest structure characterization is time consuming and due to the large number of certified wellsites in FW\_CL, 10 days of ground characterization were dedicated to the FW\_CL study site, while 4 days were associated to the AG\_CL site. A number of test plots were set up in each study site as shown in Figure 9.

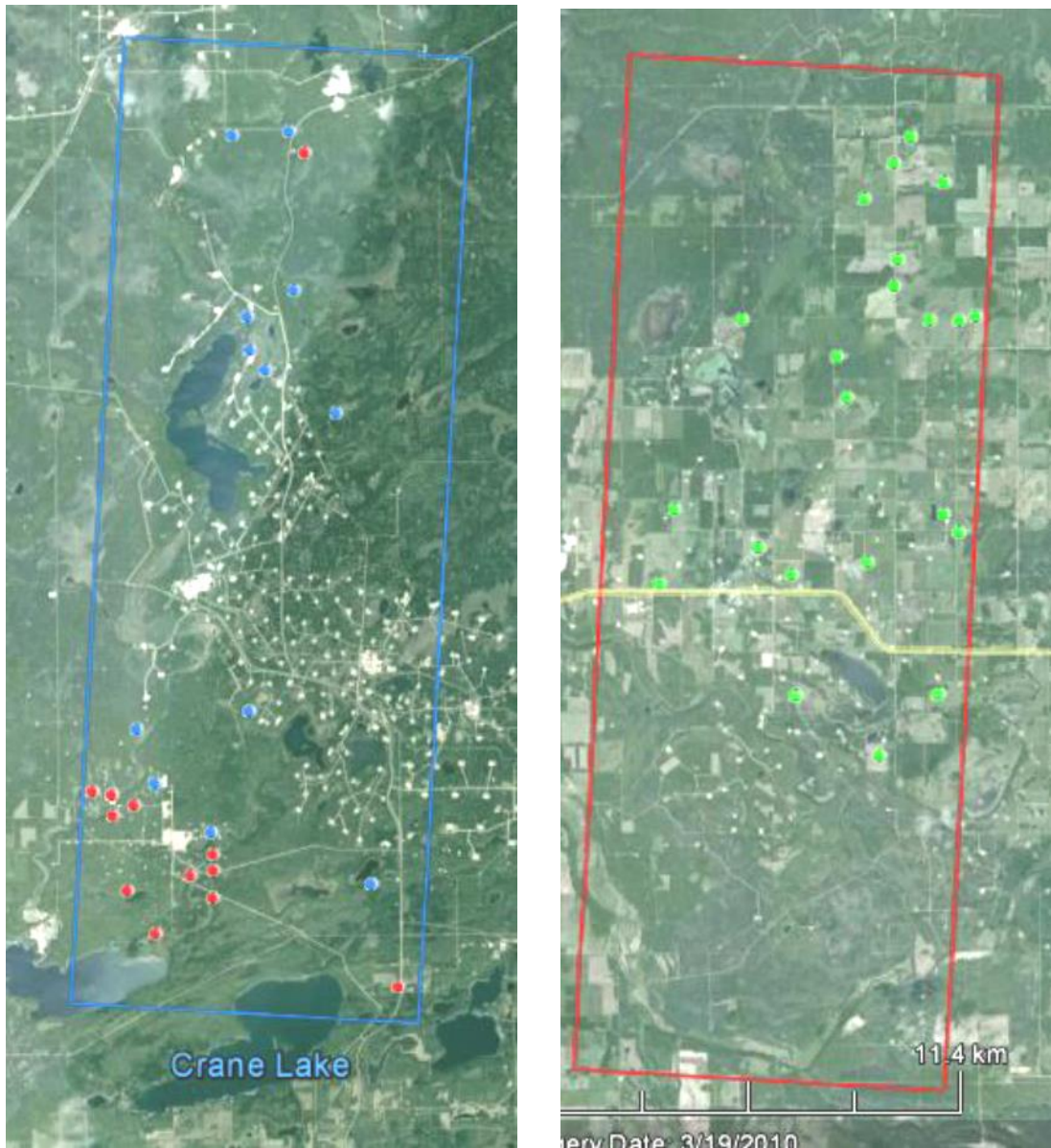


Figure 9. The wellsites sampled in the FW\_CL (left) and AG\_CL (right) study sites. Red and Blue dots denote forested sites selected based on criteria in Section 3.1.2. Green dots denote agricultural sites.

### 3.1.2 Test Plots

Test plots were selected for each wellsite following the guidelines established by Canada's National Forest Inventory (NFI; CNFI 2004). Because of the access conditions to the test sites and the complexity of the canopy structure, the measurement protocol was adjusted to ensure that a large number of certified wellsites were sampled within a reasonable time period. This was especially the case for the FW\_CL test site.

Collecting hemispherical photographs used to derive Leaf Area Index (LAI) followed the Validation of Land European Remote Sensing Instruments (VALERI) Protocol (VALERI 2014) for forested sites and the Canada Centre for Remote Sensing (CCRS) protocol for agricultural sites (Figure 10).

Test plot characterization was conducted as described in the next sections and summarized in Table 3. Prior to commencing the field work, a plan was developed that described sampling schemes, test plots, and measurement protocols (see [Appendix 2](#)).

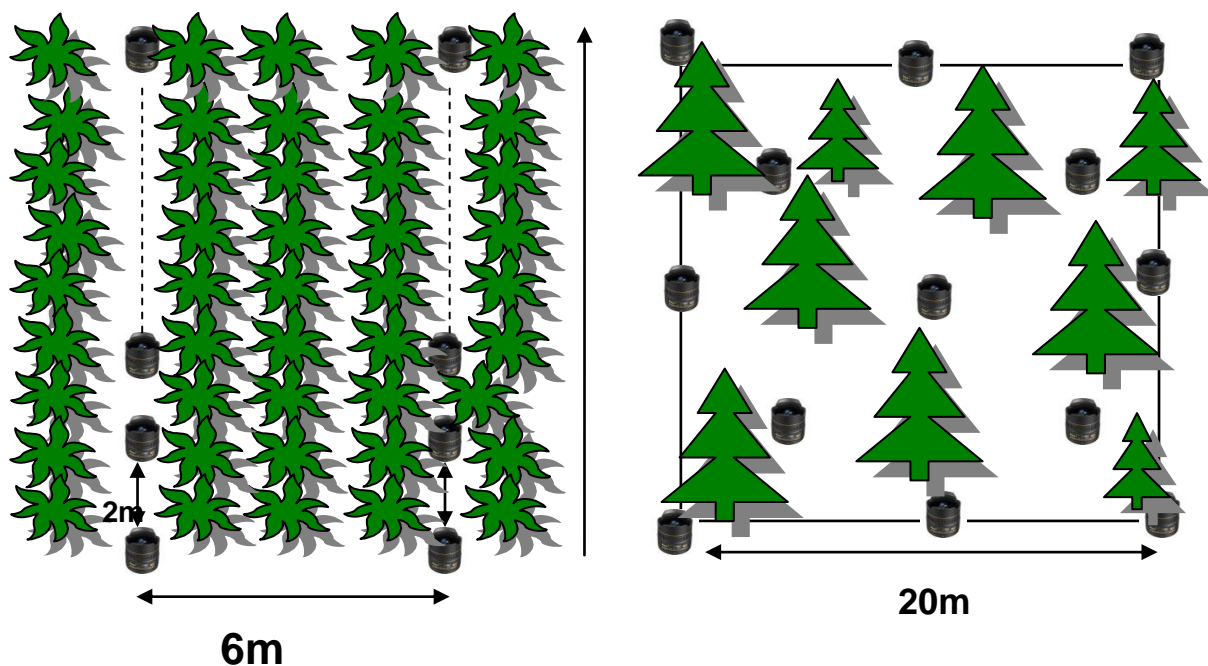


Figure 10. The sampling protocol used for collecting indirect measurements of leaf area index (LAI) using hemispherical photographs.

Left: The Canada Centre for Remote Sensing (CCRS) sampling protocol for agricultural areas.

Right: the Validation of Land European Remote Sensing Instruments (VALERI) protocol. Black lenses indicate hemispherical photographs locations.

Table 3. Agricultural and forested wellsites sampled during the 2012 Cold Lake field campaign.

Site Code	License Number	Surface Location	Well Construction Date	Reclamation Certification Date	Time Between Construction and Reclamation	Age of plot after reclamation to August 2012	Reclamation Certification Number
A10034389	34389	4-07-064-31-01	06/07/1968	18/11/1968	4 months	43 years 8 months	54-6882
A10060646	60646	4-08-063-34-06	18/10/1976	04/11/1977	1 year	34 years 8 months	54-17058
A10081012	81012	4-07-063-17-07	10/02/1980	01/02/2012	31 years 11 months	6 months	
A10121762	121762	4-07-064-30-06	04/02/1986	30/07/1987	1 year 5 months	25 years	54-25657
A10160628	160628	4-07-064-16-05	08/09/1993	29/07/1997	3 years 10 months	15 years	35448
A10162386	162386	4-07-064-20-05	19/11/1993	22/09/1998	4 years 10 months	13 years 10 months	36225
A20164151	164151	4-07-064-30-05	14/02/1994	22/09/1998	4 years 7 months	13 years 10 months	37487
F10025689	25689	4-04-066-02-01	03/03/1964	13/02/1967	2 years 11 months	45 years 5 months	55-377
F10027735	27735	4-04-065-03-14	20/02/1965	15/11/1967	2 years 8 months	44 years 8 months	55-816
F10087962	87962	4-04-064-32-10	07/02/1981	31/12/1985	4 years 10 months	26 years 7 months	
F10088251	88251	4-04-064-28-15	27/02/1981	31/12/1985	4 years 10 months	26 years 7 months	
F10088252	88252	4-04-064-28-02	01/03/1981	31/12/1985	4 years 9 months	26 years 7 months	
F10105627	105627	4-04-064-28-07	18/02/1984	14/10/2008	24 years 7 months	3 years 9 months	NE1-08-40100
F10109579	109579	4-04-064-32-15	03/11/1984	23/11/2007	23 years	4 years 8 months	NE1-07-41385
F10135076	135076	4-04-064-24-14	26/07/1988	11/02/1993	4 years 6 months	19 years 5 months	NER 93 0053
F10176511	176511	4-04-066-10-03	13/02/1996	17/05/1999	3 years 3 months	13 years 2 months	NEB 99 2E017
F10181679	181679	4-04-066-03-15	09/02/1996	13/02/2012	16 years	5 months	
F10182632	182632	4-04-066-10-11	14/01/1996	17/05/1999	3 years 4 months	13 years 2 months	NEB 99 2E032
F10191968	191968	4-04-065-05-11	05/03/1997	17/05/1999	2 years 2 months	13 years 2 months	NEB 99 2E040
F10195902	195902	4-04-066-27-13	16/03/1997	17/05/1999	2 years 2 months	13 years 2 months	NEB 99 2E022
F10196012	196012	4-04-066-26-13	21/03/1997	17/05/1999	2 years 1 month	13 years 2 months	NEB 99 2E033
F20051406	51406	4-04-064-13-01	26/10/1974	31/12/1985	11 years 2 months	26 years 7 months	
F20069598	69598	4-04-064-20-13	25/07/1978	23/01/2009	30 years 5 months	3 years 6 months	NE1-09-80307
F20087929	87929	4-04-064-21-10	30/01/1981	19/01/2007	25 years 11 months	5 years 6 months	NE1-07-02382
F20087960	87960	4-04-064-20-02	23/01/1981	31/12/1985	4 years 11 months	26 years 7 months	
F20088253	88253	4-04-064-32-06	15/02/1981	31/12/1985	4 years 10 months	26 years 7 months	
F20104481	104481	4-04-064-28-03	05/02/1984	23/10/1986	2 years 8 months	25 years 9 months	NER 86 0062
F20112558	112558	4-04-064-31-10	25/01/1985	23/10/1986	1 year 8 months	25 years 9 months	NER 86 0063
F20150494	150494	4-04-066-26-11	07/01/1992	21/10/2008	16 years 9 months	3 years 9 months	NE1-08-10885
F20367845	367845	4-04-064-31-08	09/01/2007	22/03/2011	4 years 2 months	1 year 4 months	
F20368906	368906	4-04-064-31-01	03/02/2007	22/03/2011	4 years 1 month	1 year 4 months	

In the FW\_CL test site, a plot size of 20 m x 20 m was selected for large tree stands, which were mostly located in undisturbed areas and the following measurements were conducted:

- Geographic coordinates: locations of the centre and the four corners of each test plot were recorded for the forested plots using a GPS. For those certified sites dominated by grass and/or shrubs, these measurements were only recorded for the four corners.

- Land cover type: land cover, including information about the type of overstory and understorey, were recorded and a photograph of the site was taken (Figures 11 and 12).
- Hemispherical photographs: 13 upwards looking photos of the canopy and downward looking photos of the understorey were taken when in the presence of canopy overstory. Otherwise only downward looking photos were taken, especially in those certified wellsites dominated by grass and shrubs (Figures 13 and 14).
- Forest structure: A 10 m x 10 m section of each test plot was selected to characterize each of the trees having a diameter at breast height (DBH) greater than 2.8 cm. The tree species, height and DBH were recorded.



Figure 11. Photographs of land cover in the well (F20088253) and reference (RF20088253) sites.



Figure 12. Land cover of the well (AG0164151) and reference pasture sites (RAG0164151).



Figure 13. Downward and upward hemispherical photographs of the reference site RF20088253.



Figure 14. Downward facing hemispherical photograph of the reference site RAG0164151 (pasture).

For stands of small trees mostly found in reclaimed well sites, a plot size of 7 m x 7 m was selected and the same measurement procedures were applied. For this plot size, trees inside the entire 7 m x 7 m plot were characterized.

A total of 24 certified wellsites as well as their adjacent areas were characterized. Ground reference measurements were collected in 48 test plots.

In the AG\_CL study site, the following measurements were collected within 6 m x 6 m test plots selected to acquire coverage of at least 3 x 3 pixels of the airborne hyperspectral/LiDAR data and to mitigate geolocation errors of the imagery:

- Geographic coordinates: The coordinates of the four corners of each test plot were recorded using a GPS.
- Crop type: Information about the crop type and height was recorded, and a photograph of the site was taken (Figure 13).
- Hemispherical photographs: About 30 downward looking photos were taken along two parallel 30 m transects (parallel to the crop rows) separated by 6 m. The geographical coordinates of the start and end points of each transect were also recorded using a GPS. For pasture plots, 13 downward looking photos were acquired within a 20 m x 20 m test plot (Figure 14).

- **Leaf Chlorophyll:** In each test plot, relative chlorophyll measurements were collected for 10 plants using a SPAD chlorophyll meter. For each plant, three measurements were collected, one each at the base, middle, and tip of a leaf.

Out of the 22 certified wellsites visited, only eight were characterized as many of these sites were either harvested, inaccessible or in operation. Ground reference measurements were collected in 16 test plots including both wellsites and their adjacent undisturbed areas.

### **3.2 Coal Valley Field Campaign**

The field campaign in the Coal Valley study area was undertaken from August 19 to 22, 2013. The study area is located at the southeastern portion of the Coal Valley mining operations.

A pre-selection of sample sites in reclaimed areas was made before visiting the study area. After ensuring that disturbance operations were not on-going in the vicinity, test plots were set-up and ground data were collected in these sites. While touring the mine area and collecting data from reclaimed areas, a search was also conducted for reference test plots against which to compare reclaimed site data.

Three reclaimed areas were sampled where ground measurements were collected from 22 test plots located in the reclaimed mine lease areas; as well, 7 reference test plots located in undisturbed areas were characterized (Figure 15). The field protocol followed was similar to the one adopted in the Cold Lake study area. Each of these test plots corresponds to a 20 m x 20 m plot where type of land cover (Figure 16) and species were recorded in addition to collecting hemispherical photographs. A 10 m x 10 m sub-plot was then defined where structural measurements such as tree height, diameter to breast height, number of trees and tree species were collected.

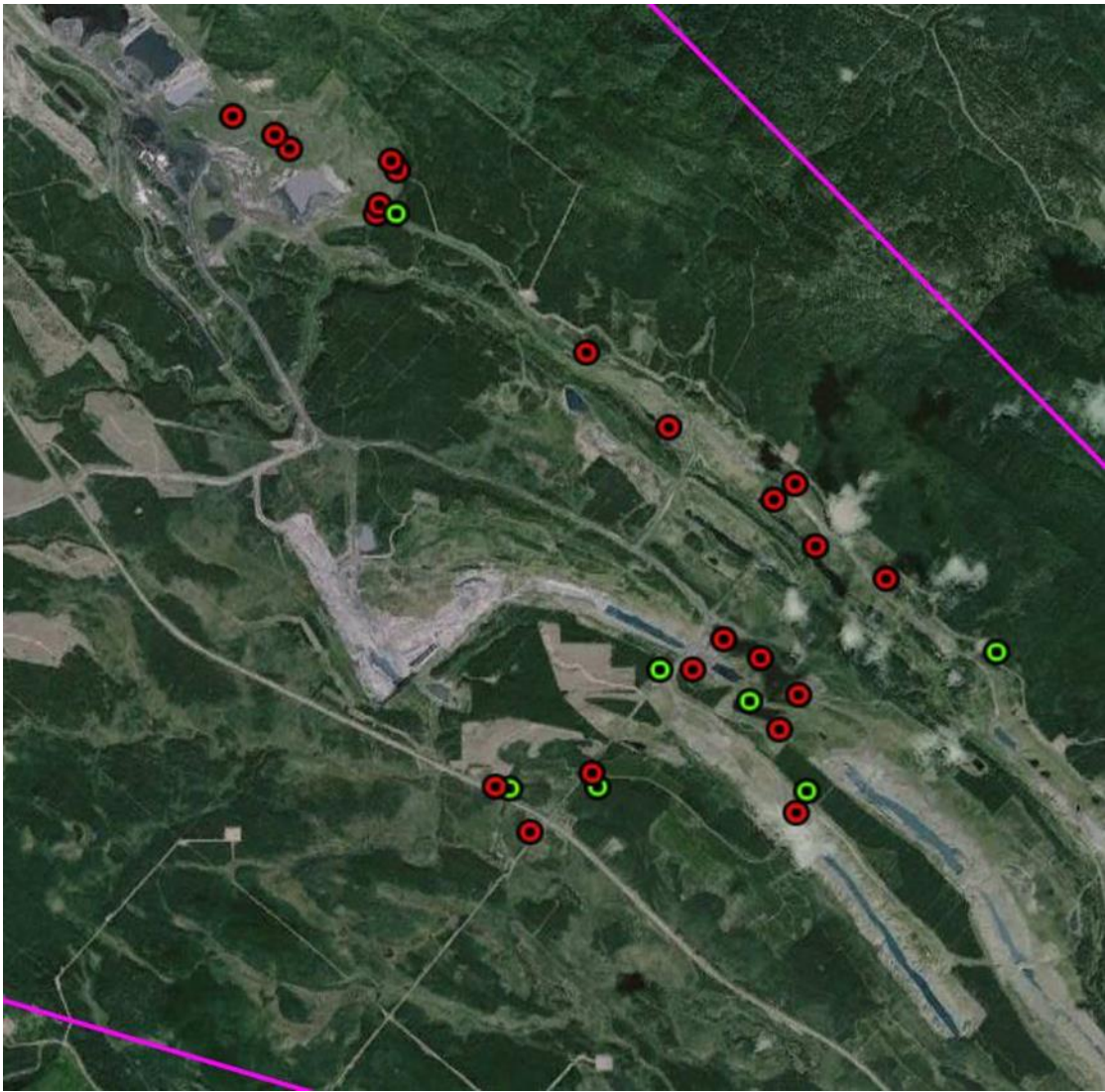


Figure 15. Test plots characterized in the Coal Valley study area in summer of 2013.  
Reclaimed (red dots) and undisturbed areas (green dots).



Figure 16. Photographs of land cover in the mine and reference areas for the Pit 14/15\_2 test plot.

### 3.3 Mattheis Ranch Field Campaign

A field visit was conducted on July 31 to the Mattheis Ranch agricultural research facility located 35 km north of Brooks, Alberta. A total of 25 wellsites were preselected based on the reclamation information provided by ESRD. A number of these sites were located in close proximity to each other, often appearing to overlap. A few sites appeared to still be in operation (close proximity of wheel marks next to extraction structures suggested that someone was visiting the sites on a regular basis). Following data collection about land condition at each reclamation site, a near-by, site appearing to be undisturbed, was chosen as a reference. Data from reclaimed and reference sites were collected at a total of four sites (Figure 17). 20 m x 20 m plots were set up and hemispherical photographs were acquired. In addition, digital photos documenting the state of these sites were also taken (Figure 18).

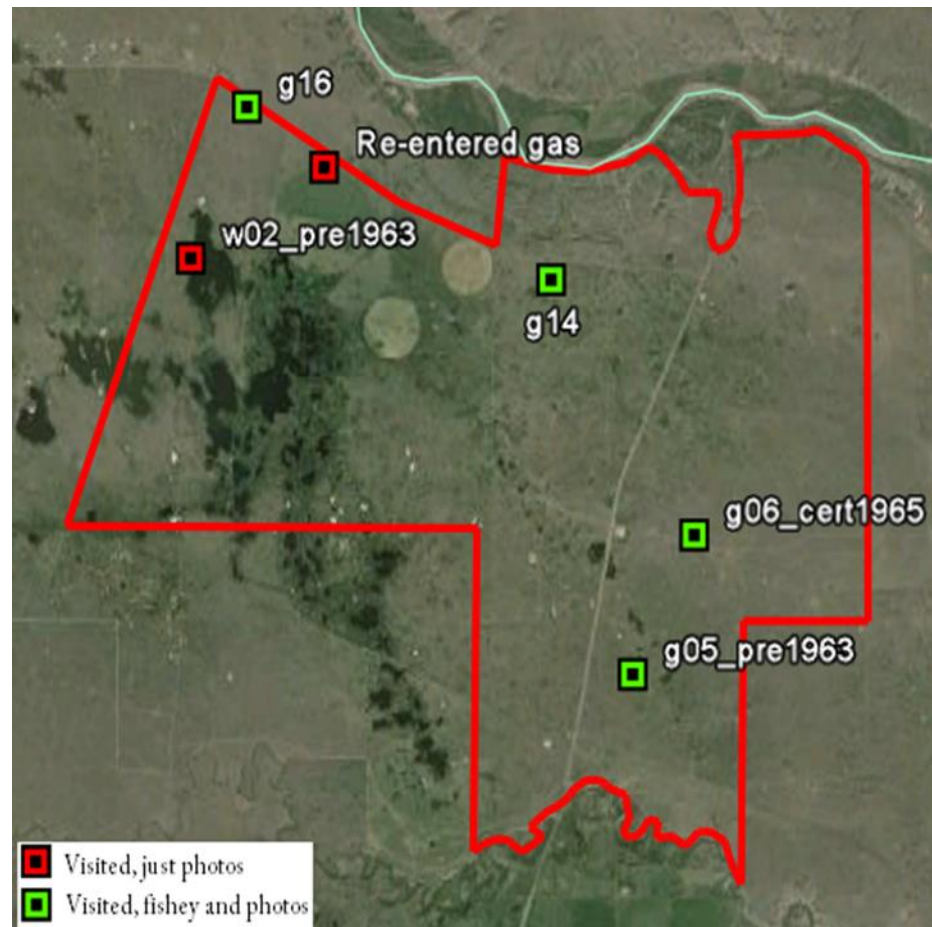


Figure 17. Test plots characterized in the Mattheis Ranch study area (red line) in July 2013.



Figure 18. Photographs of land cover in well (top) and reference (bottom) areas as observed during the Mattheis Ranch field campaign in July 2013.

### 3.4 Ground Measurements Analysis

This section addresses the ground data analysis performed, including above-ground biomass, volume, stem density, LAI, and chlorophyll content in the Cold Lake study area. The biomass, volume and stem density were considered only for the FW\_CL sites where 48 field plots, 10 m × 10 m in size, were measured to characterize the forest structure. Among these plots, 12 plots were located in wellsites which had no tree regrowth. Biomass, volume and stem density were derived for the remaining 36 plots.

#### 3.4.1 Forest Above-Ground Biomass, Volume and Stem Density

##### 3.4.1.1 Above-Ground Biomass

Above-ground biomass was calculated for FW\_CL test plots using a set of biomass equations obtained from Miao and Li (2007). Three biomass models, which historically have provided high accuracy estimation of forest above-ground biomass in the Prairie Provinces (Alberta, Manitoba, and Saskatchewan), were first tested. The following model was adopted because it was the only model that did not provide an erroneous calculation of tree biomass:

$$B = a + b \cdot DBH^2 \cdot H, \quad (1)$$

where  $B$  is the tree biomass in kg,  $DBH$  is the Diameter at Breast Height in cm,  $H$  is the tree height in m, and  $a$  and  $b$  are species-specific parameters.

The total biomass for each test plot was derived by aggregating the biomass of each individual tree within the plot. The species-specific parameters used in equation 1 are listed in Table 4, and the above-ground biomass distribution for all test plots is summarised in Figure 19.

##### 3.4.1.2 Canopy Volume

The single tree canopy volume was calculated using Penner's model (Penner et al. 1997):

$$V = \alpha \cdot 10^{-5} \cdot DBH^{\beta 1} \cdot H^{\beta 2}, \quad (2)$$

where  $\alpha$ ,  $\beta 1$  and  $\beta 2$  are species-specific parameters.

The values of these parameters used for each tree species are listed in Table 4. The total volume for each plot was derived by aggregating all single-tree volumes. The canopy volume distribution for all test plots is summarised in Figure 20.

##### 3.4.1.3 Canopy Stem Density

Stem density for each plot was computed by dividing the total number of live trees by the test plot area. The canopy stem density distribution for all test plots is summarised in Figure 21.

Table 4. Species-specific parameters used in biomass (equation 1) and volume (equation 2) models.

Tree species	Biomass <sup>1</sup>		Volume <sup>2</sup>		
	a	b	$\alpha$	$\beta_1$	$\beta_2$
Balsam Poplar	10.8106	0.01352	2.472902	1.871307	1.179970
White Spruce	6.09159	0.01499	4.328336	1.882751	1.02411
Paper Birch	4.52582	0.01769	4.328336	1.88275	1.020411
White Birch	2.54997	0.02455	5.634793	1.976455	0.803794
Trembling Aspen	0.34961	0.01916	7.491573	1.877086	0.850270
Jack Pine	2.98118	0.01679	4.421585	1.926909	1.00304
Black Spruce	2.84963	0.01699	4.328336	1.882751	1.02411
Balsam Fir	7.99821	0.01465	7.491573	1.877086	0.850270

<sup>1</sup> The parameters were adapted from Singh (1982).

<sup>2</sup> The parameters were adapted from Penner et al. (1997).

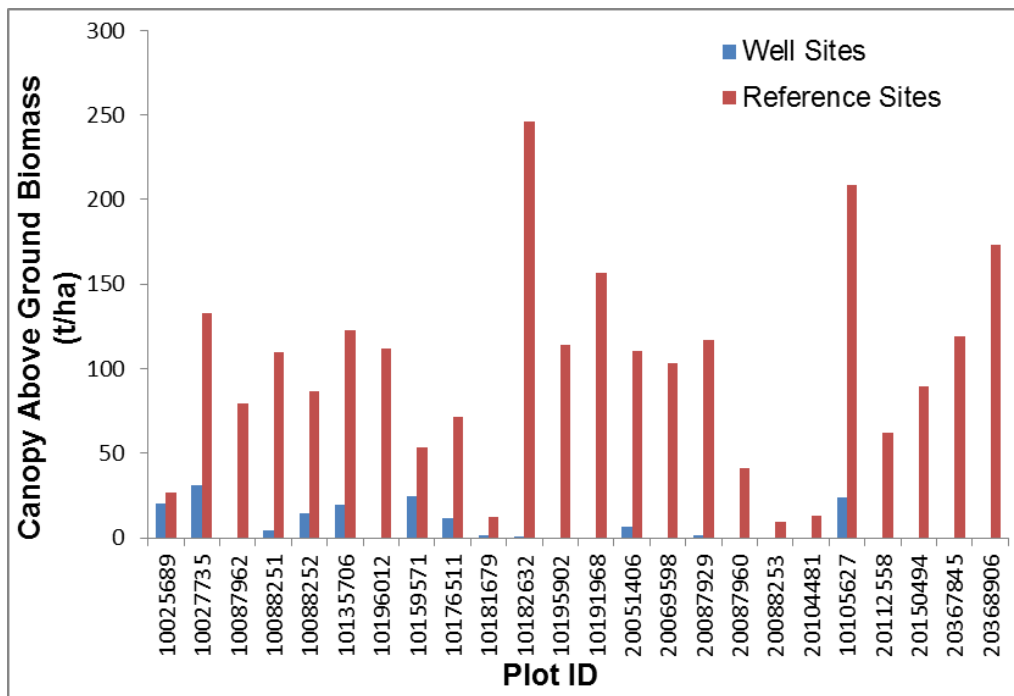


Figure 19. Above-ground biomass in forested well and reference sites for the FW\_CL study site.

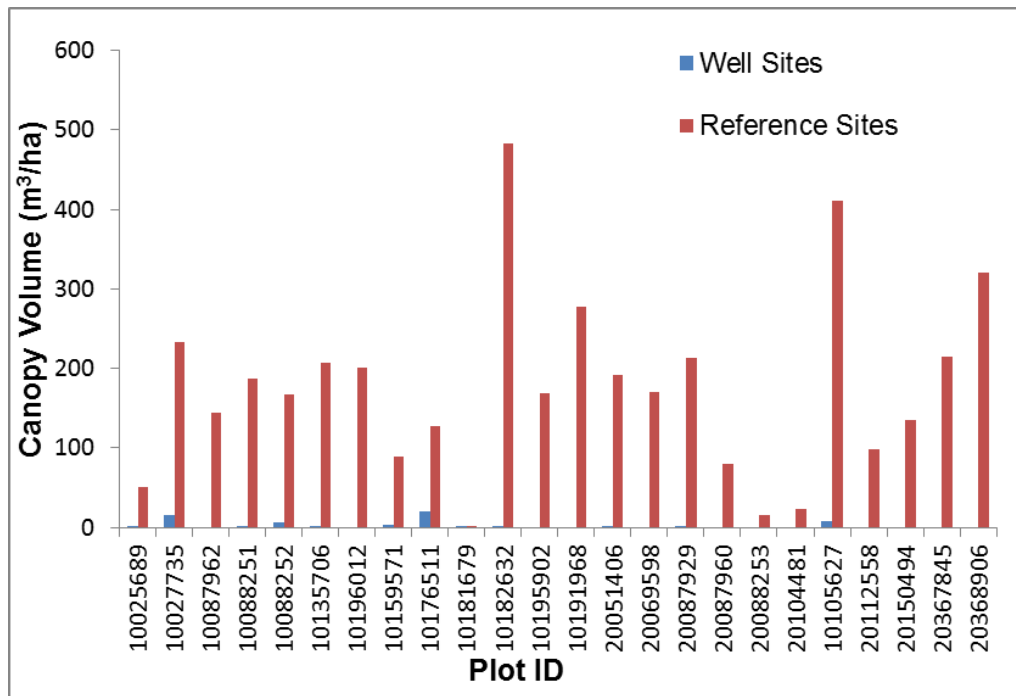


Figure 20. Canopy volume in well and reference sites for the FW\_CL study site.

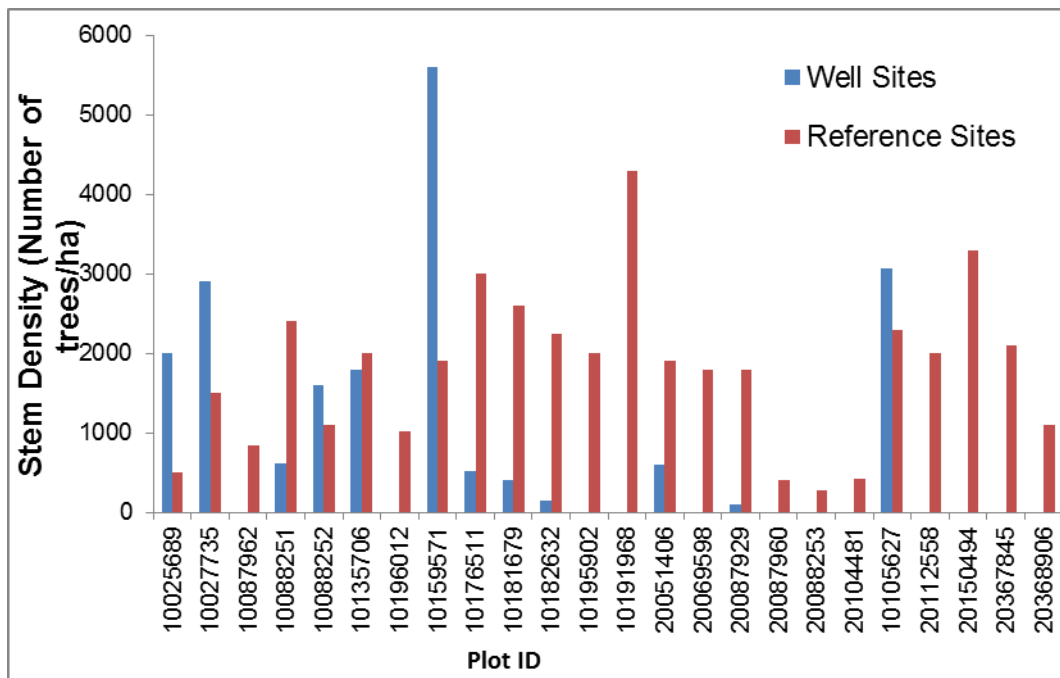


Figure 21. Stem density in forested well and reference sites for the FW\_CL study site.

### 3.4.2 Canopy Leaf Area Index (LAI)

LAI is commonly defined as the one-sided leaf area per unit horizontal ground surface area. Indirect measurement techniques are typically based on measurements of canopy gap fractions, which correspond to the probability that light is transmitted to the ground without any interaction with canopy elements. During the 2012 field campaign in Cold Lake, canopy gap fractions were measured using hemispherical photographs, which were later processed to derive LAI using the Version 6.1 of the CanEye software developed by the French National Institute of Agronomical Research (Weiss and Baret 2010). Examples of the CanEye image processing results are shown in Figures 22 and 23.

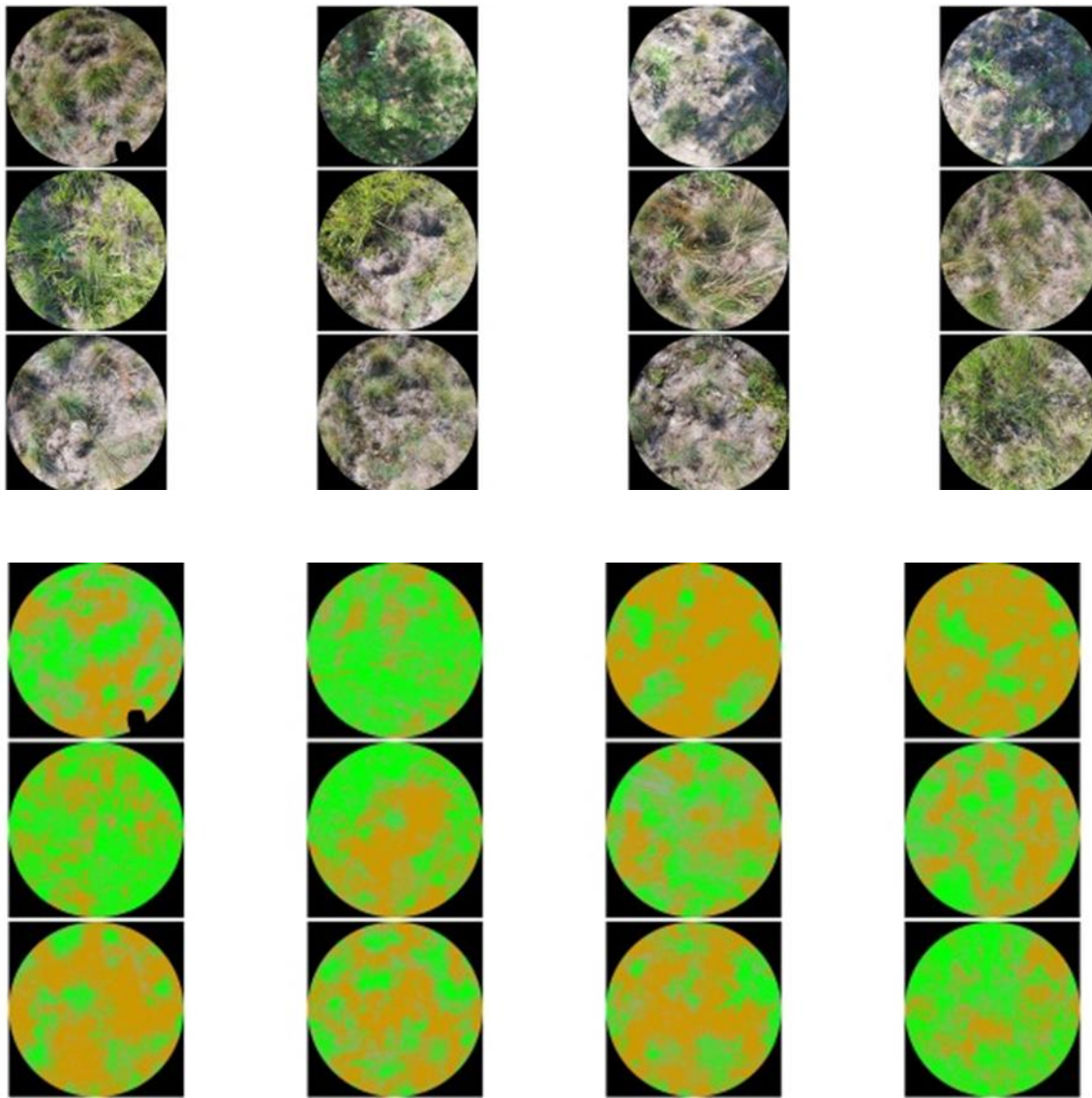


Figure 22. Downward looking hemispherical photographs (a) and classified images (b) derived using the CanEye software for the F10182632 test plot in the FW\_CL study site.

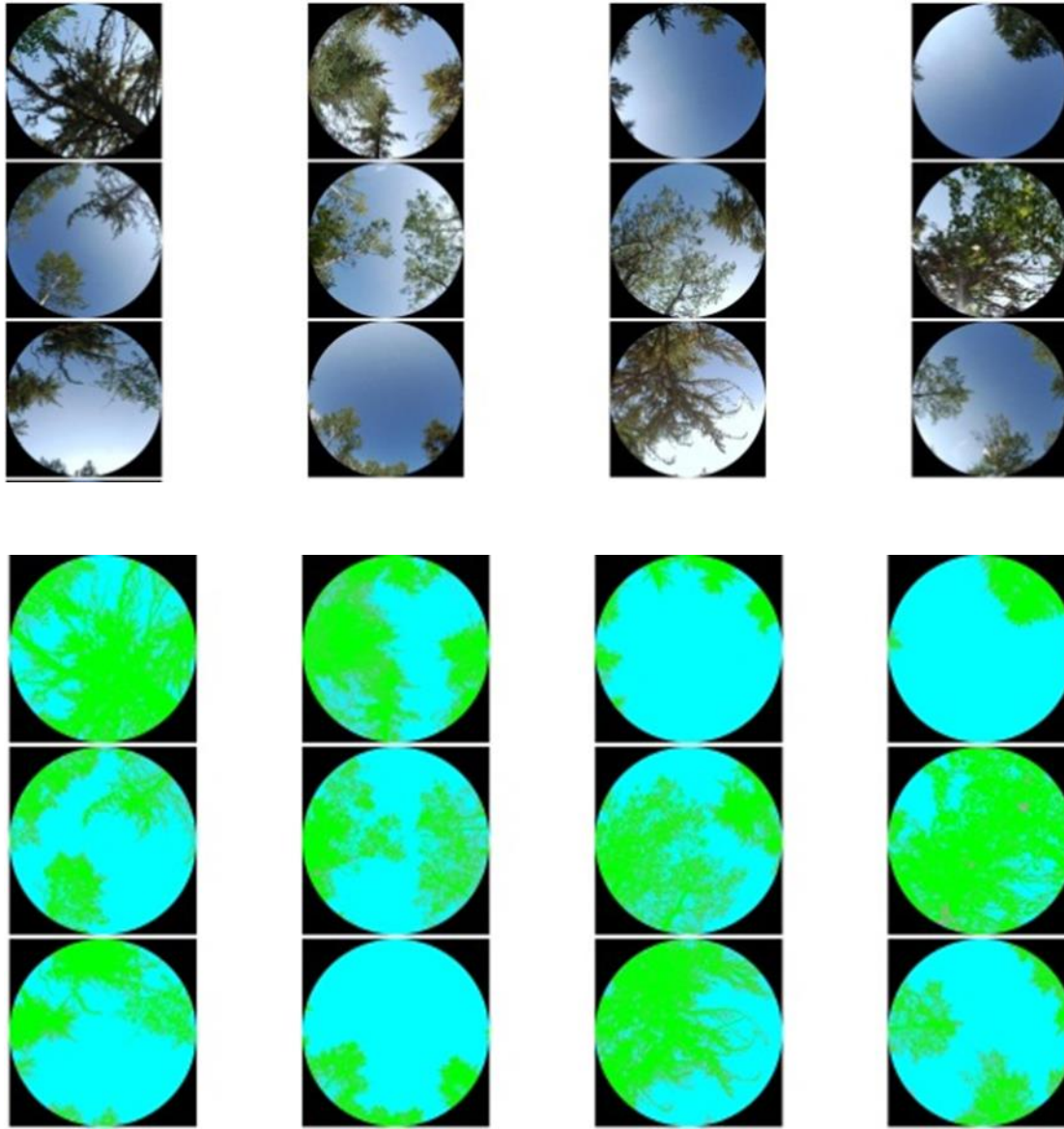


Figure 23. Upward looking hemispherical photographs (a) and classified images (b) derived using the CanEye software for the RF10182632 test plot in the FW\_CL study site.

CanEye allows the user to classify the hemispherical photographs into vegetation and non-vegetation (e.g., sky, litter, soil etc...) elements (Figure 22) and, subsequently, derive the canopy gap fraction as a function of the viewing zenith angle.

Using the canopy gap fraction model given by equation 3, a look-up-table based inversion is performed to derive LAI. Using a root-mean-square-error-based cost function, the modelled gap fraction showing the least discrepancy from the measured gap fraction is identified and the corresponding LAI is selected.

$$P_0(\theta_v, \varphi_v) = e^{-\lambda_0 G(\theta_v, \varphi_v) \cdot \frac{LAI}{\cos(\theta_v)}}, \quad (3)$$

Where  $P_0(\theta_v, \varphi_v)$  is the gap fraction,  $\theta_v$ , and  $\varphi_v$  are the zenith and azimuth view angles,  $\lambda_0$  is the canopy clumping index, and  $G(\theta_v, \varphi_v)$  is the leaf angle projection function.

Note that for forested canopies, the LAI derived using CanEye is not the true LAI but the Plant Area Index (PAI). In fact, in the classification process of vegetated/non-vegetated elements, the branches and trunks are classified as vegetated elements. For such cases, an additional correction is required to derive the true LAI using the following formula developed by Chen et al. (2006):

$$LAI = (1 - \alpha) * PAI, \quad (4)$$

where  $\alpha$  is the woody-to-total leaf area ratio.

In case of needle leaf-forest, hemispherical photographs are incapable of measuring gaps between the needles to derive the needle area index. Therefore, it is necessary to take into account the needle-to-shoot area ( $\gamma_E$ ) as follows:

$$LAI = (1 - \alpha) * \gamma_E * PAI. \quad (5)$$

LAI was calculated for all the test plots characterized in the Cold Lake study area using the collected hemispherical images as mentioned in [section 3.1.2](#). Both upward and downward LAIs were computed for the well and reference sites. They were then summed to derive the canopy LAI when canopy overstorey was present. Figure 24 summarizes the canopy LAI measurements for well and reference test plots in the FW\_CL study site.

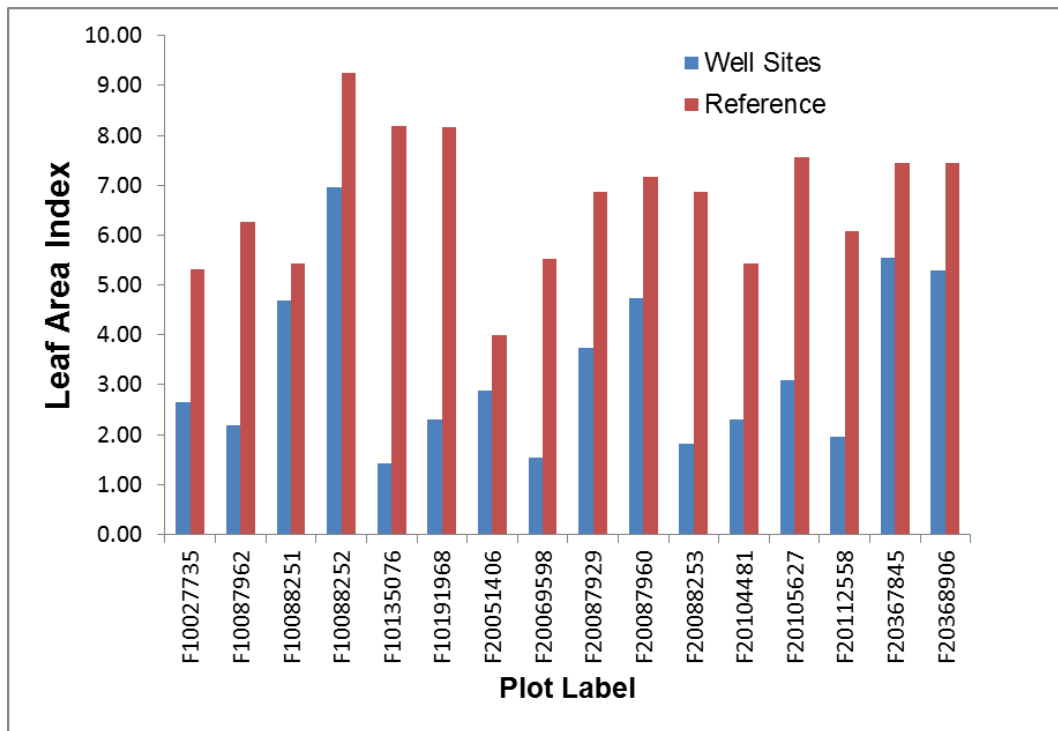


Figure 24. Canopy LAI as derived from hemispherical photographs in well and reference test plots for the FW\_CL study site.

### 3.4.3 Leaf Chlorophyll Content

Analysis of relative chlorophyll content acquired using the SPAD 502 chlorophyll meter in the field was carried out for the nine agricultural test plots (AG) and their corresponding reference plots (RAG) sampled. Because not every plot represented a pure crop, there were three broad categories considered as coverage type: canola (only crop type present), forbs, and grass. In the event that the vegetation coverage was forbs and grass, five plants were sampled each from forbs and grass, respectively.

Leaf chlorophyll analysis results are shown for forbs and grass in Figure 25 for both well and reference sites. It can be seen that differences in relative chlorophyll content occur between the well and reference sites for test plot 7 for both forbs and grass and for test plot 8 for forbs. All the differences in chlorophyll content for the other plots are within the standard deviations.

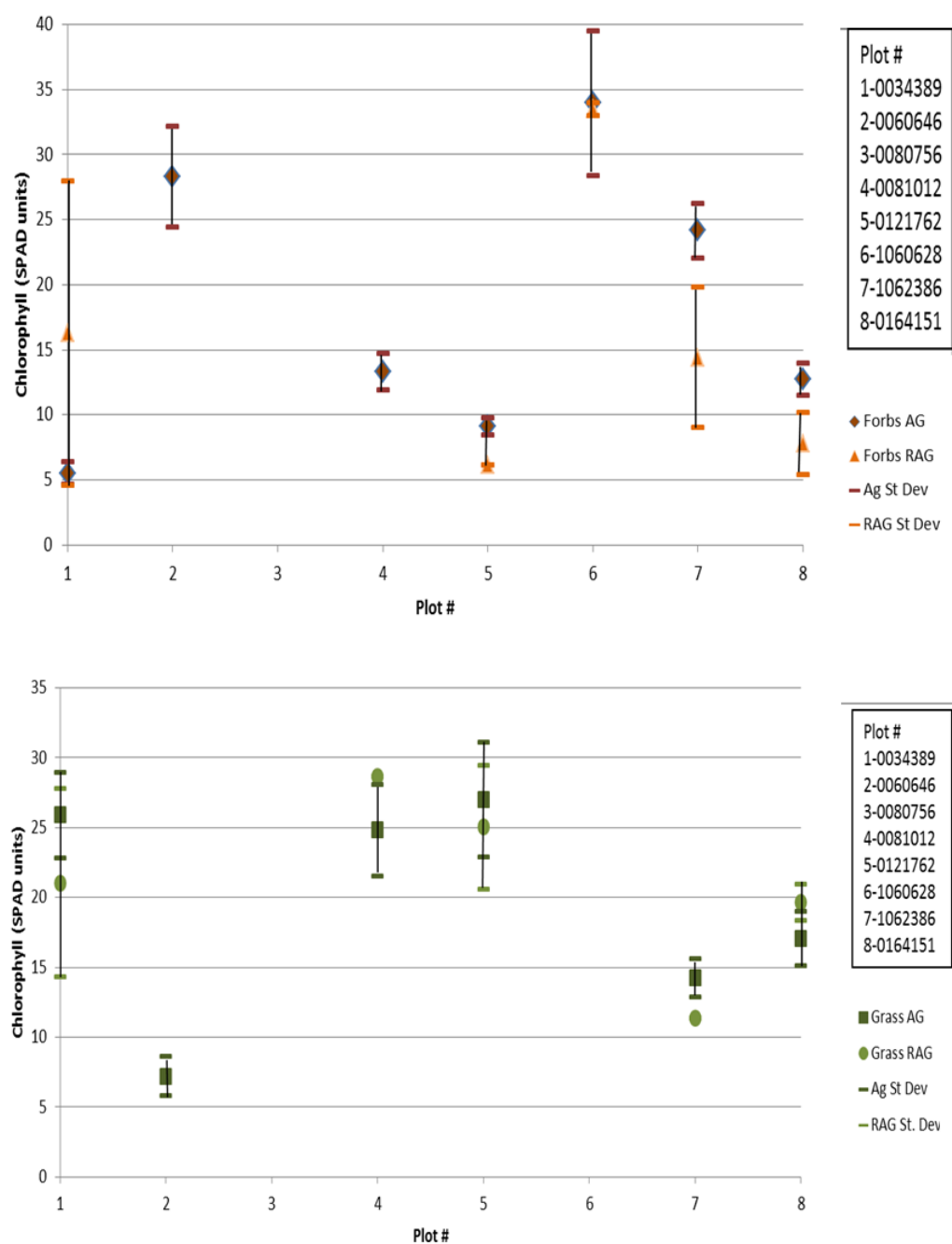


Figure 25. Averaged relative chlorophyll content of forbs (top) and grass (bottom) for all well and reference test plots within the AG\_CL study site.

## **4 METHODOLOGY – INFORMATION EXTRACTION**

To retrieve information about vegetation condition in both reclaimed and natural lands, remote sensing image data, together with the ground data collected, were investigated. A set of land products were developed within this project, including baseline land cover, land-cover change, canopy height, fractional cover, tree species and canopy LAI. In addition, multi-year profiles of vegetation index data were examined to assess vegetation regrowth in wellsites in comparison to undisturbed reference areas. Canopy structure attributes, derived using LiDAR data such as canopy height and fractional cover, were also examined to assess differences in vegetation structure between reclaimed wellsites and regenerated burnt/clear-cut areas.

While baseline land cover and change detection mapping together with multi-year vegetation index assessment were conducted for Cold Lake, Coal Valley and Lacombe study areas, the remaining products were produced only for the Cold Lake study area.

The focus on some of the study areas compared to others was mostly governed by the data availability and time limitation. An assessment of airborne hyperspectral data was conducted at a preliminary stage due to time limitation caused by the delay in the data delivery. However, the preliminary results were not included in this report as they are not conclusive.

The next sub-sections provide descriptions of the approaches adopted and the land products generated.

### **4.1 Baseline Land-Cover Mapping**

Baseline cover maps were produced using the oldest imagery available in this project. Three land-cover maps were produced using Landsat imagery acquired in 1998, 2001 and 2002 over the Cold Lake, Coal Valley and Lacombe study areas, respectively. These land-cover maps can be used as a baseline for assessing land cover in any reclaimed area associated with oil and gas wellsites or mine areas that were established after the imagery acquisition date.

The land-cover classification was performed using the supervised Support Vector Machine (SVM) technique. A set of thematic classes were defined for each study area as shown in Figures 26 and 27. For this purpose, a number of regions of interest were first selected based on visual inspection for use as training data.

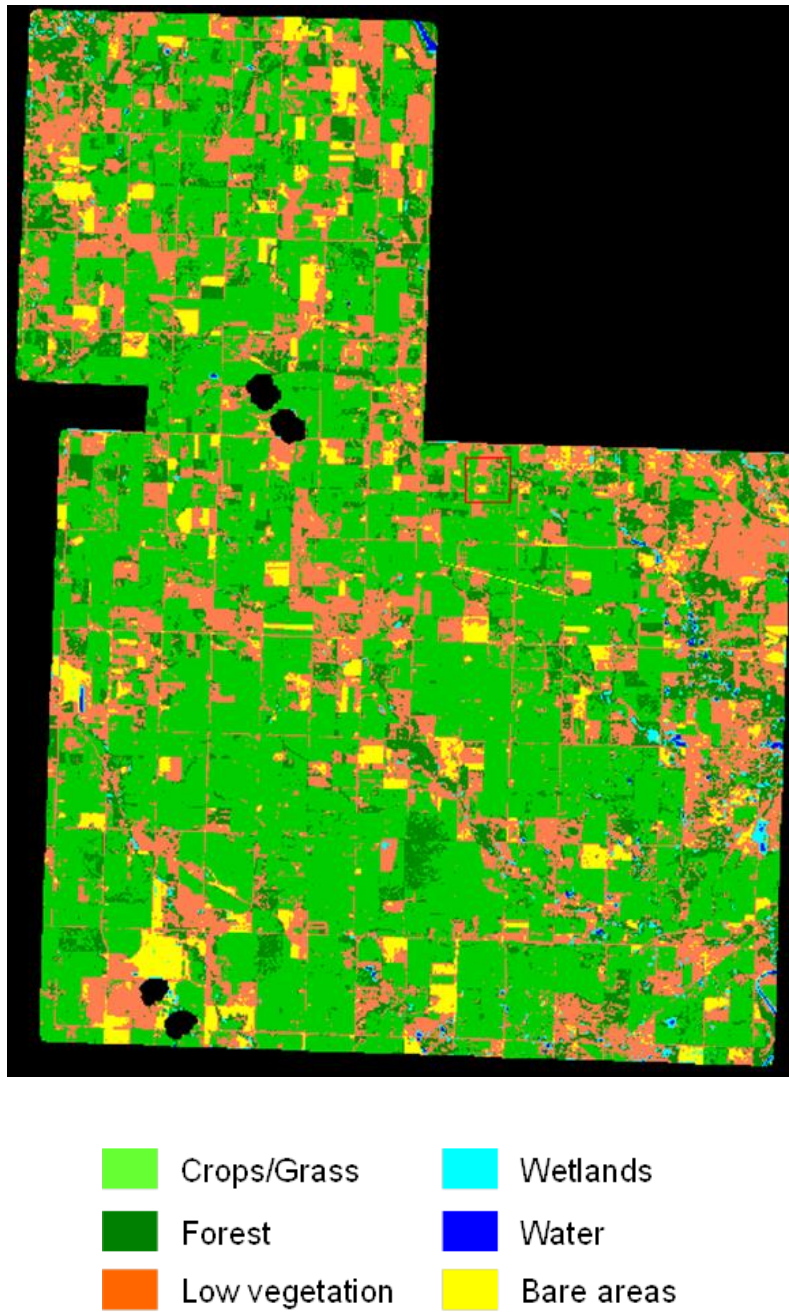


Figure 26. 30 m land-cover map of the Lacombe study area using Landsat imagery acquired in 2001.

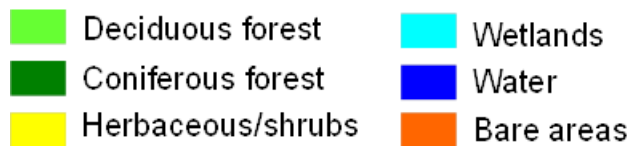
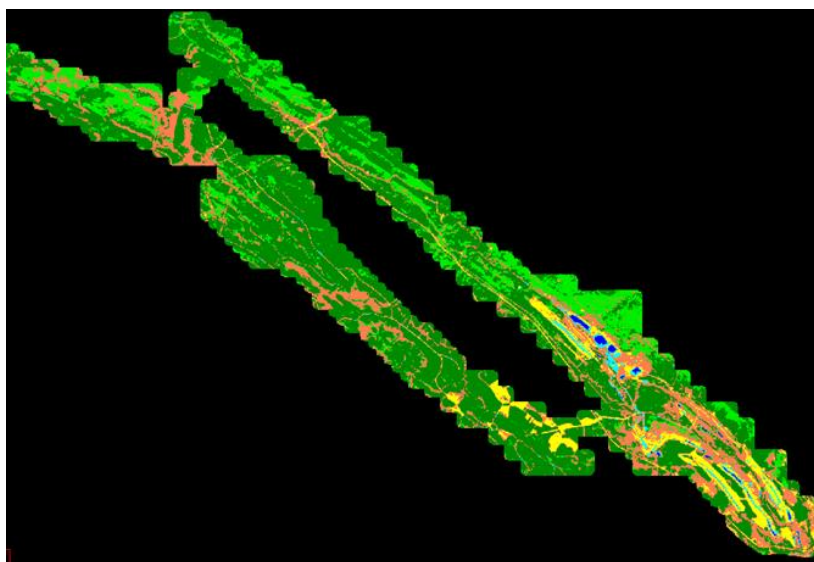
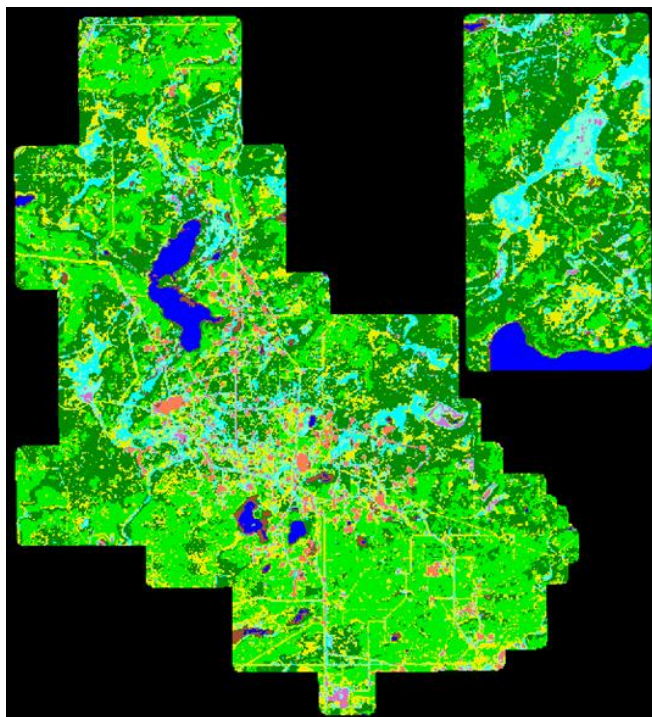


Figure 27. 30 m land-cover maps over the Cold Lake (top) and Coal Valley study (bottom) areas using Landsat imagery acquired in 1998 and 2002, respectively.

An accuracy assessment was then conducted for each land-cover map using a new set of regions of interest for validation. Three accuracy measures were examined as follows:

- Overall accuracy: the probability that pixels in the land-cover map have been correctly classified.
- User accuracy: the probability that pixels for a given class of the land-cover map have been correctly classified.
- Producer accuracy: the probability that a given land-cover class on the ground was correctly represented in the land-cover map.

For the Lacombe study area, overall accuracy equaled 86% with User and Producer accuracies ranging from ~ 77% to 94%. A 90% overall accuracy was found for the Coal Valley study area with User and Producer accuracies ranging from 77% to 100% except for wetlands. The latter had 38% and 52% for User and Producer accuracies, respectively. Finally, for the Cold Lake study area, the overall accuracy obtained was about 80% with User and Producer accuracies ranging between 66% and 100%.

#### 4.2 Monitoring Change Using Multispectral Satellite Imagery

A change detection procedure was applied to the Normalized Difference Vegetation Index (NDVI; Rouse et al. 1974) data derived using the oldest image and the most recent acquired before 2012 over the Cold Lake and Coal Valley study areas to determine the type of changes that occurred between these two years. NDVI is a mathematical transformation of the RED and NIR spectral bands based on the following formula:

$$NDVI = \frac{(R_{NIR} - R_{RED})}{(R_{NIR} + R_{RED})}, \quad (6)$$

where  $R_{RED}$  and  $R_{NIR}$  are surface reflectances acquired in the RED and NIR bands, respectively.

Figures 28 and 29 show false-colour composites of Landsat TM 5 acquired in 1998 and 2011 over Cold Lake, and in 2001 and 2009 for Coal Valley. Each pair of images was acquired not more than 12 days apart for each study area, which suggests that the acquisition time difference should have little effect on vegetation phenology assuming that the meteorological conditions are similar for these years.

The change detection was performed using the Spectral Processing Exploitation and Analysis Resource (SPEAR) tool<sup>12</sup> used in the ENVI image processing software. This tool allows assessing the areas that have experienced changes between two distinct points of time by subtracting the NDVI between two dates.

---

<sup>12</sup> See <http://www.exelisvis.com/docs/spearchangedetection.html>

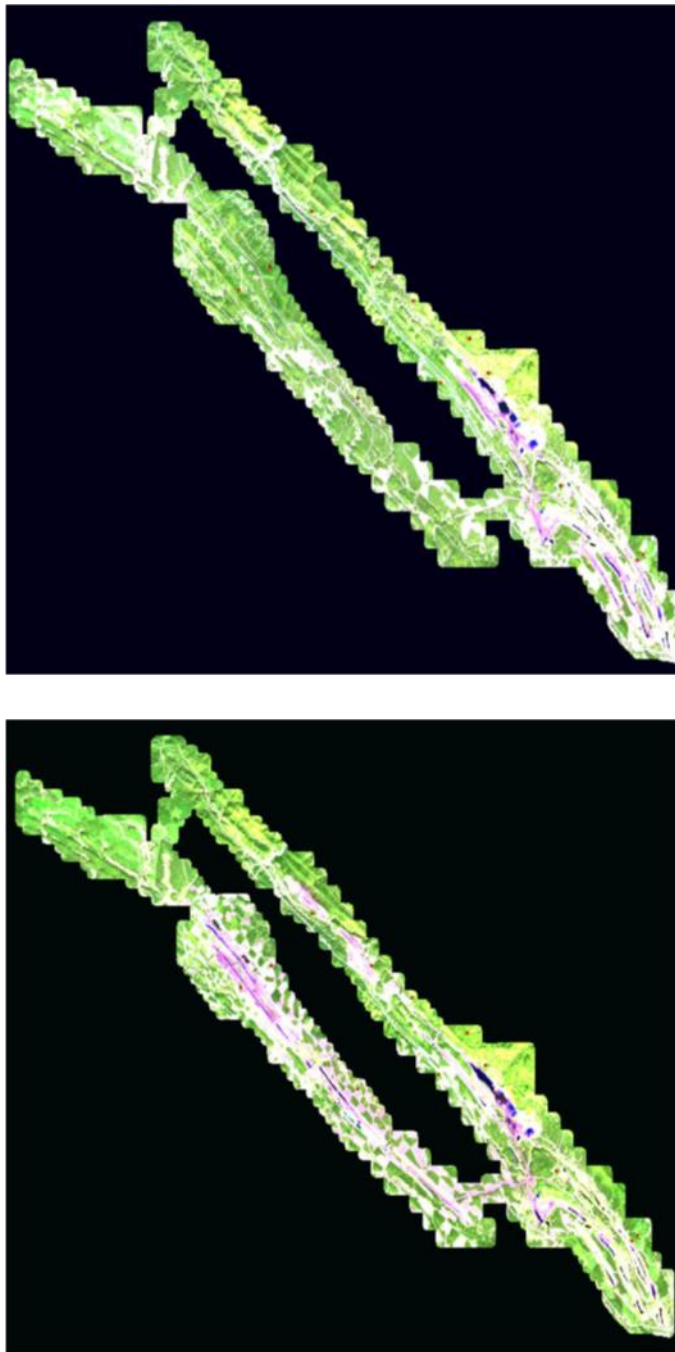


Figure 28. Landsat colour composites over the Coal Valley study area acquired in 2001 (top) and 2009 (bottom).  
SWIR band in red, NIR band in green and RED band in blue.



Figure 29. Landsat colour composites over the Cold Lake study area acquired in 1998 (top) and 2011 (bottom).  
SWIR band in red, NIR band in green and RED band in blue.

The results of change detection are illustrated for Cold Lake and Coal Valley in Figures 30 and 31. A decrease or an increase in NDVI between the oldest image and the most recent one was associated with land disturbance or vegetation regrowth, respectively. These two land statuses correspond to an absolute NDVI difference ranging from 0.15 to 1. An absolute NDVI variation, smaller than 0.15, seems to be associated with natural variations resulting from the inter-annual variation of meteorological conditions. This behaviour was observed especially in wetland areas.

Figure 32 shows two examples of the change detection results over the Cold Lake area where the land was cleared for oil and gas exploration, resulting in an increase of the number of well pads and access roads. The revegetated areas, derived from the change detection process showing the areas where vegetation recovery has occurred between 1998 and 2011, are also illustrated. Some residual errors were also associated with the revegetation detection, which seems to be due to a natural change in the land condition caused by a possible variation in the meteorological conditions between the two selected years.

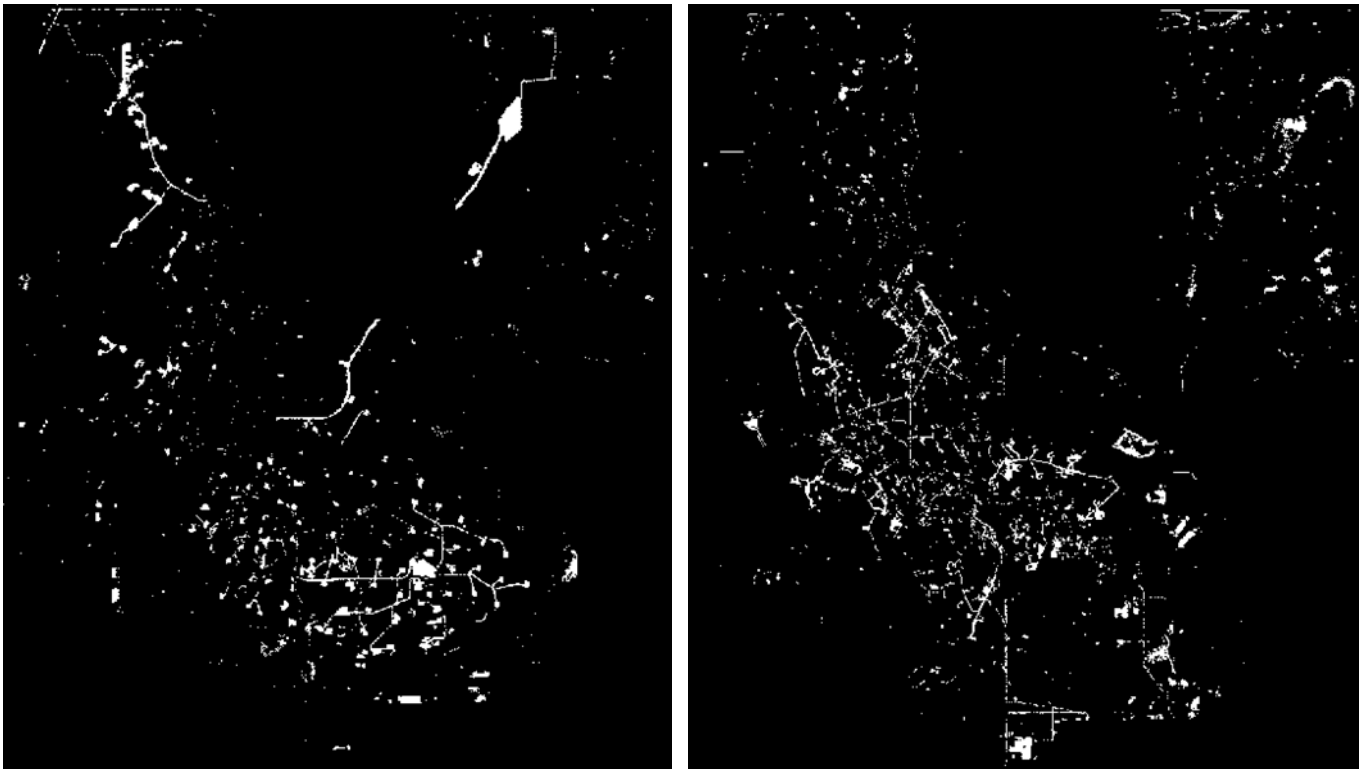


Figure 30. Change detection maps showing the areas that have been cleared (left) or revegetated (right) between 1998 and 2011 in the Cold Lake study site. Changes are indicated in white.

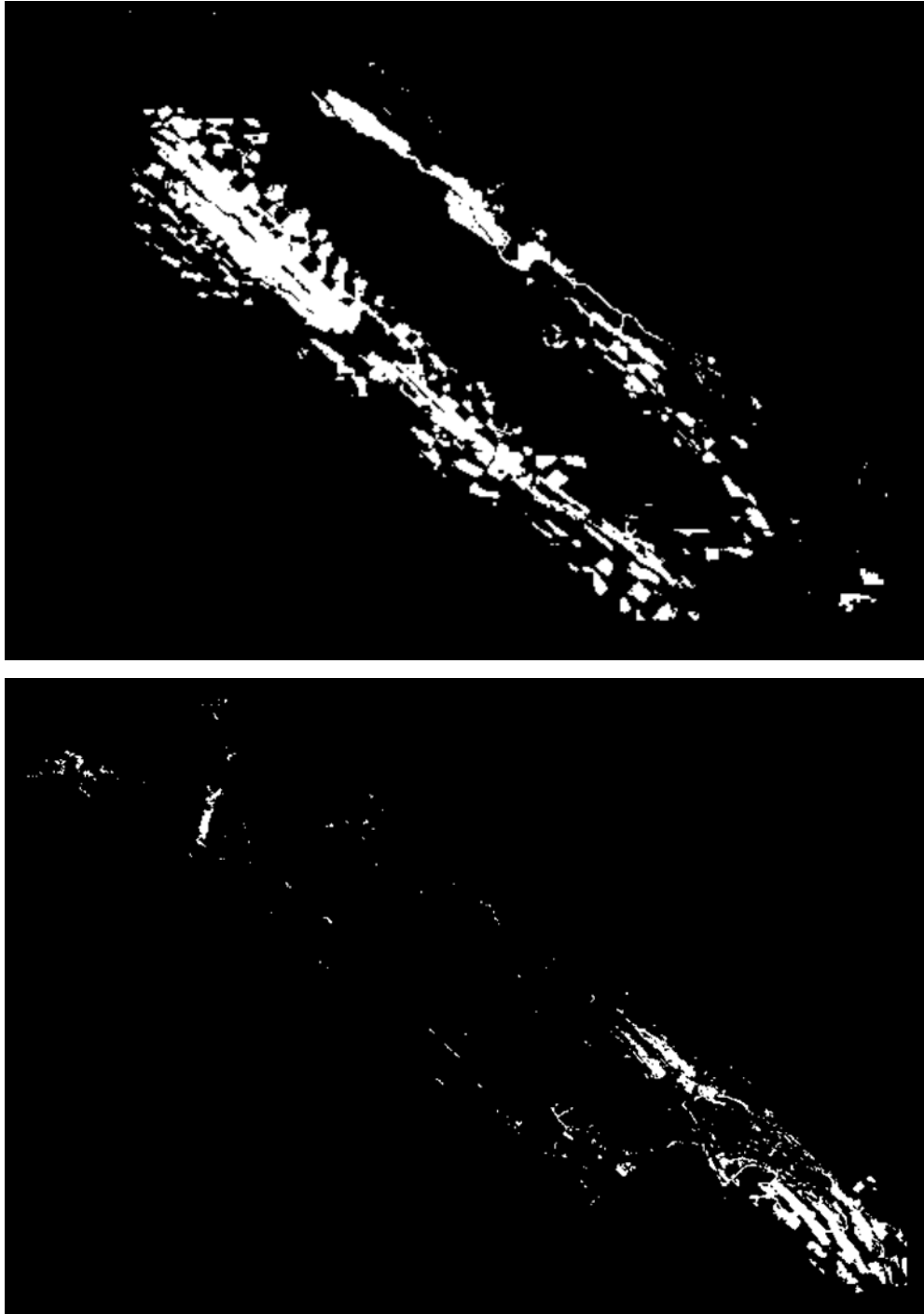


Figure 31. Change detection maps showing the areas in the Coal Valley study site that have been cleared (top) or re-vegetated (bottom) between 2001 and 2009. Changes are indicated in white.

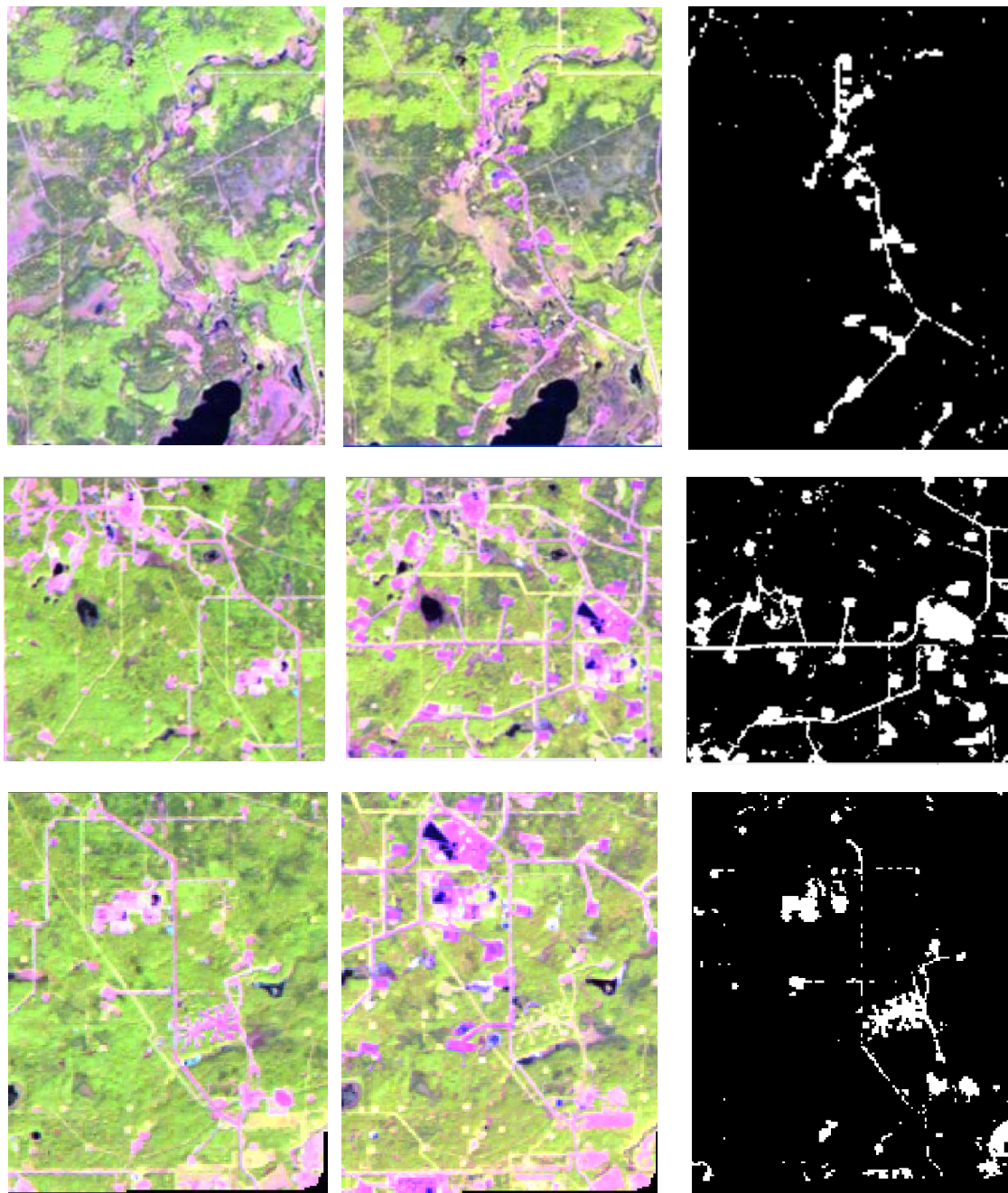


Figure 32. Examples of areas that were cleared or revegetated in the Cold Lake study area after 1998.

Left (1998) and center (2011): subsets of Landsat false colour composite where the SWIR, NIR, and RED bands are displayed in red, green and blue colours, respectively.

Right: change detection map where white colour corresponds to areas where the change has occurred.

Figure 33 illustrates few examples of the change detection results over the Coal Valley study area. A significant increase in cleared area coverage is observed between 2001 and 2009, indicating an increase in the coal mining development. Revegetation was mostly concentrated in the south of the Coal Valley area. However, it seems that some sites in the north of the study area are misclassified as it appears from both images that these areas correspond to mining ponds. This can be corrected by applying a water mask to remove these areas.

The change detection approach was not extended to the Lacombe study area, because major variations in NDVI are strongly affected by the difference in the land use between different years (e.g., non-cultivated versus cultivated fields, seeding of different crop types with different phenological cycles).

#### 4.3 Assessment of Multi-Temporal Satellite Multispectral Imagery for Monitoring Reclamation Trend

Vegetation indices (VI's) are mathematical transformations of surface reflectance acquired at a given number of spectral bands. These indices have been largely used for retrieving information about vegetation condition such as leaf area index, canopy cover and canopy biomass, which can be related to some of the reclamation criteria for assessing vegetation growth and productivity.

A large suite of VI's has been developed and they have shown different performances (e.g., better sensitivity to large canopy biomass, insensitive to canopy background and/or atmospheric correction) due to the type of spectral bands and/or the correction parameters used (Fernandes et al. 2003, Huete 1988, Huete et al. 1997, Jordan 1969, Kauffman and Tanre 1992).

Due to the sensitivity of these indices to canopy biomass, multi-year VI's data were examined to assess the temporal trend of vegetation productivity. A number of VI's were tested including:

1. Normalized Difference Vegetation Index (NDVI; section 4.2) and
2. Atmospherically Resistant Vegetation Index (ARVI) expressed as follows (Kauffman 1992):

$$ARVI = \frac{(R_{NIR} - 2R_{RED} - R_{BLUE})}{(R_{NIR} + 2R_{RED} - R_{BLUE})} , \quad (7)$$

where  $R_{RED}$ ,  $R_{NIR}$  and  $R_{BLUE}$  are surface reflectances acquired in the RED, NIR and BLUE bands, respectively.

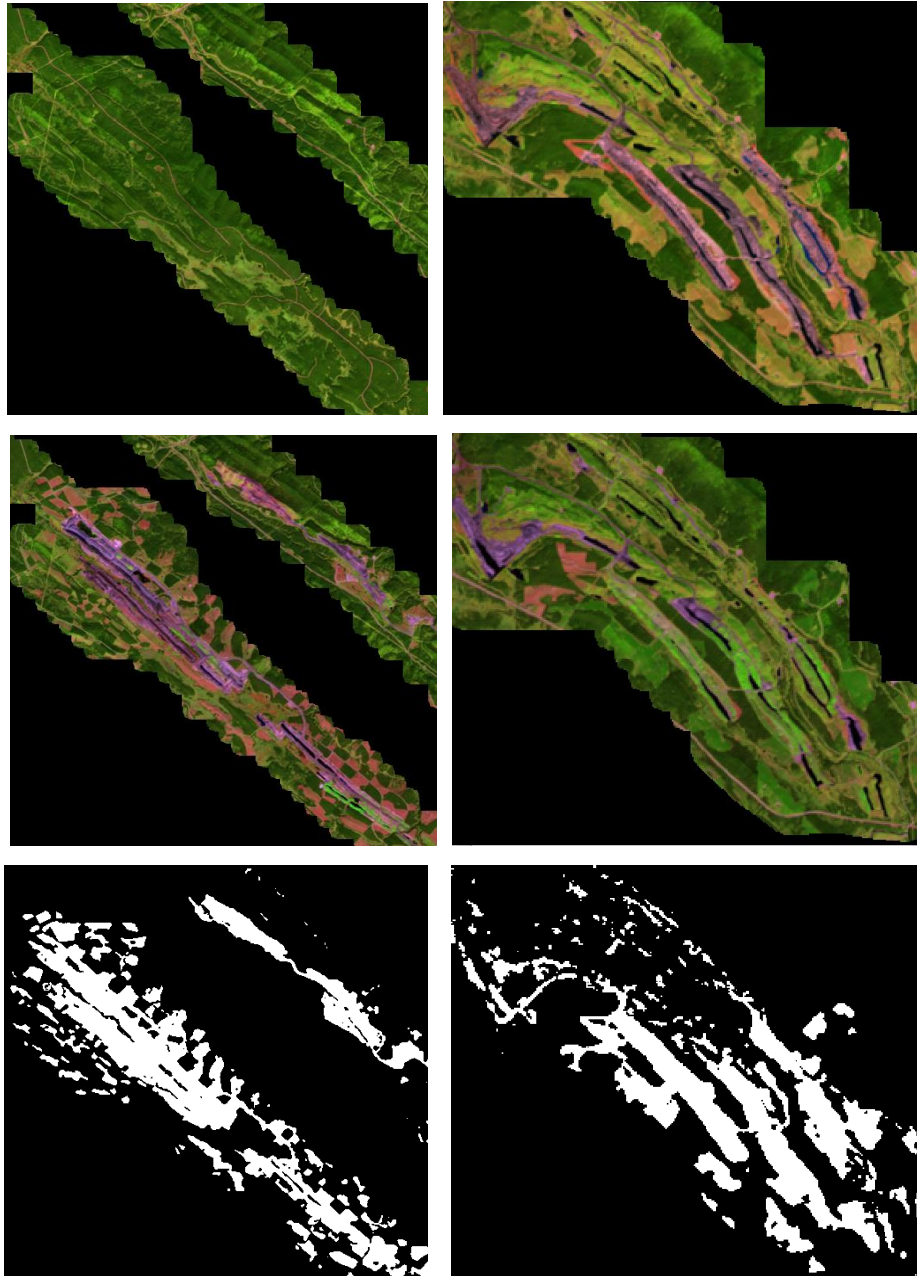


Figure 33. Examples of areas that were cleared or revegetated in the Coal Valley study area between 2001 (top) and 2009 (middle).  
 Top and Middle: subsets of Landsat false-colour composite where the SWIR, NIR, and RED bands are displayed in red, green and blue colours respectively.  
 Bottom: change detection map where the white colour corresponds to areas of change.

3. Simple Ratio (SR) expressed as follows (Jordan 1969):

$$SR = \frac{R_{NIR}}{R_{RED}}, \quad (8)$$

where  $R_{RED}$  and  $R_{NIR}$  are surface reflectances acquired in the RED and NIR bands, respectively.

4. Infrared Simple Ratio (ISR) expressed as following (Fernandes et al. 2003):

$$ISR = \frac{R_{NIR}}{R_{SWIR}}, \quad (9)$$

where  $R_{NIR}$ , and  $R_{SWIR}$  are surface reflectances acquired in the NIR and SWIR bands, respectively.

5. Enhanced Vegetation Index (EVI) expressed as follows (Huete et al. 1994):

$$EVI = 2.5 \frac{(R_{NIR} - R_{RED})}{(R_{NIR} + 6R_{RED} - 7.5R_{BLUE} + 1)}, \quad (10)$$

where  $R_{RED}$ ,  $R_{NIR}$  and  $R_{BLUE}$ , are surface reflectances acquired in the RED, NIR and BLUE bands, respectively.

6. Soil Adjusted Vegetation Index (SAVI) expressed as follows (Huete 1988):

$$SAVI = 1.5 \frac{(R_{NIR} - R_{RED})}{(R_{NIR} + R_{RED} + 0.5)}, \quad (11)$$

where  $R_{RED}$  and  $R_{NIR}$  are surface reflectances acquired in the RED and NIR bands, respectively.

Multi-year VI data were analyzed to determine the vegetation condition within the well and mine sites and its temporal trend in comparison to the adjacent areas. The multi-year assessment was separately performed for each of the Landsat and SPOT datasets available. The series of images selected were acquired between July 30th and August 31st for Cold Lake, August 8th and September 14th for Coal Valley and July 4th and July 29th for Lacombe.

This approach implies two main assumptions as follows:

- Variation in vegetation condition for a given study site did not change significantly during the selected time period, and
- Inter-annual meteorological conditions are similar and do not significantly affect changes in phenology. This would have a small effect on VI multi-year variability.

Image registration was first applied to all the images available over a given study area to minimize any geolocation errors between the images. This will assure that the same pixel is compared over all the images available. The assessment approach adopted is adapted from Alberta Environment and Sustainable Resource Development (2012). The main modification is related to the control area delineation.

Figure 34 illustrates the scheme used in the assessment process. Lease or mine polygons enclosed in the shapefile provided by ESRD were first overlaid on top of the multi-year VI imagery. A buffer area was delineated to exclude pixels located in the transitional area between the well or mine boundaries and the adjacent lands. These pixels are not included in the assessment, because their associated signal could result from the contribution of both on- and off- lease areas. Accordingly, a one-pixel buffer width was considered. A control area was then delineated around the buffer zone using a two-pixel width.

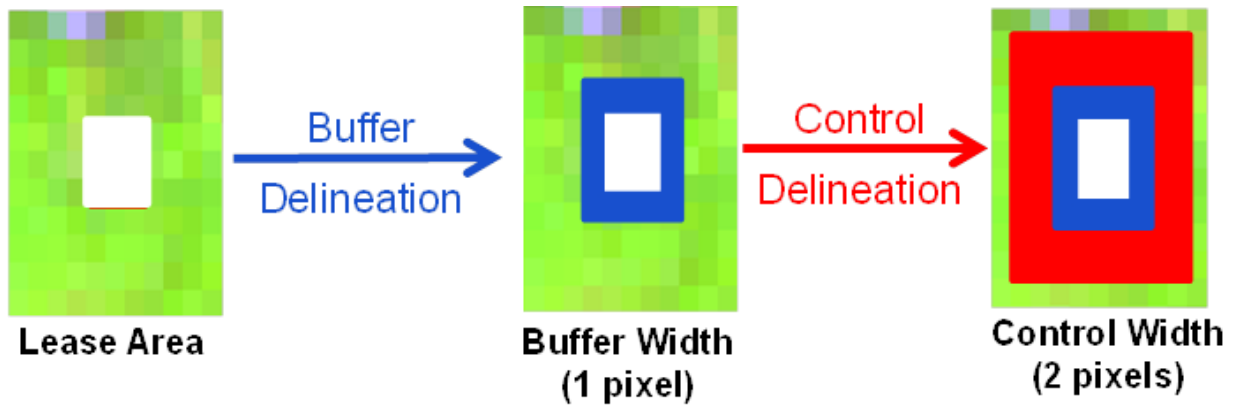


Figure 34. The control area delineation scheme used for lease area assessment.

VI values for each pixel within the lease and control areas were extracted for each of the available years. The data were then organized for each area based on the land-cover types available. The change detection disturbance mask addressed in [section 4.2](#) was used to exclude any pixels previously disturbed from the control area. Statistical parameters including average, standard deviation (STD), minimum and maximum values were computed for each cover type in the lease and control areas. The VI temporal trend for each pixel in the lease area was then compared to the average VI temporal trend in the control area using the same type of land cover. A disagreement flag was defined for each available year when the VI value for a given lease pixel was not within  $\pm 2$  STD from the control average VI. Figure 35 illustrates examples of multi-year VI assessment for three wellsites located in the study area of Cold Lake using NDVI.

The first example illustrates average NDVI for both wellsite and control areas, showing a consistent similarity for the five years selected covering a period from 1998 to 2011. The second example shows that the NDVI average of the wellsite is within the variation range of the control area, except for 2009 where the lease NDVI average is lower than that of the control. Finally,

the third example illustrates similarity between the lease NDVI average and the control except for the last three years where the lease NDVI average is higher, suggesting that the vegetation condition for these years is slightly better than in the reference area.

The effect of the type of VI used on the reclamation assessment results were assessed as shown in Figure 36. In this case, comparing NDVI, ISR and SR for the same wellsite, shows that the assessment results are sensitive to the type of VIs used. ISR shows a slightly different temporal trend in early years. Specifically, NDVI identified three years (1998, 2003, and 2009) where lease and control areas were found in disagreement, while SR isolated only one year (2003), while ISR showed that the disagreement occurred for all the five years considered. These differences require further assessment on the ground to identify, which of these indices better captures the difference in vegetation condition between the lease and control areas.

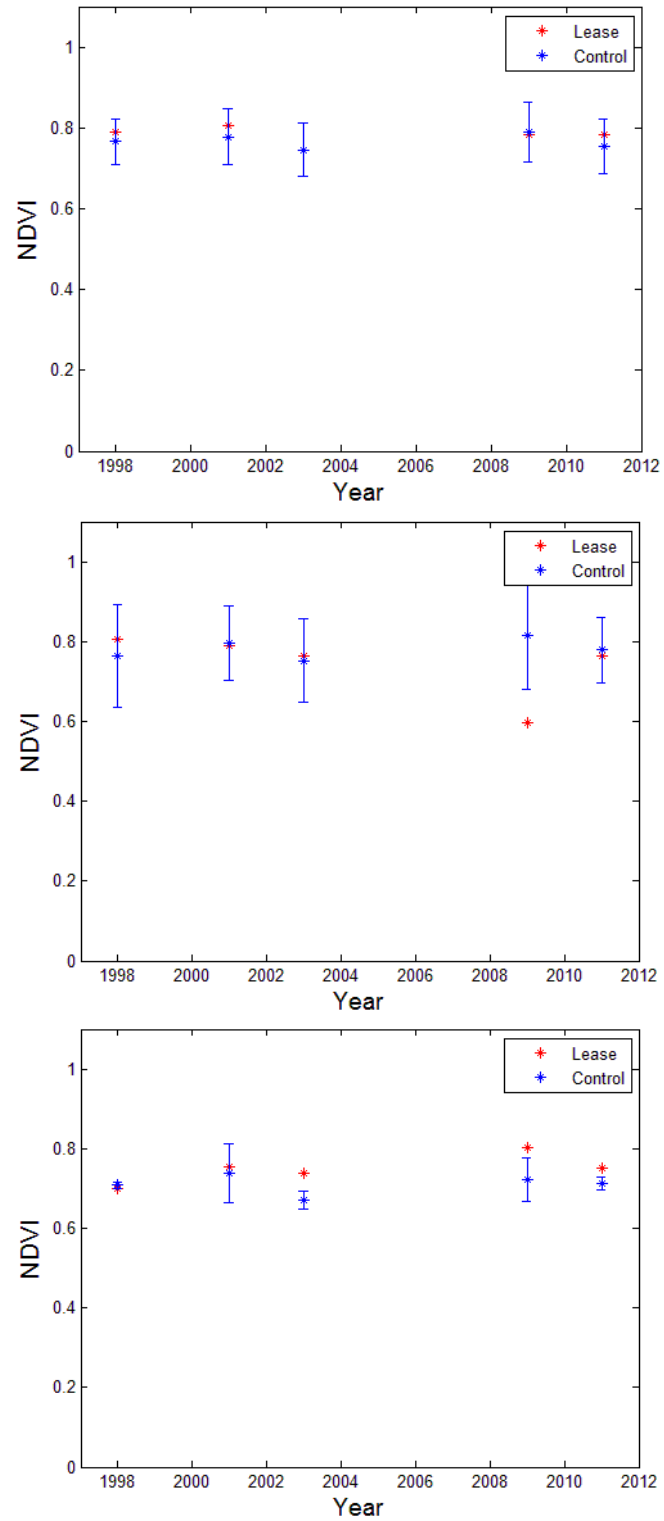


Figure 35. Examples of NDVI temporal trend plots for three different certified wellsites in the Cold Lake study area.

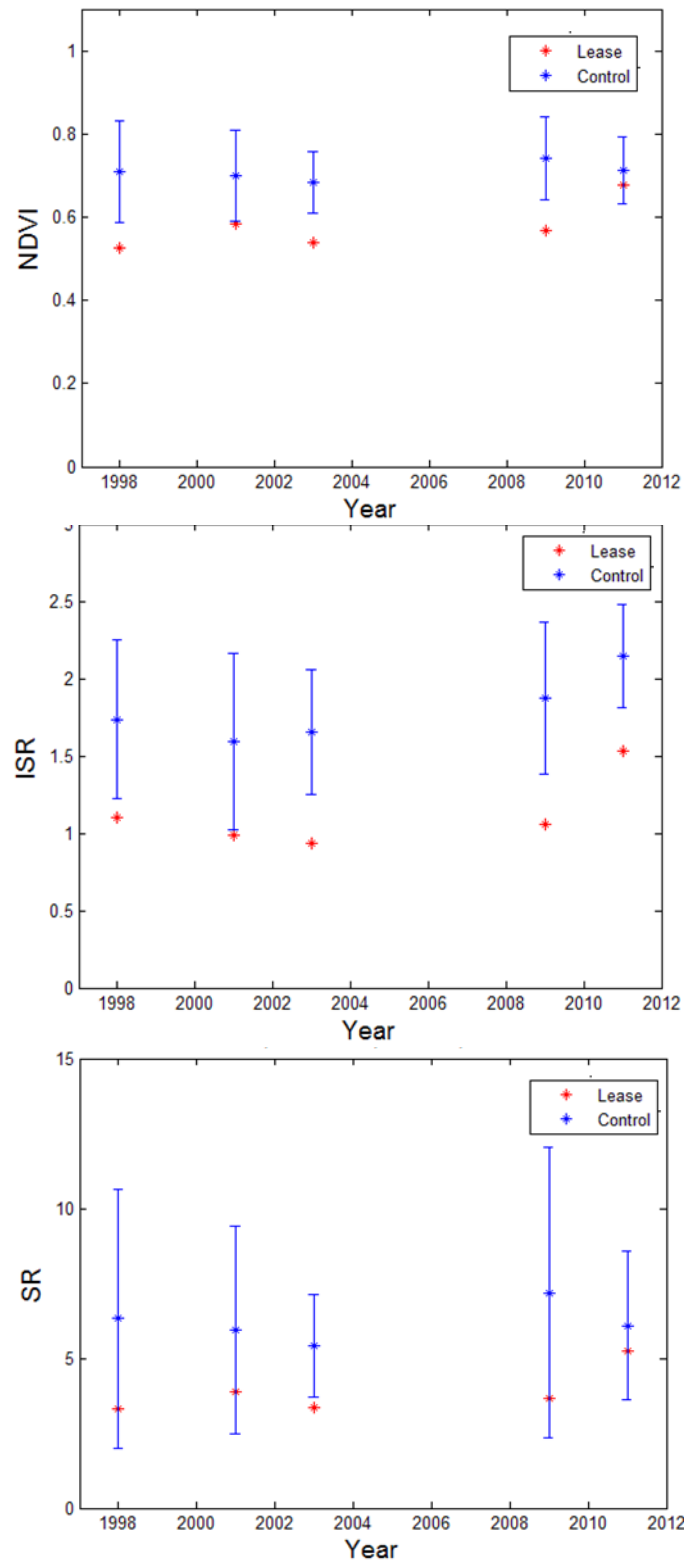


Figure 36. Temporal trend plots for three different VIs including SR, NDVI and ISR for a certified wellsite in the Cold Lake study area.

#### 4.4 Mapping Canopy Structure Using LiDAR

The 2006 LiDAR data acquired over the Coal Valley and Cold Lake study areas and provided by ESRD, as well as the 2012 LiDAR data collected over the Cold Lake study area during the 2012 field campaign, were processed to derive canopy height and canopy fractional cover. The FUSION/LDV software (McGaughey 2014) developed by the United States Department of Agriculture (USDA) was used to process LiDAR data. Point cloud data were filtered to separate canopy returns from ground returns. For each study site, a 10 m digital elevation model was created together with two geospatial maps of canopy height and canopy fractional cover. A 2 m height break was used to derive canopy cover, which is calculated as the proportion of vegetation returns above this height break. Figures 37, 38 and 39 illustrate these products for the Cold Lake and Coal Valley study areas.

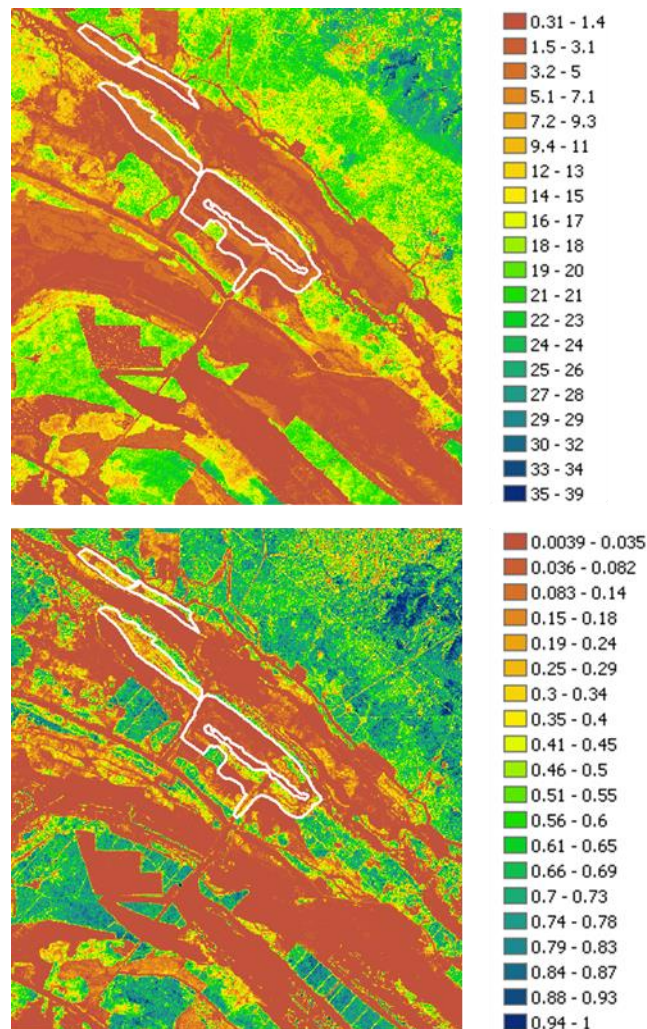


Figure 37. Canopy height (top) and canopy fractional cover (bottom) derived using the ESRD 2006 LiDAR data over the Coal Valley study area.

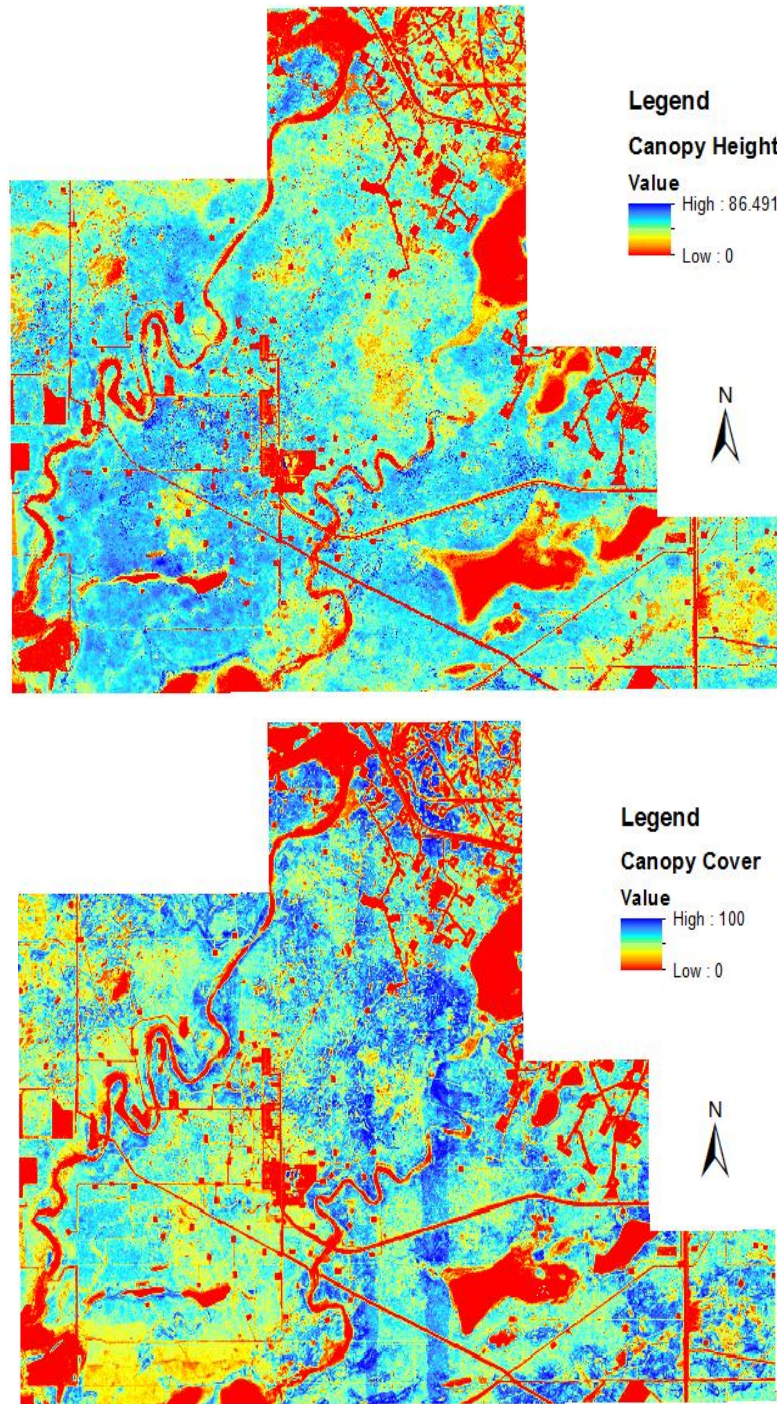


Figure 38. Canopy height (top) and canopy fractional cover (bottom) derived using the ESRD 2006 LiDAR data over the Cold Lake study area.

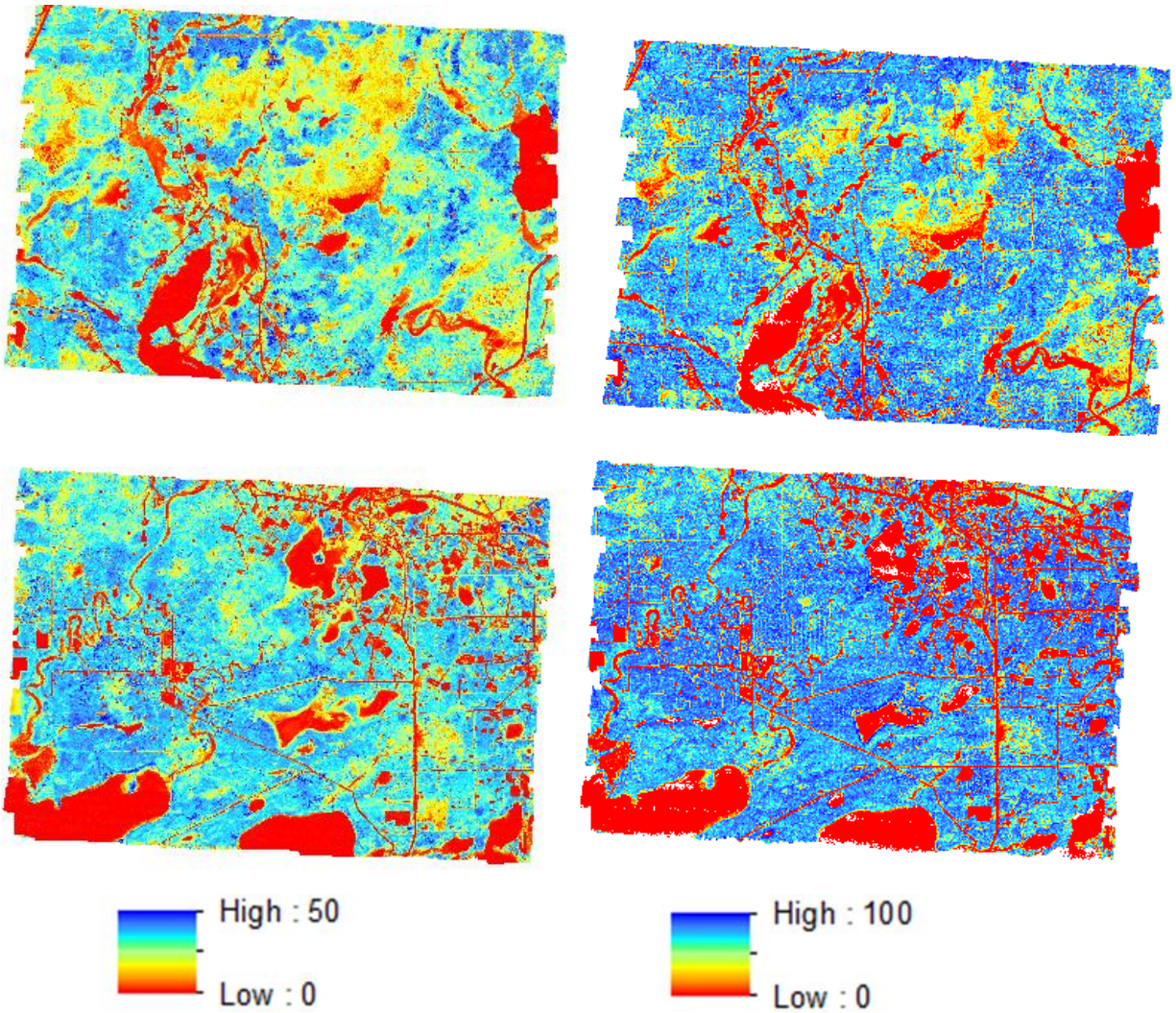


Figure 39. Canopy height (left) and canopy fractional cover (right) derived using the 2012 LiDAR data over the Cold Lake study area.

#### 4.5 Assessment of Canopy Structure within Reclaimed Wellsites in the Cold Lake Study Area Using LiDAR Data

The LiDAR-based canopy height and canopy fractional cover products were used to assess canopy structure within a set of certified wellsites in the Cold Lake study area (Figure 40). The Alberta Vegetation Inventory (AVI) was used to select non-oil and gas disturbance sites to be used as reference for assessing canopy structure in the selected oil and gas wellsites.

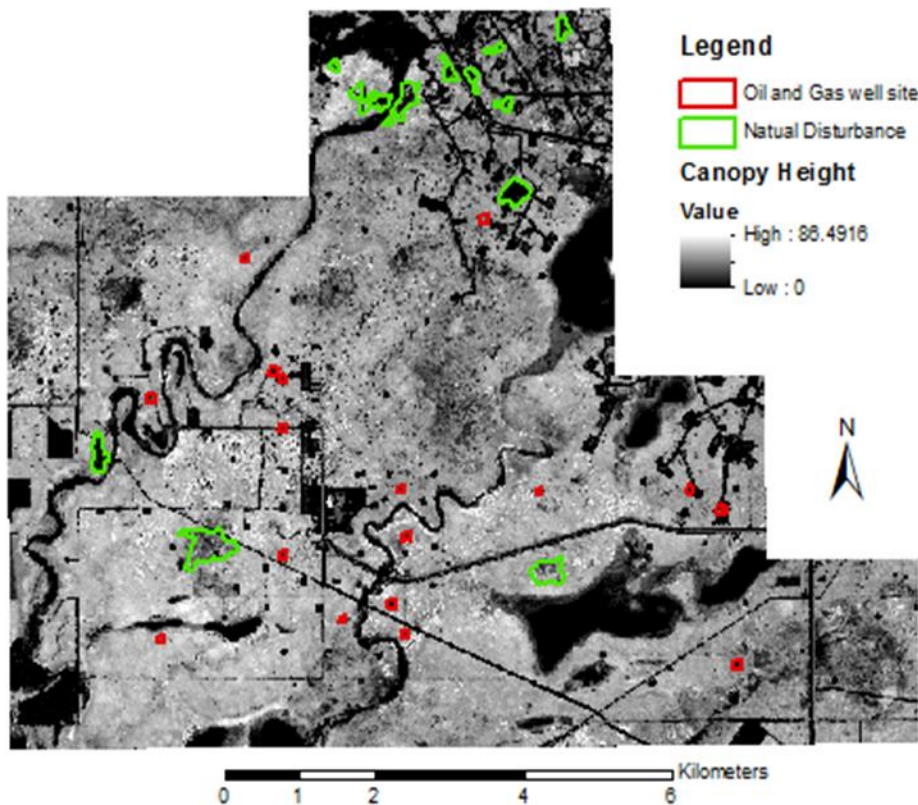


Figure 40. Certified wellsites (red) and non-oil-and-gas related disturbed areas (green) as extracted from the AVI data and overlaid on top of the LiDAR canopy height map.

Table 5 summarizes the certification and disturbance dates for certified wellsites and non-oil-and-gas disturbances, respectively. Due to the absence of this information for some non-oil-and-gas disturbed sites, these were visually inspected using the 1998 Landsat imagery and were found to be similar to adjacent disturbances that have occurred in 1995 and 1997. Therefore, it has been assumed that these sites were most likely disturbed around the same period and 1996 was used as the year of disturbance. This resulted in a set of well/reference pairs to be assessed. The average values of canopy height and canopy cover were first calculated for each of the certified and non-oil-and-gas disturbed sites. The differences in canopy height and cover averages between the certified sites and those areas that were disturbed (e.g., fire, logging) within the six years prior to the certification year of a given wellsite were then calculated as illustrated in Figure 41. Each of the certified wellsites had at least one reference site to be compared to. Differences in canopy height averages between certified and reference sites range between -10 m and + 10 m while differences in canopy cover averages vary from - 45% to about 10%.

Table 5. The certification and disturbance dates for the selected certified wellsites and non-oil-and-gas disturbances.

The dates in blue were assumed after examining 1998 satellite imagery as no information about the disturbance year was available in the AVI data.

Well Site	UWI	Certification_YR
Well1	00/07-28-064-04-4/0	14/10/2008
Well2	00/10-21-064-04-4/0	19/01/2007
Well3	02/10-31-064-04-4/0	23/10/1986
Well4	00/15-28-064-04-4/0	31/12/1985
Well5	00/10-32-064-04-4/0	31/12/1985
Well6	AA/11-25-064-04-4/0	03/09/1992
Well7	00/07-29-064-04-4/0	31/12/1985
Well8	00/10-19-064-04-4/0	31/12/1985
Well9	AA/13-25-064-04-4/0	03/09/1992
Well10	00/13-21-064-04W4/0	07/04/2005
Well11	00/07-32-064-04-4/0	11/09/2006
Well12	00/14-03-065-04-4/0	15/11/1967
Well13	AA/11-05-065-04-4/0	17/05/1999
Well14	00/06-24-064-04-4/0	09/10/2001
Well15	AA/14-21-064-04-4/0	22/03/2011
Well16	00/14-32-064-04-4/0	23/11/2007

Reference Site	Disturbance_YR
REF1	1997
REF2	1997
REF3	2001
REF4	1990
REF5	1995
REF6	0 (1996)
REF7	0 (1996)
REF8	0 (1996)
REF9	0 (1996)
REF10	0 (1996)
REF11	0 (1996)
REF12	0 (1996)
REF13	0 (1996)

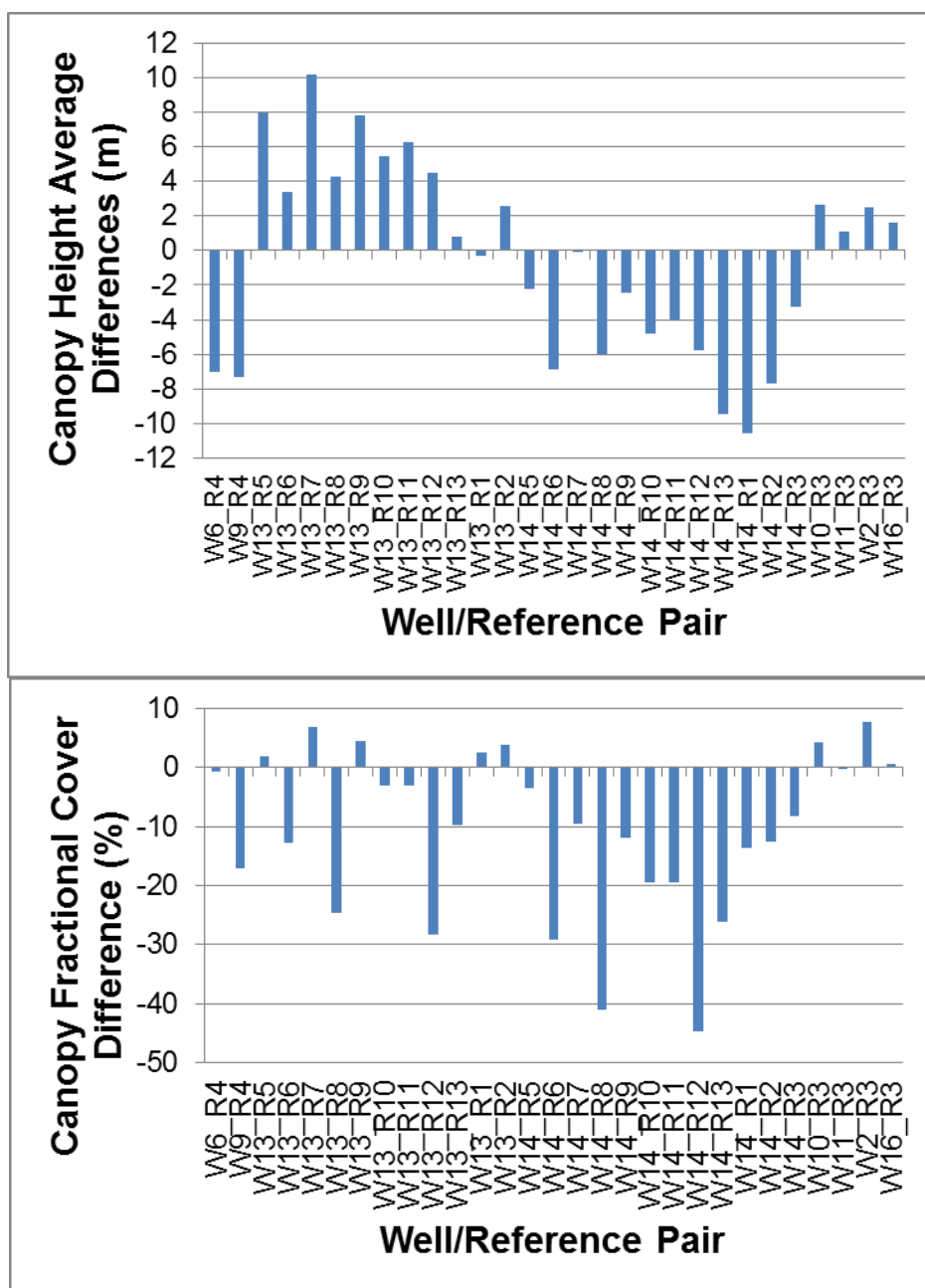


Figure 41. Differences in canopy height (top) and fractional cover (bottom) averages between certified wellsites and non-oil-and-gas disturbed sites.

A Mann-Whitney U statistical test was conducted to determine if there is a significant difference in the canopy height and canopy cover sets of data between certified wells and non-oil-and-gas disturbed areas for each well/reference pair. This test is suitable for non-normally distributed data. A two-tailed test with a 95-% confidence level was performed. Seven certified wellsites (6, 9, 10, 11, 13, 14, and 16) were found to have no significant difference in canopy height, while six sites (2, 9, 10, 11, 13, and 14) had no difference in canopy cover with at least one reference

site. Only five sites (9, 10, 11, 13, and 14) verified the hypothesis of no difference for both canopy cover and canopy height.

#### 4.6 Mapping Tree Species Using Multi-/Hyperspectral and LiDAR Data

Multispectral and hyperspectral data alone and combined with LiDAR data were assessed for mapping species composition. The scope of this assessment was to determine the performance of the sensors selected in the MOPRA project and the benefits from using additional information related to canopy architecture through LiDAR data. Because these data are less available than optical multispectral data, such as SPOT and RapidEye, due to the associated cost, the impact of the LiDAR data acquisition date on the species mapping results was also assessed by comparing LiDAR data acquired within few days to weeks from multispectral data to the ESRD LiDAR data archive acquired in the fall of 2006 (leaf-off). The 2012 LiDAR data were collected in August 2012 (leaf-on), resulting in six years difference between these two LiDAR data acquisitions. The next few sub-sections summarize the approaches adopted.

##### 4.6.1 Assessment of RapidEye and LiDAR Data in the Cold Lake Study Area

The performance of RapidEye alone and in combination with LiDAR data was assessed for mapping tree species in the Cold Lake study area. The following three questions were investigated:

1. Will classification accuracy improve when combining RapidEye with LiDAR data?
2. How sensitive is the classification accuracy to the type of classifier used?
3. How does the LiDAR acquisition date affect the classification accuracy?

Species classification made use of the five RapidEye bands (surface reflectances) in addition to the red-edge NDVI. This index was calculated using the following equation:

$$\text{Rededge NDVI} = \frac{(\rho_{NIR} - \rho_{rededge})}{(\rho_{NIR} + \rho_{rededge})}, \quad (7)$$

where  $\rho_{NIR}$  and  $\rho_{rededge}$  are surface reflectances in the RapidEye NIR and red-edge bands, respectively.

The 2006 LiDAR data provided by ESRD and the 2012 LiDAR data acquired over Cold Lake were processed using the FUSION/LDV software. LiDAR point cloud data were filtered to extract the ground returns and generate a 5 m Digital Elevation Model (DEM) consistent with the RapidEye spatial resolution. The canopy-height model and the percentile heights were derived for all points within a 5 m cell including, 50, 75, 80 and 95 percentiles. Using all LiDAR returns, the percentages of returns above a predefined set of height-break values ranging from 1.4 m to 21.4 m using a 2 m step were calculated within a 5 m cell as follows to stratify the canopy structure profile:

$$\text{Percent\_Returns}_{\text{Height-Break}} = (\text{All Returns above Height-Break} / \text{Total Returns}) * 100. \quad (8)$$

In addition, average intensity, terrain slope and aspect were also derived at 5 m resolution. A hierarchical classification scheme composed of two levels of detail was applied (Table 6). Level-2 classification was only applied to the area classified as forest in Level-1. Five species were classified, including Trembling Aspen, Tamarack, Balsam Poplar, Black Spruce, White Spruce, and Jack Pine.

Table 6. The classification hierarchy used for tree species mapping.

Level-1	Level-2
Grasses	X
Shrubs	X
Water	X
Non-vegetation	X
Forest	Trembling aspen (AW)
	Tamarack (LT)
	Balsam poplar (PB)
	Black spruce (SB)
	White spruce (SW)
	Jack pine (PJ)

Reference samples were selected from the 2012 field data and the Alberta Vegetation Inventory Database (AVI) to be used for training and validation of the classification. A total of 106 samples were selected for level-1, while for Level-2, the samples were selected in AVI polygons where the forest cover is above 50% and the percentage cover of the dominant species is above 80%. The 2012 field data collected within the 48 plots, including tree species, height, and DBH, were also used. Plots, where dominant species have more than 80% volume, were selected as reference sets for the level-2 classification. In total, 169 samples were selected for this classification. A total of 70% of the reference pixels was used as training samples and 30% was saved for validation. The SVM classifier and Random Forest decision tree (RF) classification approaches were assessed using the R-project software<sup>13</sup>. The classified images were then extracted for use in ENVI for a post-classification assessment.

Level-1 classification was produced with an overall accuracy of 97.6% (Figure 42). Good Producer and User accuracies were achieved for the forest class, which were equal to 97.1% and 88.7%, respectively.

---

<sup>13</sup> See <http://www.r-project.org/>

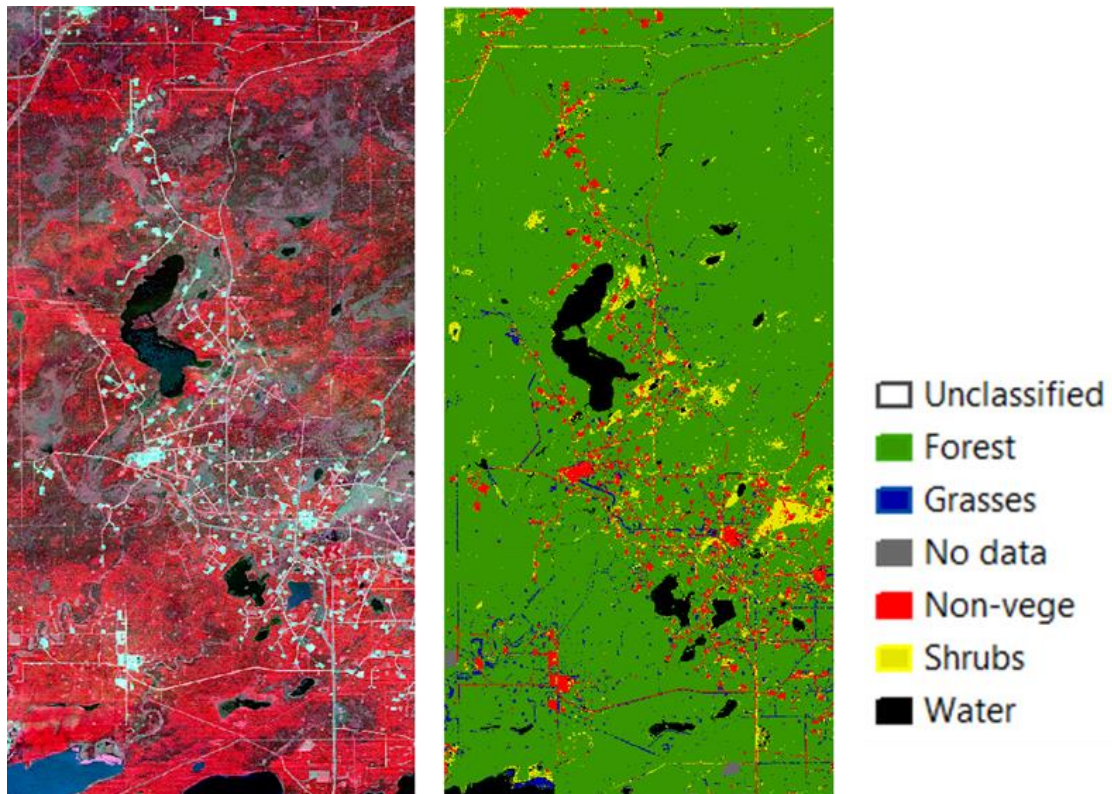


Figure 42. The 2012 RapidEye image acquired over the Cold Lake study area (left) and the corresponding Level-1 classification map (right).

Accuracy assessment of RF tree species classification using RapidEye compared to the 2012 LiDAR/RapidEye is summarized in Table 7. The results show that the overall accuracy was significantly higher when combining LiDAR and RapidEye data (65%) with more than 23% increase compared to RapidEye alone. An increase in both Producer and User accuracies, ranging between 10% and 40%, was observed for all species except Balsam Poplar.

Using the RF classifier, accuracy per species ranged from 54% to ~ 88%, except for Balsam Poplar where it did not exceed 44%. Figure 43 shows the RF tree species classification map.

Table 7. Accuracy assessment of species classification using RF for both RapidEye and 2012 LiDAR/RapidEye data.

Class	2012 RapidEye		2012 LiDAR/RapidEye	
	Prod. Acc.	User. Acc.	Prod. Acc.	User. Acc.
AW	50.00	60.78	88.71	78.57
LT	36.59	43.48	65.85	65.85
PB	39.66	31.94	34.48	44.44
PJ	41.33	31.63	57.33	55.84
SB	53.91	63.92	83.48	73.28
SW	31.25	29.70	54.17	62.65
<b>Overall Accuracy</b>	42.42%		65.57%	

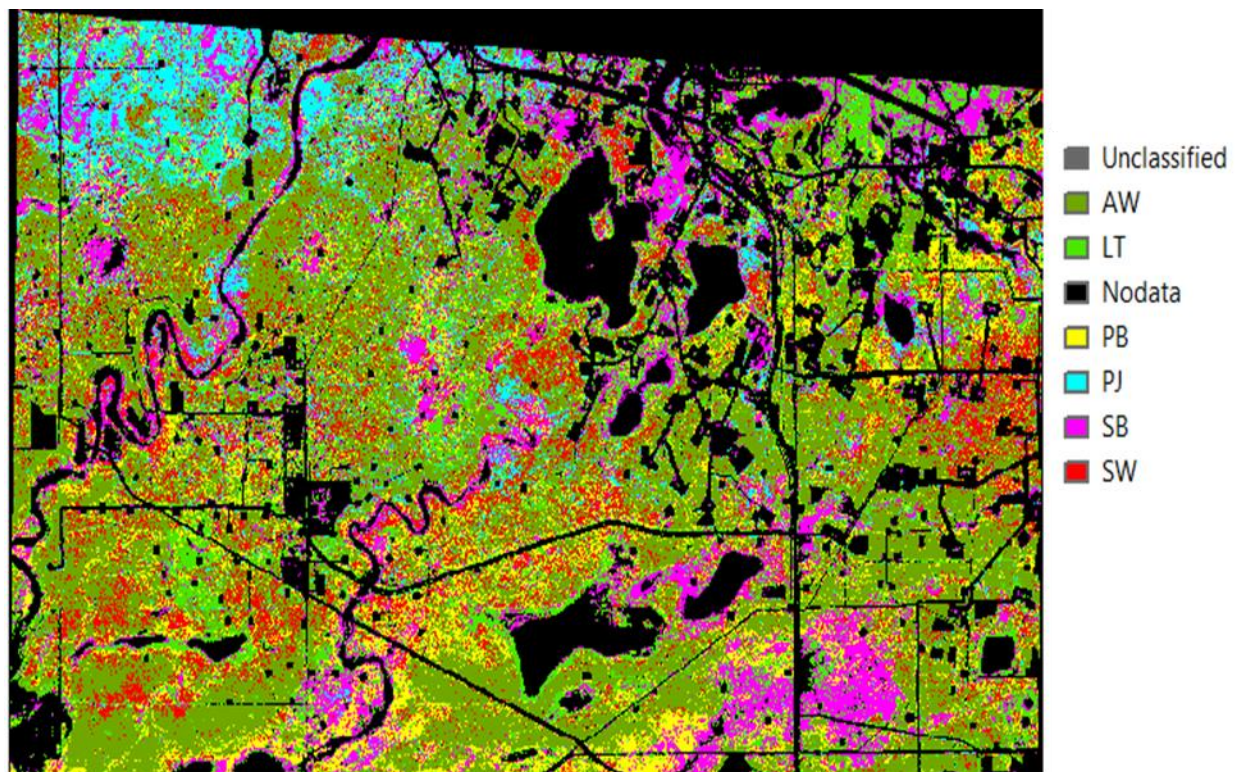


Figure 43. 5 m species map using the RF classifier and the 2012 LiDAR/RapidEye data over the Cold Lake study area.

The accuracy assessment results using the SVM and RF classifiers are summarised in Table 8. The overall classification accuracy is more than 12% higher when using the RF classifier. This increase is also observed per species with an increase of User and Producer accuracies ranging between 7% and 32%, except for tamarack with a 13% decrease in Producer accuracy.

Table 8. Accuracy assessments using 2012 LiDAR/RapidEye data for SVM and RF classifiers.

Class	SVM		RF	
	Prod. Acc. (%)	User Acc. (%)	Prod. Acc. (%)	User Acc. (%)
<b>AW</b>	70.97	75.86	88.71	78.57
<b>LT</b>	78.05	60.38	65.85	65.85
<b>PB</b>	27.59	25.4	34.48	44.44
<b>PJ</b>	45.33	46.58	57.33	55.84
<b>SB</b>	51.30	62.11	83.48	73.28
<b>SW</b>	44.79	46.24	54.17	62.65
<b>Overall Accuracy</b>	53.28%		65.57%	

The species classification map and accuracy assessment results associated with the use of LiDAR data acquired at different dates (2006 and 2012) are illustrated in Figure 44 and Table 9, respectively. The difference in overall accuracy was moderate and did not exceed 3%.

Improvement in Producer and User accuracies was species dependent. An increase between 3% and 12% was observed for Trembling Aspen, Tamarack, Balsam Poplar and Black Spruce with the most significant improvement observed for Balsam Poplar. However, a decrease in Producer and User accuracy was observed for White Spruce (14%) and Jack Pine (5%), respectively.

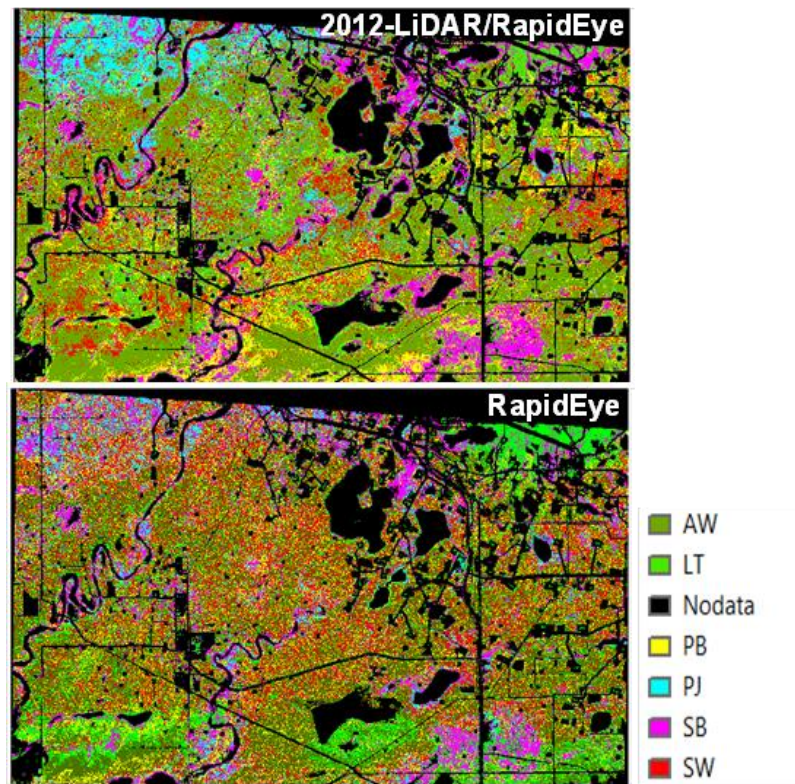


Figure 44. 5 m species maps using RF classifier together with the 2012 LiDAR/ RapidEye (top) and RapidEye (bottom) data.

Table 9. Accuracy assessments using the RF classifier for 2006 and 2012 LiDAR combined with RapidEye imagery.

Class	2006 LiDAR/RapidEye		2012 LiDAR/RapidEye	
	Prod. Acc.	User Acc.	Prod. Acc.	User Acc.
	(%)	(%)	(%)	(%)
AW	85.48	76.81	88.71	78.57
LT	56.10	60.53	65.85	65.85
PB	22.41	41.94	34.48	44.44
PJ	52.00	60.00	57.33	55.84
SB	78.26	67.16	83.48	73.28
SW	68.75	58.41	54.17	62.65
Overall Accuracy	62.91%		65.57%	

Assessing the impact of the type of input data used in the RF classification on the resulting accuracy showed that the most relevant input data for species classification using 2012 LiDAR/RapidEye data are: the NIR and red-edge bands, DEM, terrain slope, red-edgeNDVI, and canopy height.

#### **4.6.2 *Assessment of SPOT-5 and LiDAR Data in the Cold Lake Study Area***

The same approach developed in section 4.6.1 was applied to assess SPOT-5 and 2012 LiDAR data for mapping tree species. Based on the best results obtained in the previous section, the decision tree (RF) approach was adopted for this assessment. The main spectral differences between SPOT-5 and RapidEye are: (1) the absence of the SWIR band and (2) the presence of the blue and red-edge band in the RapidEye data.

The 2012 LiDAR/SPOT-5 species map and the corresponding accuracy assessment results are illustrated in Figure 45 and Table 10, respectively. The 53% overall accuracy is about 13% lower compared to the combined RapidEye and LiDAR overall accuracy (~ 66%). Comparison of per-species-accuracy between SPOT-5/LiDAR and RapidEye/LiDAR data shows a decrease in Producer and User accuracies ranging between 7% and 37% for Trembling Aspen, Tamarack, White Spruce, and Black Spruce. Producer and User accuracies for these species range from 50% to ~ 76%, except for White Spruce which has the lowest accuracies of 18% and 32%, respectively. However, an improvement in per-species accuracy was observed for Jack Pine and Balsam Poplar when using SPOT-5/LiDAR data. Up to a 13% increase in Jack Pine accuracies was observed bringing Producer and User accuracies to 66% and 69%, respectively. About a 6% improvement was observed for the Balsam Poplar, where Producer accuracy increased up to 40%, while the User accuracy decreased to 31%.

These results suggest that an accuracy of 50% or higher can be achieved using SPOT-5/LiDAR data for the following species: Trembling Aspen, Tamarack, White Spruce and Black Spruce. Assessment of the impact of the type of input data used in the RF classification process on the resulting accuracy showed that the most relevant input data for species classification when using SPOT-5/LiDAR data are: the NIR and SWIR bands, DEM, terrain slope, NDVI and percentage of LiDAR returns above 1.4 m.

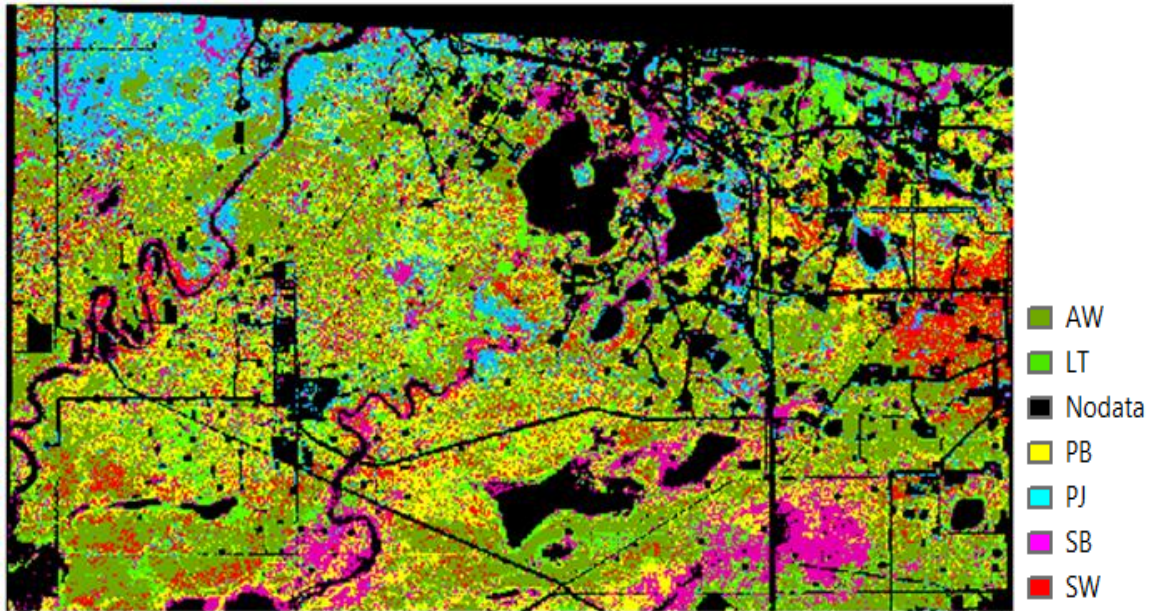


Figure 45. 10 m tree species map of the Cold Lake study area using the RF classifier together with the 2012 LiDAR/SPOT-5 data.

Table 10. Accuracy assessment results using the RF classifier for 2012 LiDAR/SPOT-5.

Class	Random Forest	
	2012 LiDAR/SPOT-5	
	Prod. Acc. (%)	User. Acc. (%)
AW	75.69	66.06
LT	58.93	50.38
PB	40.63	31.14
PJ	66.41	69.11
SB	59.26	65.98
SW	17.86	32.47
Overall Accuracy	52.76%	

#### 4.6.3 Assessment of Hyperspectral CHRIS and LiDAR Data for Mapping Tree Species in the Cold Lake Study Area

Hyperspectral CHRIS and LiDAR data were assessed for mapping tree species in the Cold Lake study area. Hyperspectral data were classified alone and combined with LiDAR data using the SVM technique. As for multispectral data, a classification hierarchy was used for species mapping. The first hierarchy consisted of a land-cover classification to isolate forested from non-forested areas. The six tree species introduced in the previous section (Table 6) were used to further classify the forested areas. Selection of regions of interests (ROI) was made using both the AVI and aerial ortho-photos acquired over the Cold Lake study area. In addition, ground measurements were also used to assist in the region of interest selection. 70% of these regions of interest were used for the SVM classifier training, while the other 30% were utilized for the species map validation. The 34 m CHRIS-based species map is shown in Figure 46.

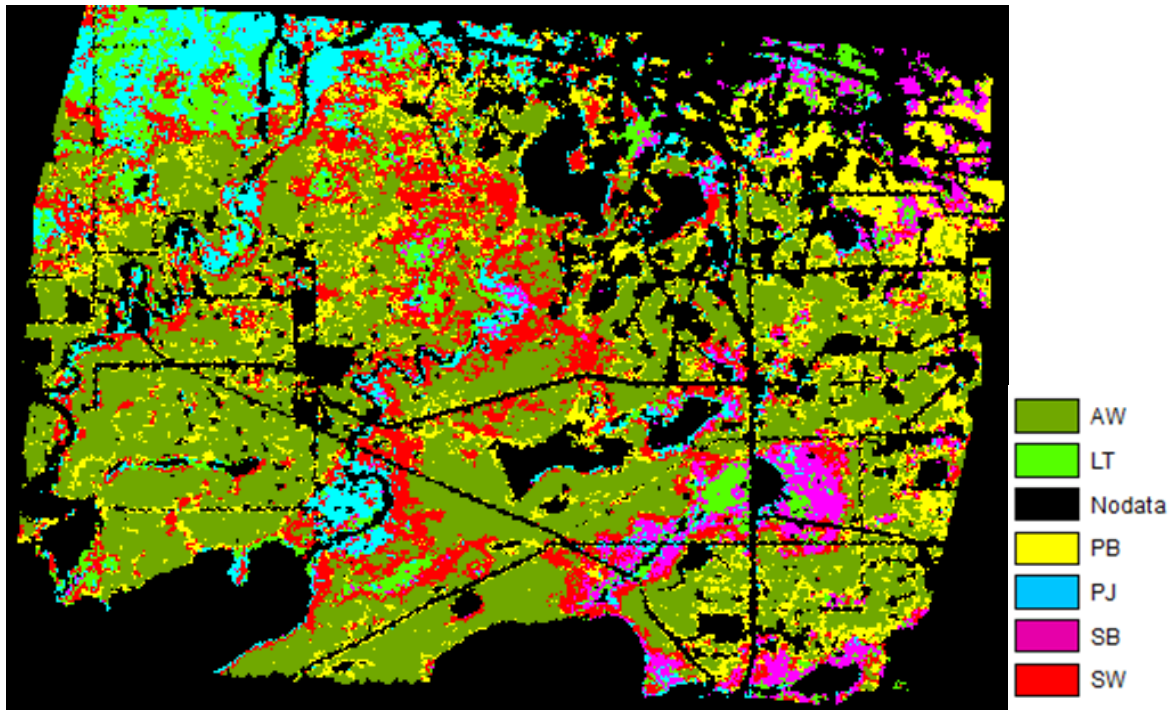


Figure 46. 34 m tree species map of the Cold Lake study area using the CHRIS data and SVM classifier.

The accuracy assessment results (Table 11-Top) showed that CHRIS data can map tree species with an overall accuracy of 79%. Both Producer and User accuracies exceeded 73%, reaching up to 93% per species. The only exception is Black spruce which had a Producer accuracy equal to about 55%. Including LiDAR data in the classification process increased the overall accuracy up to 84% (Table 11-Bottom). Differences in User and Producer accuracies between CHRIS and LiDAR/CHRIS species classification showed a small decrease in this latter of up to 3% for most

of the tree species considered. However, an increase ranging between 1% and 6% was observed for Balsam Poplar, White Spruce, and Black Spruce. This increased the Black Spruce Producer accuracy to ~ 61%.

Table 11. Accuracy assessment results using the SVM classifier for CHRIS (top) and 2012 LiDAR/CHRIS data (bottom).

Class	2012 CHRIS - SVM	
	Prod. Acc. (%)	User. Acc. (%)
<b>AW</b>	96.33	89.74
<b>LT</b>	79.80	80.61
<b>PB</b>	73.00	85.71
<b>PJ</b>	84.54	77.36
<b>SB</b>	54.55	83.72
<b>SW</b>	93.10	76.06
<b>Overall Accuracy</b>	79.18%	

Class	2012 LiDAR/CHRIS - SVM	
	Prod. Acc. (%)	User. Acc. (%)
<b>AW</b>	96.79	89.41
<b>LT</b>	77.78	80.21
<b>PB</b>	71.43	86.67
<b>PJ</b>	82.47	74.07
<b>SB</b>	60.61	83.33
<b>SW</b>	91.38	80.30
<b>Overall Accuracy</b>	83.62%	

#### 4.7 Mapping Leaf Area Index in Cold Lake

A 20 m LAI map was produced for the Cold Lake study area using the 2012 SPOT-5 data (Figure 47). These data were first up-scaled from 10 m to 20 m resolution to match the spatial scale of the field plots where LAI ground measurements were collected. A land-cover classification map was then generated using the up-scaled SPOT-5 image together with the SVM classifier.

Canopy LAI ground measurements collected in 48 test plots were used to develop two LAI empirical models based on SR and ISR indices (Figure 48). Both understory and overstory LAI's were added to derive canopy LAI. The first LAI empirical model was developed for conifer forest using SR, while the second model was generated using the ISR index for the remaining land-cover types, including mixed forest, deciduous forest, and shrubs/herbaceous. The mean absolute errors between LAI-model estimates and ground measurements were equal to 1.4 for both models.

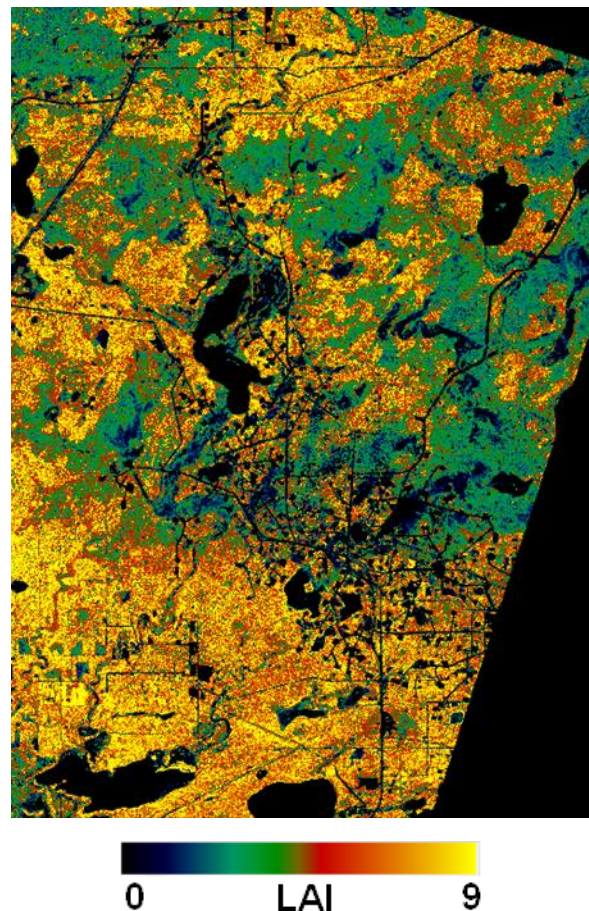


Figure 47. 20 m leaf area index map of the Cold Lake study area produced using LAI-VI empirical models and SPOT-5 data.

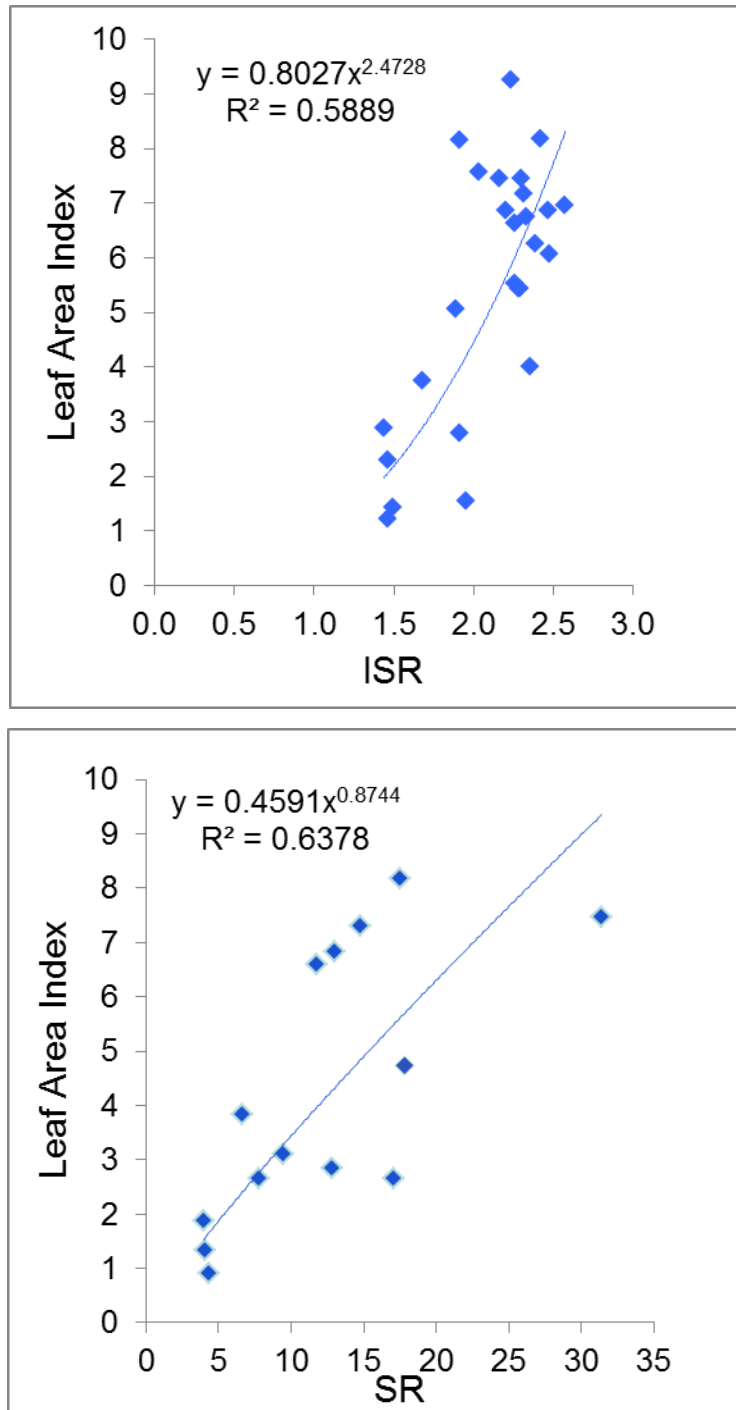


Figure 48. LAI-VI empirical models developed using VIs derived from SPOT-5 data and ground measurements collected in July 2012 at the Cold Lake study area.  
 Bottom: Coniferous forest;  
 Top: Deciduous forest, Mixed Forest, and Herbaceous/shrubs.

## 5 MOPRA MONITORING SYSTEM DEVELOPMENT

The processing chain developed within the MOPRA project was implemented within a monitoring system made of two modules to automate all the tasks required to derive information about land condition in reclaimed sites as well as their associated landscape.

The first module is *the Remote Sensing Data Processing Toolbox* where all the steps required to correct the at-sensor signal, derive the surface reflectance and the land products addressed in [section 4](#) were packaged.

The second module is *the Stand-Alone Assessment Tool* where the multi-year vegetation index assessment approach was implemented.

### 5.1 MOPRA Remote Sensing Data Processing Toolbox

This software was implemented as an ENVI plug-in that is accessible through the ENVI menu system. The toolbox provides the capabilities for processing and characterizing vegetation conditions using LiDAR and optical-passive remote sensing technologies as follows:

1. baseline mapping,
2. change detection, and
3. retrieval of information about vegetation condition in reclaimed areas.

The focus of the system is how to effectively integrate a set of data pre-processing/information extraction tools using existing remote sensing processing techniques (commercial, open source and in-house) to automate the processing chains for mapping and monitoring purposes.

A detailed description of the MOPRA processing toolbox is given in [Appendix 3](#).

### 5.2 MOPRA Stand-Alone Assessment Tool

The approach, adopted for monitoring vegetation condition in reclaimed areas using multi-year VI (section 4.3), was implemented within a software package including two executables, the reclamation assessment and temporal trend tools. This package was developed using the Matlab software<sup>14</sup>. In addition to the information related to land cover and change detection, the reclamation assessment tool can handle additional information if available related to land condition such as tree species, LAI, canopy height and fractional cover. The products provided by these tools are shapefiles where all the information related to land condition in reclaimed and reference areas is compiled in addition to the VI temporal trend plots that illustrate the profile of vegetation condition in reclaimed areas compared to reference sites. These tools have been intensively tested in ESRD and have been improved through the lifetime of this project based on ESRD's feedback. A more detailed description of the MOPRA stand-alone assessment package is provided in [Appendix 4](#).

---

<sup>14</sup> See <http://www.mathworks.com/products/matlab/>

## 6 CONCLUSIONS

This report addresses the work that has been conducted within the MOPRA project. The project provided the opportunity to assess remote sensing technologies including optical multi-/hyperspectral and LiDAR data, for monitoring vegetation condition in reclaimed wellsites and mine areas. The land products derived from remote sensing provide information related to some of the landscape and vegetation assessment parameters adopted within the 2010 reclamation criteria document (Alberta Environment and Sustainable Resource Development, 2013), such as bare areas, vegetation species, land-use change, canopy height, percent canopy cover and vegetation quantity/quality.

The choice of the sensors to be assessed was governed by the size of the features to be monitored as well as the data availability necessary for an operational use. Because wellsite sizes range between one to three hectares, sensors that have a spatial resolution better or equal than 30 m were selected including Landsat (30 m), SPOT (10 to 20 m) and RapidEye (6.5 m). LiDAR data were considered within this project due to the unique information they provide about canopy structure. Although this type of data is often associated with a considerable cost which may limit its use on an operational basis, LiDAR data assessment was motivated by the large LiDAR data archive owned by the Government of Alberta as well as the regular LiDAR acquisitions made by energy companies over their lease areas. In the latter case, these data are mostly used to produce terrain elevation models for landform monitoring and to our knowledge not for canopy monitoring.

Although hyperspectral data are not yet available for operational monitoring, these data were also assessed within this project in preparation for the future hyperspectral missions, such as EnMAP and PRISMA to be launched in 2017 or beyond. Within this context, the hyperspectral CHRIS data were tested over one of the study areas.

The major achievements within this project were as follows:

- Development of land-cover based maps over the Cold Lake, Coal Valley and Lacombe study areas. These 30 m land-cover maps were produced using the oldest Landsat images available within this project. These products provide information about the type of land cover present prior to oil and gas extraction and mining operations. This provides a baseline to which the land cover, established in reclaimed areas, can be compared. Further analysis of this information can be combined with existing and planned lease coverage to assess and forecast the impact of wellsites and mining area development on vegetation loss per land-cover type. The same approach could be applied to assess vegetation recovery per land-cover type in reclaimed areas by using a land-cover map produced at a recent date.
- Development of change detection maps over the Cold Lake and Coal Valley study areas using the oldest and most recent Landsat data available within this project. These 30 m change-detection maps provide information about vegetation loss and vegetation regrowth between these two dates. Application of this approach to all available years will provide information about the rate at which these two processes

take place during a given time period. This will allow a comprehensive assessment of land-use development, which will support decisions related to an integrated resources management system.

- Development of tree species maps over Cold Lake using multispectral SPOT and RapidEye, hyperspectral CHRIS and LiDAR data. Classification accuracies range from moderate to high depending on the type of data used. RapidEye combined with LiDAR data provided more than 55% user accuracy for most of the tree species considered in this work. These results need to be assessed with regards to the type of tree species commonly used in the reclamation process. For example, assuming that Trembling Aspen, Black Spruce and White Spruce are used in revegetation of reclaimed lands, these species were mapped with an accuracy of 63%, 73% and 79%, respectively. CHRIS hyperspectral data provided the best accuracy results exceeding 77% for all the species considered. These results are encouraging in view of the future hyperspectral sensors to be launched in about a three- to four-year time frame, which are expected to perform better in mapping species due to a higher spectral resolution and coverage.
- Development of canopy structural attribute maps, including canopy height and canopy fractional cover, using LiDAR data. This kind of information can be used to assess vegetation structure in reclaimed lands with regards to natural succession occurring elsewhere, such as clear-cuts and burnt areas. An example of this assessment was conducted in the Cold Lake study area to isolate wellsites showing no significant statistical difference in canopy height and fractional cover when compared to clear-cut/burnt areas. In addition, this information could also be used in combination with forest height models to determine if the condition in reclaimed areas converges towards model predictions.
- Development of a leaf area index (LAI) map for the Cold Lake study area. This information can be further analyzed to determine the distribution of LAI in reclaimed areas and determine how it compares to the LAI of clear-cut burnt areas. It can also be used together with land-cover maps to inter-compare various reclaimed areas, which have the same land-cover type to quantify differences in these areas and assess possible causes, such as natural variability or difference in reclamation strategies.
- Development of a multi-year assessment approach for monitoring vegetation productivity in reclaimed areas using adjacent areas as a reference. Comparison of vegetation index (VI) values between reclaimed and reference areas allow to capture differences between these areas at a given point in time as well as discrepancies in their temporal trajectories. A flag, based on a pre-defined criterion, permits to isolate reclaimed areas that are different from reference areas.
- Development of the MOPRA monitoring system including:
  - *The Remote Sensing Data Processing Toolbox* developed as an ENVI plug-in is an integration of the approaches developed in this project to derive land products

in reclaimed and natural lands in an automated mode that minimizes the work load involved in using various software packages, and

- *The Stand-Alone Assessment Tool*, made of two executables, integrates the multi-year VI assessment of reclaimed areas and can be run without any software purchase. The package is user friendly and requires basic training, which will facilitate its use by consultants, industry and regulatory staff.

## **7 KEY REMARKS AND RECOMMENDATIONS**

The achievements of the MOPRA project have highlighted the benefits that remote sensing technologies can provide in support of reclamation monitoring efforts. Having access to a synoptic view of reclaimed lands at the landscape and regional level is of value for assessing land-use cumulative effects and making decisions in line with an integrated resources management system.

While the MOPRA outcomes have shown promise in this direction, there is still a need to test and validate the information extraction approaches adopted as well as the monitoring system developed on various landscapes, such as wetlands, rangelands, agriculture and forested areas. Although this project has focused on reclaimed wellsites and reclaimed areas within coal mines, the work undertaken can be applicable to natural areas as well as reclaimed lands that have been disturbed due to other sources of activities, such as transportation corridors, wind energy, sand and gravel operations, oil sands mines as well as pipelines.

To move towards an integration of remote sensing technologies as an operational monitoring tool, the MOPRA monitoring system would require further testing involving consultants, industry (e.g., oil and gas, coal mine, wind energy farms), and monitoring organizations (Alberta Environmental Monitoring, Evaluation and Reporting Agency – AEMERA) and regulatory agencies (e.g., Alberta Energy Regulator, ESRD). This will allow assessing the remote-sensing-based information related to reclamation and disturbance condition using expertise on the ground. Therefore, this assessment will determine the value of remote sensing-based information and define how it can be integrated within the current reclamation monitoring strategies.

Integration of the MOPRA monitoring system could be envisaged on one hand to augment reclamation assessment by using multi-temporal data when regular field visits are required to aid in prioritizing resources (i.e., staff time, remote access), and on the other hand to gather information about reclaimed areas where access is difficult due to terrain ruggedness. Moreover, the MOPRA monitoring system could be of significant value for post-certification monitoring to ensure that reclamation success is being met and provide an increased level of assurance to Albertans. The monitoring system could also be applied to assess different reclamation strategies, which would provide insights for future strategies and policy decisions (e.g., criteria).

Integration of the MOPRA monitoring system within reclamation assessment activities would also require an easy and consistent access to the system, which would be a prerequisite for an extensive usage by the reclamation monitoring community. Within this context, it is

recommended that the system would be incorporated within a web-based monitoring system, where the user can submit a request for a specific area through a dedicated website and receive the associated results through ftp.

Finally, it would be beneficial to extend the capabilities of the current MOPRA monitoring system to take advantage of other research outcomes related areas such as agriculture or rangelands. Some of the aspects that could be investigated would be invasive species infestations as well as stress monitoring.

## **8 REFERENCES**

Alberta Environment and Sustainable Resource Development, 2012. Monitoring procedures for site reclamation in Alberta, temporal monitoring of reclamation success using satellite remote sensing. Alberta Environment and Sustainable Resource Development, Edmonton, Alberta. 51 pp.

Alberta Environment and Sustainable Resource Development, 2013. 2010 Reclamation Criteria for Wellsites and Associated Facilities for Forested Lands. Alberta Environment and Sustainable Resource Development, Edmonton, Alberta. 81 pages.  
<http://www.environment.gov.ab.ca/info/library/8364.pdf> [Last accessed May 9, 2014].

Berk, A., G.P. Anderson, L.S. Bernstein, P.K. Acharya, H. Dothe, M.W. Matthew, S.M. Adler-Golden, J.H. Chetwynd, S.C. Richtsmeier, B. Pukall, C.L. Allred, L.S. Jeong and M.L. Hoke, 1999. MODTRAN4 Radiative Transfer Modeling for Atmospheric Correction. IN: Proceedings of SPIE Optical Spectroscopic Techniques and Instrumentation for Atmospheric and Space Research III, 19-21 July 1999, Vol. 3756.

Chen, J.M., A. Govind, O. Sonnentag, Y.Q. Zhang, A. Barr and B. Amiro, 2006. Leaf area index measurements at Fluxnet-Canada forest sites. *Agricultural and Forest Meteorology* 140(1-4): 257-268.

CNFI, 2004. Canada National Forest Inventory, Ground Sampling Guidelines. 97 pages.  
[https://nfi.nfis.org/documentation/ground\\_plot/Gp\\_guidelines\\_v4.1.pdf](https://nfi.nfis.org/documentation/ground_plot/Gp_guidelines_v4.1.pdf).

Fernandes, R., C. Butson, S. Leblanc and R. Latifovic, 2003. A Landsat TM/ETM+ based accuracy assessment of leaf area index products for Canada derived from SPOT4/VGT data. *Canadian Journal of Remote Sensing* 29(2): 241-258.

Huete, A.R., 1988. A soil-adjusted vegetation index (SAVI). *Remote sensing of Environment* 25: 295-309.

Huete, A.R., H.Q. Liu, K. Batchily and W. van Leeuwen, 1997. A comparison of vegetation indices over a global set of TM images for EOS-MODIS. *Remote Sensing of Environment* 59: 440-451.

Jordan, C.F., 1969. Derivation of leaf-area index from quality of light on the forest floor. *Ecology* 50: 663-666.

Kaufman, Y.J. and D. Tanre, 1992. Atmospherically resistant vegetation index (ARVI) for EOS-MODIS. *IEEE Transaction in Geoscience Remote Sensing* 30: 261-270.

McGaughey, R.J., 2014. FUSION/LDV: Software for LiDAR data analysis and visualization. Version 2.80. Pacific Northwest Research Station, US Forest Service, Portland, Oregon.

Miao, Z. and C. Li, 2007. Biomass estimates for major boreal forest species in west-central Canada. Natural Resources Canada, Canadian Forest Service, Canadian Wood Fibre Centre, Edmonton, Alberta. Information Report FI-X-002. 37 pp.  
[http://nofc.cfs.nrcan.gc.ca/bookstore\\_pdfs/28300.pdf](http://nofc.cfs.nrcan.gc.ca/bookstore_pdfs/28300.pdf)

Penner, M., K. Power, C. Muir, R. Tellier and Y. Wang, 1997. Canada's forest biomass resources: Deriving estimates from Canada's forest inventory. Natural Resources Canada, Canadian Forest Service, Pacific Forest Centre, Victoria, British Columbia. Information Report BC-X-370. 33 pp. <http://www.cfs.nrcan.gc.ca/pubwarehouse/pdfs/4775.pdf>

Rouse, J.W., R.H. Haas, J.A. Schell and D.W. Deering, 1974. Monitoring vegetation systems in the Great Plains with ERTS. IN: Freden, S.C., E.P. Mercanti and M. Becker (Editors). Third Earth Resources Technology Satellite-1 Symposium. Volume I: Technical Presentations. NASA SP-351, NASA, Washington, D.C. pp. 309-317.

Singh, T., 1982. Biomass equations for ten major tree species of the prairie provinces. Natural Resources Canada, Canadian Forest Service, Northern Forest Research Centre, Edmonton, Alberta. Information Report NOR-X-242.

VALERI, 2014. Validation of Land European Remote Sensing Instruments.  
<http://w3.avignon.inra.fr/valeri/> [Last accessed May 9, 2014].

Weiss, M. and F. Baret, 2010. CAN-EYE V6.1 User Manual. EMMAH laboratory (Mediterranean environment and agro-hydro system modelisation). French National Institute of Agricultural Research (INRA).

## **9 GLOSSARY**

### **9.1 Terms**

#### **Atmospheric Correction**

Process of correcting the at-sensor radiance data to remove the atmosphere contribution to the signal and derive the surface reflectance.

#### **Classifier**

A technique based on pattern recognition principles used in remote sensing to classify the image data into a number of categorical classes (e.g., land-cover, land-use, species ...).

#### **Geomatics**

The branch of science which addresses the collection, analysis, and interpretation of spatial data relating to the earth's surface.

### **Geometric Correction/Geo-rectification/Ortho-rectification**

Image data acquired by airborne and spaceborne sensors containing geometric errors due to the Earth's curvature and terrain relief. These errors can be corrected by matching coordinates of physical features in the image to the geographic coordinates of these features in an existing map or collected using global positioning system (GPS).

### **Hyperspectral Image**

A remote sensing image acquired in narrow contiguous (using a large number) bands (> 20) across the electromagnetic spectrum.

### **Image Pixel**

The smallest unit in a remote sensing image.

### **Image Registration**

The process of matching two different remote sensing images pixel by pixel.

### **Laser Return**

A portion of the laser light energy which is sent back towards the LiDAR system after having an interaction with a given target (e.g., top of tree, ground).

### **Multispectral Image**

A remote sensing image acquired in a small number of spectral bands ranging between 3 and 20.

### **Point Cloud Data**

A set of data points defined by X, Y, and Z coordinates, which correspond to the locations where laser pulses emitted by a LiDAR system had an interaction with an object.

### **Pre-processing**

A series of processes which consist of applying radiometric, atmospheric and geometric correction to remote sensing data to improve data quality and extract information with higher accuracy.

### **Producer Accuracy**

The probability that a given land-cover class on the ground was correctly represented in the classification map.

### **Radiometric Correction**

Process of correcting for radiometric errors (e.g., noise) caused by failure or mis-calibration of the sensor, as well as atmospheric and topographic effects, which affect the actual brightness value of the imaged surface.

### **Red-edge Region**

A spectral region between 680 nm and 730 nm where a rapid change in vegetation [reflectance](#) is observed.

## **Spatial Resolution**

The size of the smallest possible feature that can be detected in a remotely sensed imagery.

## **Spectral Band**

A spectral range defined by the spectral response function, where a remote sensor acquires data.

## **User Accuracy**

The probability that pixels for a given class of the land-cover map have been correctly classified.

## **9.2 Acronyms**

AISA	Airborne Imaging Hyperspectral Systems
ARVI	Atmospherically Resistant Vegetation Index
ATIC	Alberta Terrestrial Imaging Centre
ATCOR3	Atmospheric and Topographic Correction
AVI	Alberta Vegetation Inventory
CCRS	Canada Centre for Remote Sensing
CHRIS	Compact High Resolution Imaging Spectrometer
DBH	Diameter at Breast Height (trees)
DEM	Digital Elevation Model
ELC	Equivalent Land Capability
ENVI	ENvironment for Visualizing Images
ESA	European Space Agency
ESRD	Alberta Environment and Sustainable Resource Development
ETM	Enhanced Transverse Mercator
EVI	Enhanced Vegetation Index
FLAASH	Fast Line-of-sight Atmospheric Analysis of Spectral Hypercubes
GPS	Global Positioning System
HRV	High Resolution Visible
HRVIR	High Resolution Visible Infra-Red
ISR	Infrared Simple Ratio
LAI	Leaf Area Index
LiDAR	Light Detection and Ranging

MOPRA	Monitoring Procedures for Reclamation in Alberta
NDVI	Normalized Difference Vegetation Index
NFI	National Forest Inventory
NIR	Near-Infrared
OSRIN	Oil Sands Research and Information Network
PAI	Plant Area Index
RF	Random Forest
ROI	Region of Interest
RS	Remote Sensing
SAVI	Soil Adjusted Vegetation Index
SEE	School of Energy and the Environment
SPEAR	Spectral Processing Exploitation and Analysis Resource
SPOT	Satellite Pour l'Observation de la Terre
SR	Simple Ratio
SRI	Simple Ratio Index
STD	Standard Deviation
SVM	Support Vector Machine
SWIR	Short-Wave-Infrared
TM	Transverse Mercator
USDA	US Department of Agriculture
VALERI	Validation of Land European Remote Sensing Instruments
VI	Vegetation Index
VIS	Visible
VNIR	Visible and Near-InfraRed

## APPENDIX 1: Examples of Spatial High-Resolution Sensors Characteristics and Data Costs

Sensor Name	Swath (km)	Spatial Resolution (m)	No. of Bands	Cost	Comment	Cost estimate 60 km x 60 km
Landsat Thematic Mapper (TM)	185	30 (ms <sup>1</sup> )	6 (ms)	No Cost	public (180 km x 180 km)	0
Enhanced TM+	185	30 (ms) 15 (pan <sup>2</sup> )	6 (ms) 1 (pan)	No Cost	public (180 km x 180 km)	0
SPOT HRV	117	20 (ms)	3 (ms)	\$800 Arch. <sup>3</sup> \$1200 New	(60 km x 60 km)	800 (Arch.) 1,200 (New)
		10 (pan)	1 (pan)	\$800 Arch. \$1200 New		800 (Arch.) 1,200 (New)
SPOT HRVIR	117	20 (ms),	4 (ms)	\$800 Arch. \$1200 New	(60 km x 60 km)	800 (Arch.) 1,200 (New)
		10 (pan)	1 (pan)	\$800 Arch. \$1200 New		800 (Arch.) 1,200 (New)
SPOT HRG	60-80	10 (ms),	4 (ms)	\$1.80 - \$4.00 / km <sup>2</sup>	Prices vary based on area coverage	7,200
		2.5, 5 (pan)	1 (pan)	\$1.80 - \$6.00 / km <sup>2</sup>		10800 (pan – 2.5 metre)
IRS LISS	145	25 (ms)	4 (ms)	2400.00 Euro	(140 km x 140 km )	2,057
				1500.00 Euro	(70 km x 70 km)	
Quick Bird	16.5	2.4-2.8 (ms)	4 (ms)	\$14.00 / km <sup>2</sup> Arch. (US\$)	Min. order cost: \$1800	48,329 (Arch.) 69,040 (New)
		0.6-0.7 (pan)	1 (pan)	\$20.00 / km <sup>2</sup> New (US\$)	Min. order size: 25 km <sup>2</sup>	48,329 (Arch.) 69,040 (New)
IKONOS	11.3	3.2-4 (ms)	4 (ms)	\$10.00 / km <sup>2</sup> Arch. (US\$)	Min. order size (New): 100 km <sup>2</sup>	34,520 (Arch.) 69,040 (New)
		0.8-1 (pan)	1 (pan)	\$20.00 / km <sup>2</sup> New (US\$)	Min. order size (Arch.): 49 km <sup>2</sup>	45,20 (Arch.) 69,040 (New)
Worldview 2	16.4	1.8-2.4 (ms)	7 (ms)	\$14.00 / km <sup>2</sup> Arch. (US\$)	Min. order cost: \$1800	48,329 (Arch.) 69,040 (New)
		0.46-0.52 (pan)	1 (pan)	\$20.00 / km <sup>2</sup> New (US\$)	Min. order size: 25 km <sup>2</sup>	48,329 (Arch.) 69,040 (New)
Geoeye 1	15.2	1.65 (ms)	4 (ms)	\$12.50 / km <sup>2</sup> Arch. (US\$)	Min. order size (New): 100 km <sup>2</sup>	43,150 (Arch.) 89,6301 (New)
		0.41 (pan)	1 (pan)	\$25.00 / km <sup>2</sup> New (US\$)	Min. order size (Arch.): 49 km <sup>2</sup>	43,150 (Arch.) 89,6301 (New)
Formosat 2	24	8 (ms)	4 (ms)	\$3680.00 Arch.	(24 km x 24 km)	11,040 (Arch.)
		2 (pan)	1 (pan)	\$5180.00 New		15,540 (new)
RapidEye	77	5 (ms)	5 (ms)	0.95 Euro / km <sup>2</sup>	Discounts / over 5000 Euro Min. order: 1000 km <sup>2</sup>	4,689
ASTER	60	15 (VNIR <sup>4</sup> )	9 (ms)	No Cost	public	0
		30 (SWIR <sup>5</sup> )				

All costs are C\$ unless otherwise specified

<sup>1</sup>ms = multispectral

<sup>2</sup>pan = panchromatic

<sup>3</sup>Arch. = Archived

<sup>4</sup>VNIR = Visible Near-Infra-Red

<sup>5</sup>SWIR = Short-Wave Infra-Red

## APPENDIX 2: MOPRA Field Plan – Cold Lake Study Area

### 1. Introduction

This document summarizes the field plan undertaken in the Cold Lake area in late July 2012. As part of the MOPRA project, a number of oil and gas well sites in this area were characterized on the ground. The objective is to acquire ground measurements to describe the vegetation and its condition on well sites as well as the adjacent areas. Two study sites were visited during this campaign. The “ColdLake\_FW” is located north west of Cold Lake and mostly dominated by forests and wetlands while the “ColdLake\_AG”, located south west of Cold Lake, is dominated by cultivated areas. Figure 1 illustrates these study sites. The polygons correspond to the areas that had an airborne hyperspectral/LiDAR data acquisition over the summer.

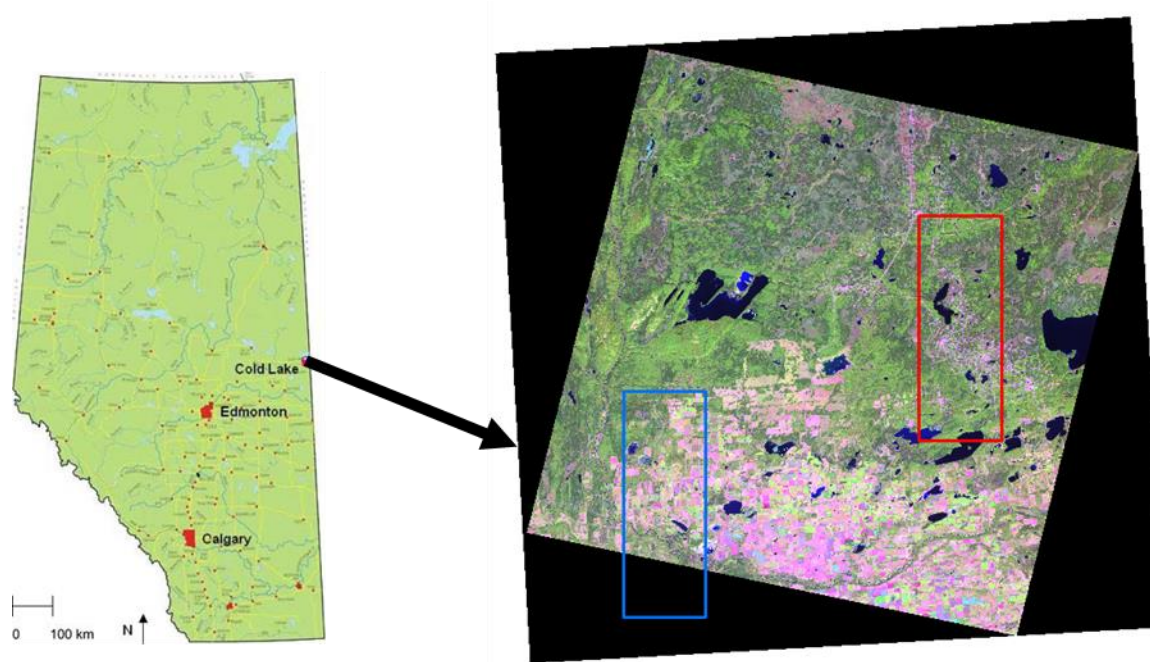


Figure 1. Location of the Cold Lake study area in Alberta. The red and blue polygons, overlaid on a SPOT-4 colour composite image, correspond to the sites that had an AISA/LiDAR acquisition.

### 2. Sampling Scheme

The sampling plan was governed by the location of the certified well sites in the “ColdLake\_FW” and the “ColdLake\_AG” sites. The goal of this field campaign was to sample about 30 certified well sites and their adjacent areas in each study site, taking into account the variability in their certification issue date, their land cover/land use as well as the temporal trend of their Normalised Difference Vegetation Index (NDVI) derived from the LANDSAT TM/ETM+ data acquired during the 1998 to 2011 period (Figure 2). For this purpose, the forest

inventory data available through the Alberta Vegetation Inventory (AVI) were examined so that different forest architecture in terms of species composition and crown closure could be sampled at the “ColdLake\_FW” site (Figure 3).

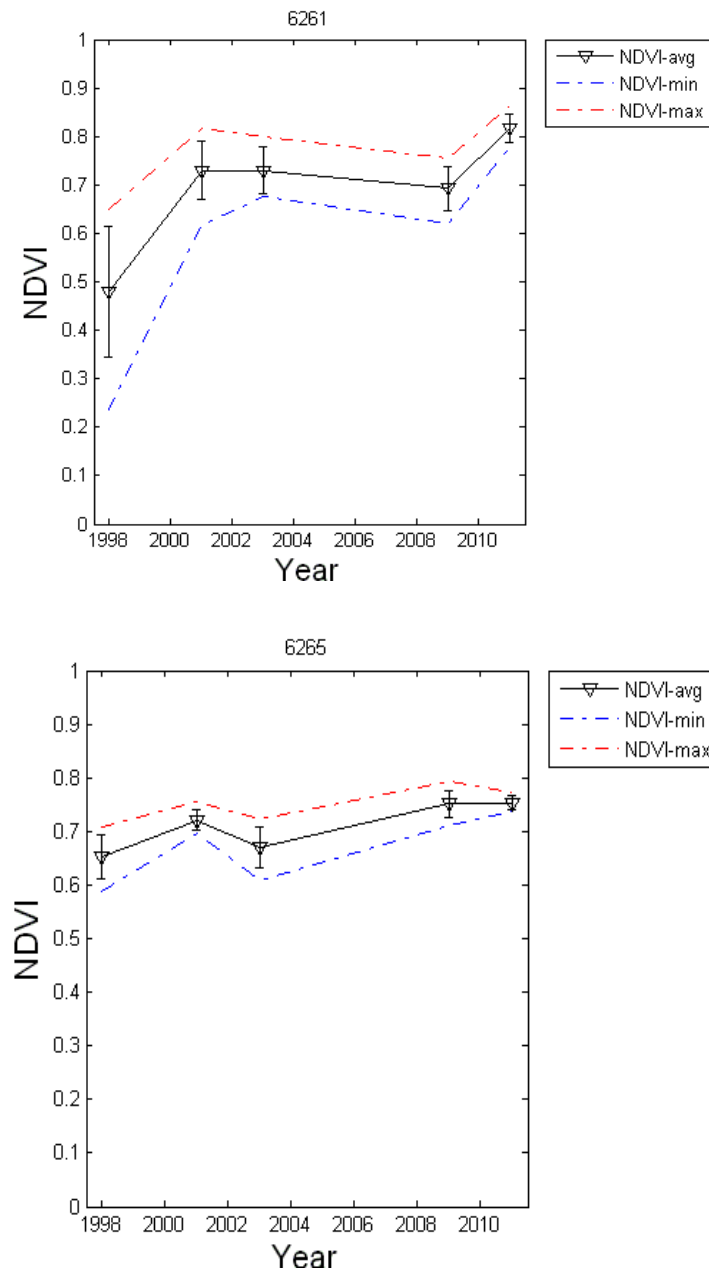


Figure 2: Temporal profile of the Normalized Difference Vegetation Index (NDVI) derived from LANDSAT/TM data acquired from 1998 to 2011 for two reclaimed well sites (#6261 and #6265). The average, maximum, and minimum NDVI values derived over the whole well site are plotted in black, red and blue, respectively.

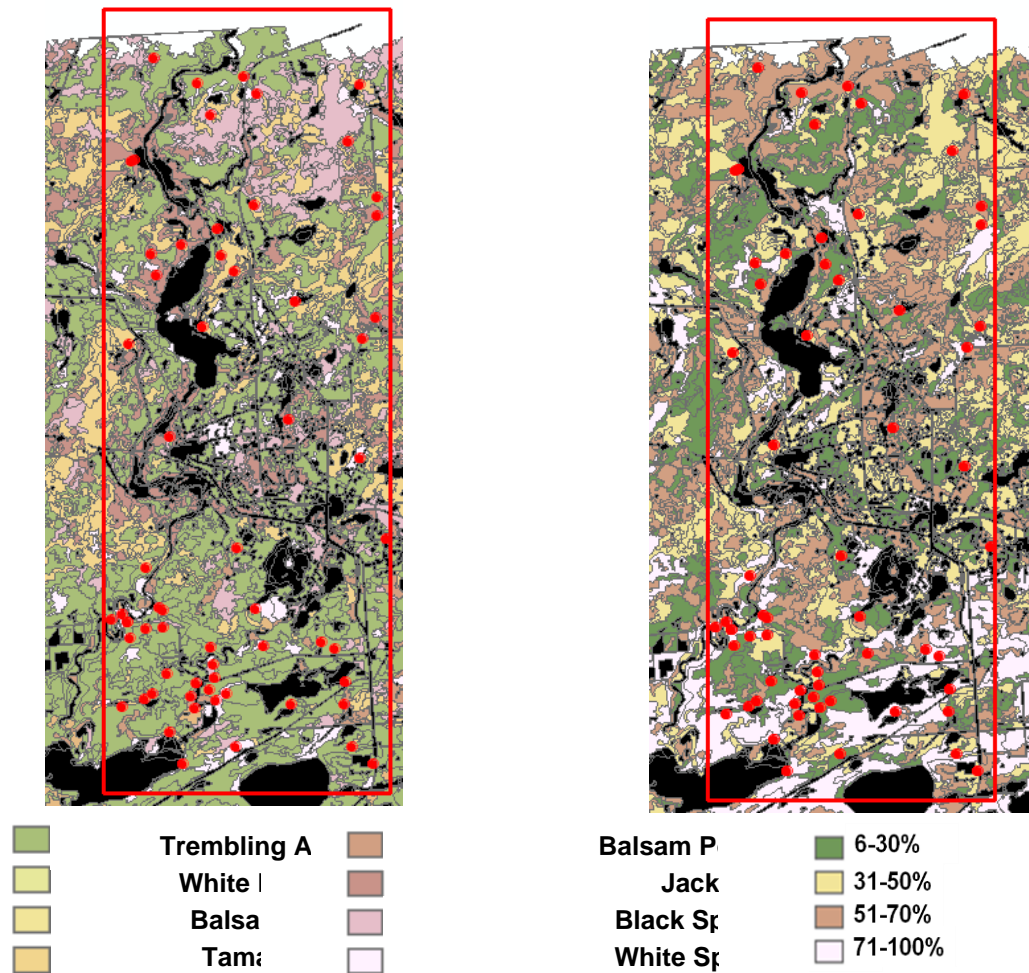


Figure 3: Alberta Vegetation inventory data over the ColdLake\_FW study site illustrating the most dominant species (left) and canopy closure (right). Red dots indicate well sites that received a reclamation certificate.

### 3. Variables of Interest

A set of variables was estimated or measured in the field including:

- Land cover/land use,
- Tree species,
- Number of trees,
- Tree height,
- Tree diameter at breast height (DBH),

- Crop height,
- Leaf Area Index (LAI; half the total surface area of green foliage per unit horizontal ground area),
- Canopy fractional cover (percent of horizontally projected canopy on the ground),
- Leaf chlorophyll content ( a green pigment found in the chloroplasts of leaves necessary for the photosynthesis process, which allows plants to absorb energy from light), and
- Tree mortality.

#### 4. Test Plots

A 6 m x 6 m plot equivalent to 3 x 3 pixel size of the airborne acquisition was established in the “ColdLake\_AG” study site to mitigate any geolocation error in the airborne remote sensing data.

For the “ColdLake\_FW” study site, test plots were established following Canada’s National Forest Inventory (NFI) guidelines. Further adjustments were considered to balance the time available and the number of plots sampled:

- For a stand of large trees a 20 m x 20 m plot was first established and 10 m x 10 m subplot was selected where tree height and DBH were measured for trees with a diameter to breast height greater than or equal to 2.8 cm.
- For a stand of small trees, mostly located on reclaimed wellsites, a 7 m x 7 m plot was established for measuring tree height and DBH for all trees.

These test plots were established on the well site as well as on adjacent areas. The geographical coordinates of the plot corners and center (only for forested areas) were recorded using a handheld GPS.

#### 5. Measurements Protocol

Table 1 summarizes the variables that were measured or visually estimated at the selected test plots.

Table 1. A list of the variables of interest characterized on the ground.

Variable	Measurement Method
Land cover/land use	Visual
Tree species	Visual

<b>Variable</b>	<b>Measurement Method</b>
Number of trees	Visual
Tree height	Inclinometer
Tree DBH	Measured at 1.30 m from the tree ground base
Crop height	Measuring tape
Leaf Area Index	Hemispherical Photographs
Canopy fractional cover	Hemispherical Photographs
Leaf chlorophyll content	SPAD-502 Chlorophyll metre
Tree mortality	Visual

## 5.1 Forested Plots

### Site Assessment and Tree Structure

- Identify and tag the plot centre and its four corners,
- Record the land-cover type for both canopy overstory and understorey,
- Identify trees to measure (DBH > 2.8 cm for a stand of large trees and all trees for a stand of small trees),
- Measure and record tree attributes (DBH, height),
- Record tree species (Table 2),
- Record live/dead status, and
- Paint spray the measured tree before moving to the next one to avoid confusion.

Table 2. A list of the most common trees species in the Cold Lake area.

<b>Code</b>	<b>Common Name</b>	<b>Species Name</b>
Aw	Trembling Aspen	<i>Populus tremuloides</i>
Bw	Paper birch	<i>Betula papyrifera</i>
Pb	Balsam poplar	<i>Populus balsamifera</i>

Code	Common Name	Species Name
Fa	Alpine fir	<i>Abies lasiocarpa</i>
Fb	Balsam fir	<i>Abies balsamea</i>
Lt	Tamarack	<i>Larix laricina</i>
Pj	Jack pine	<i>Pinus banksiana</i>
Pl	Lodgepole pine	<i>Pinus contorta</i>
Sb	Black spruce	<i>Picea mariana</i>
Sw	White spruce	<i>Picea glauca</i>

### Leaf Area Index / Canopy Cover

Indirect measurements of leaf area index and canopy cover were undertaken using digital hemispherical photographs (DHP). The photographs were later processed using the CANEYE software to derive these two variables:

- The Validation of Land European Remote sensing Instruments (VALERI) protocol was used for this purpose. Measurements were made over 20 m x 20 m plots for both short and tall trees stands (Figure 4).
- 13 upward (overstory) and 13 downward (understory) looking photographs were taken.
- All downward-mode photos were acquired in automatic mode while the operator was facing the sun to minimize the shadow effect.
- All upward-mode photos were taken back to the sun and in automatic mode.

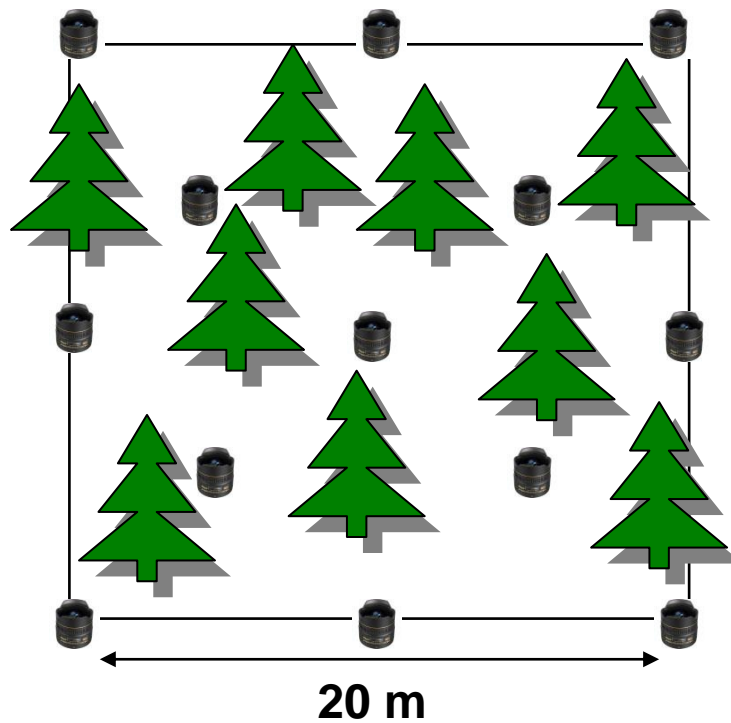


Figure 4. The Validation of Land European Remote sensing Instruments (VALERI) sampling protocol.

## 5.2. Agriculture Plots

### Site Assessment

- Mark the four corners of the test plot with a flag or a stake,
- Identify the crop type,
- Take note of any sign of stress, and
- Take 10 random measurements of canopy height.

### Chlorophyll content

- Select 10 random plants for chlorophyll measurements, and
- Acquire measurements over the two uppermost fully developed leaves at the base, middle, and tip of the leaf using the SPAD-520 chlorophyll meter.

### Leaf Area Index / Canopy Cover

Indirect measurement of leaf area index and canopy cover were undertaken using digital hemispherical photographs (DHP). The photographs were later processed using the CANEYE software to derive these two variables as follows:

- Following the Canada Centre for Remote Sensing protocol, measurements were made over two 30 m transects oriented parallel to the rows and separated by a 6 m distance as illustrated in Figure 5.
- Photographs were acquired every 2 m in the upward mode for crops taller than 50 cm and in downward mode if the crop height was smaller than 50 cm. A total of 32 photos were acquired.
- All downward-mode photos were acquired in automatic mode, while the operator was facing the sun to minimize the shadow effect.
- All upward-mode photos were taken back to the sun and in automatic mode.

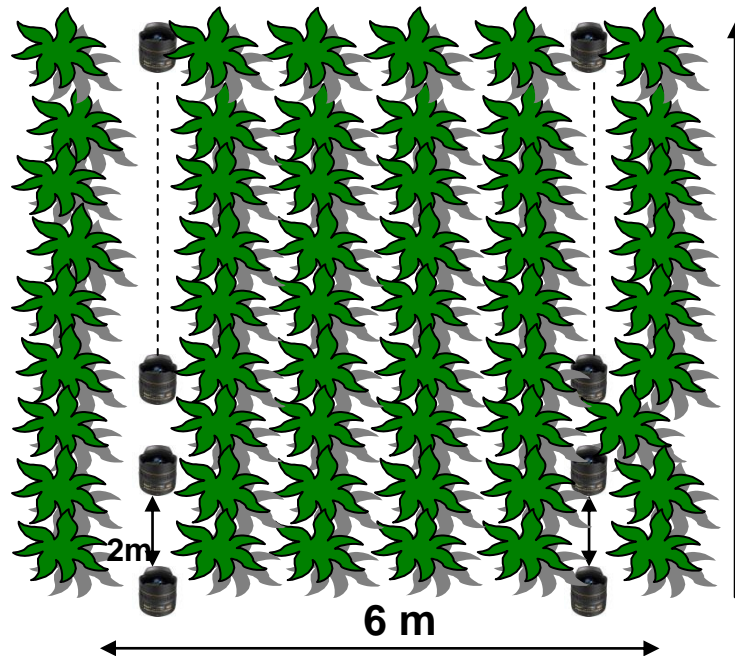


Figure 5. The Canada Centre for Remote Sensing (CCRS) sampling protocol.

## **APPENDIX 3: Remote Sensing Data Processing Toolbox: ENVI-Plug in**

### **1. Introduction**

This document describes the overall structure and major functions of the software toolbox developed within the *Monitoring Procedures for Site Reclamation in Alberta (MOPRA) project*. This software was implemented as an *ENVI plug-in* that is accessible through the ENVI menu system. The toolbox provides the capabilities for processing and characterizing vegetation conditions using LiDAR and optical-passive remote sensing technologies as follows: (1) baseline mapping, (2) change detection, and (3) retrieval of information of vegetation condition in reclaimed areas. The focus of the toolbox is how to effectively integrate a set of data pre-processing/information extraction modules using existing remote sensing processing software (commercial, open source and in-house) to automate the processing chains for mapping and monitoring purposes.

It should be pointed out that the toolbox described here is modified from the System Design document (ATIC-2012-009) based on the feedback from the Alberta Government. The following changes have been made to ensure the major functionalities:

1. All the hyperspectral modules have been dropped because there are no operational data available;
2. The reclamation assessment tool for the temporal Monitoring of reclamation condition was not implemented in the plug-in toolbox due to the difficulty to integrate the Matlab code into the ENVI plug-in toolbox; and
3. Functions to calculate the LAI, biomass and stem density were dropped due to a lower priority and time constraints.

#### ***1.1 Intended Audience***

This document is intended to be used by the developers of the different software components involved in the monitoring toolbox and the users of the toolbox.

#### ***1.2 Purpose of this Appendix***

This document is intended to provide a high-level introduction of the monitoring toolbox. The detailed information on individual algorithms and implementation is not included in this appendix.

#### ***1.3 Acronyms in this Appendix***

Below is a list of acronyms used in this document.

ARVI	Atmospherically Resistant Vegetation Index
------	--

ATIC	Alberta Terrestrial Imaging Centre
ATMSCOR	Automatic aTMOSpheric CORrection
BCAL	Boise Center Aerospace Laboratory
CAP	Centre d'Archivage et de Prétraitement
CSM	Canopy Surface Model
DEM	Digital Elevation Model
DIMAP	Digital Image MAP
DN	Digital Number
EVF	ENVI Vector Format
EVI	Enhanced Vegetation Index
GDAL	Geospatial Data Abstraction Library
GUI	Graphical User Interface
HRV	High Resolution Visible
IDL	Interactive Data Language
ISR	Infrared Simple Ratio
LAI	Leaf Area Index
LiDAR	Light Detection and Ranging
LAS	LASer
MAD	Multivariate Alteration Detection
LUT	Look-Up Table
MODIS	Moderate Resolution Imaging Spectroradiometer
MODTRAN	MODerate resolution atmospheric TRANsmission
MOPRA	MONitoring Procedures for site Reclamation in Alberta
NDVI	Normalized Difference Vegetation Index
NITF	National Imagery Transmission Format
RMSE	Root Mean Squared Error
ROI	Region of Interest
RS	Remote Sensing
RF	Random Forest
SAVI	Soil Adjusted Vegetation Index

SRI	Simple Ratio Index
SMA	Spectral Mixture Analysis
SPOT	Satellite Pour l'Observation de la Terre
SRTM	Shuttle Radar Topography Mission
SVM	Support Vector Machine
USGS	U.S. Geological Survey
VI	Vegetation Index

## **2. Toolbox Overview**

The purpose of the toolbox is to provide a toolbox for mapping and monitoring the vegetation condition on wellsite areas using spaceborne and airborne remote sensing technologies and associated image data. The toolbox supports the following major mapping requirements:

1. Baseline mapping to capture the pre-disturbance condition of mines and wellsites,
2. Temporal (multi-year) monitoring of vegetation recovery in reclaimed areas, and
3. Retrieval of information about vegetation condition in reclaimed areas.

### **2.1 Toolbox Components**

The main components of the toolbox and their functionalities are listed in the following sections.

#### **2.1.1 Requirements of the Hardware and Operating System**

There are no special hardware requirements for the mapping/monitoring toolbox. The hardware requirements are mainly determined by the ENVI software. However, the larger RAM (> 8GB) is preferred since some processing tasks demand more memory space.

The mapping/monitoring toolbox will run as a plug-in toolbox built on top of the commercial software ENVI, incorporating customized algorithms (developed at ATIC), open source and free software. The plug-in toolbox has been designed, implemented and tested on the Windows platforms (Windows XP and Windows 7). It runs on both 32-bit and 64-bit systems.

#### **2.1.2 Software Components**

Generally speaking, the monitoring/mapping toolbox is not a complete geospatial processing software. It is an integrated platform to facilitate the user to efficiently carrying out the mapping and monitoring tasks.

Figure 1 shows the general architecture of the toolbox. Its core component is the ENVI software, different packages, such as open source (GDAL, R, etc.) and in-house tools (ATMOSCOR, etc.), will be integrated through the IDL interface.

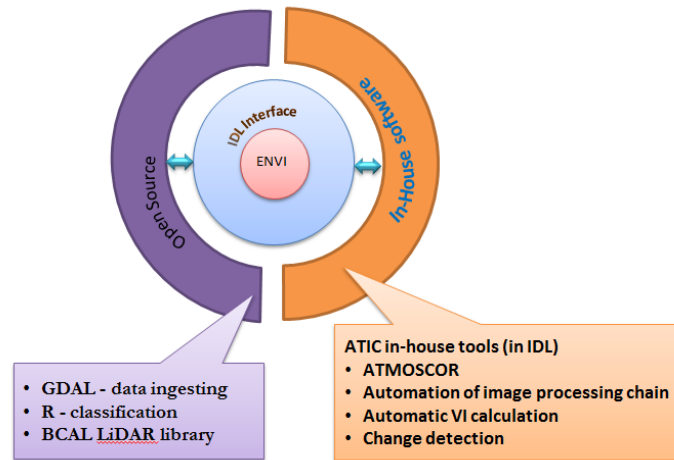


Figure 1: Overall architecture of the MOPRA mapping/monitoring toolbox (GDAL = Geospatial Data Abstraction Library, R = R language, ATMOSCOR = Automatic Atmospheric Correction).

The design of the MOPRA toolbox is modularized for better maintenance and future expansion. It includes five major components as follows:

- Data ingestion,
- Image Preprocessing:
  - Radiometric normalization, and
  - Geometric rectification,
- Information extraction:
  - Classification (baseline mapping),
  - Vegetation indices, and
  - Vegetation characterisation using LiDAR data,
- Change detection, and
- Results assembly.

Figure 2 presents a detailed overview of the whole toolbox.

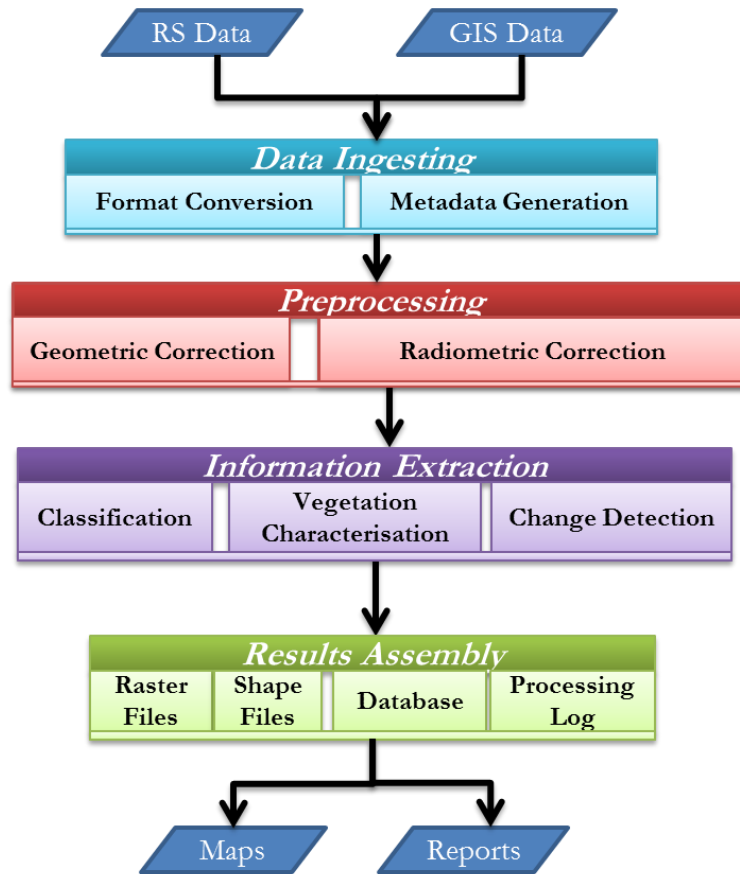


Figure 2: Overview of the MOPRA mapping/monitoring toolbox architecture.

### 2.1.3 Strategy for the MOPRA Mapping/Monitoring Toolbox Implementation

To facilitate easy utilization of the toolbox, core functions of the mapping/monitoring toolbox have been grouped into different categories based on the mapping requirements and embedded into the ENVI-menu system (Figure 3). Each menu/button in this interface is associated with a graphical user interface (GUI) for selection of input/output files and specification of different parameters according to the selected preprocessing/analysis procedure. The detailed menu layout for the current version is shown in Figure 4.

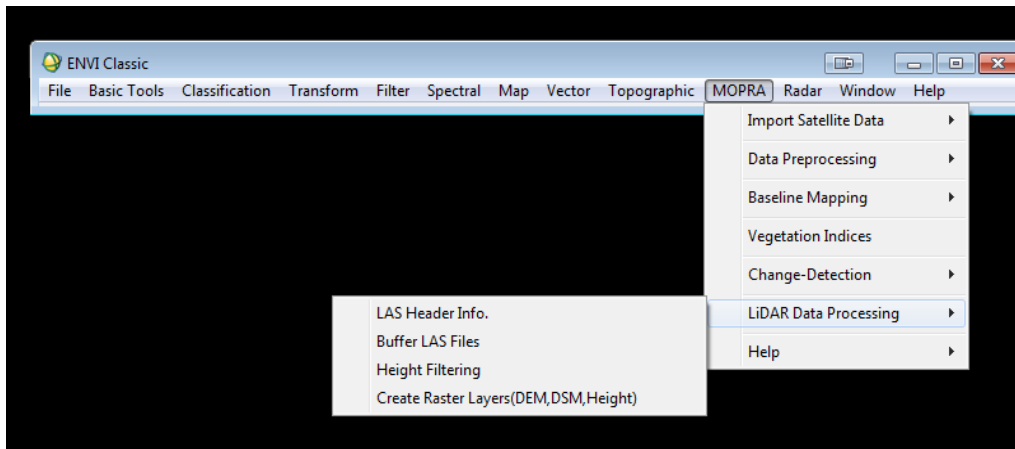


Figure 3: Schematic view of the MOPRA mapping/monitoring toolbox menu.

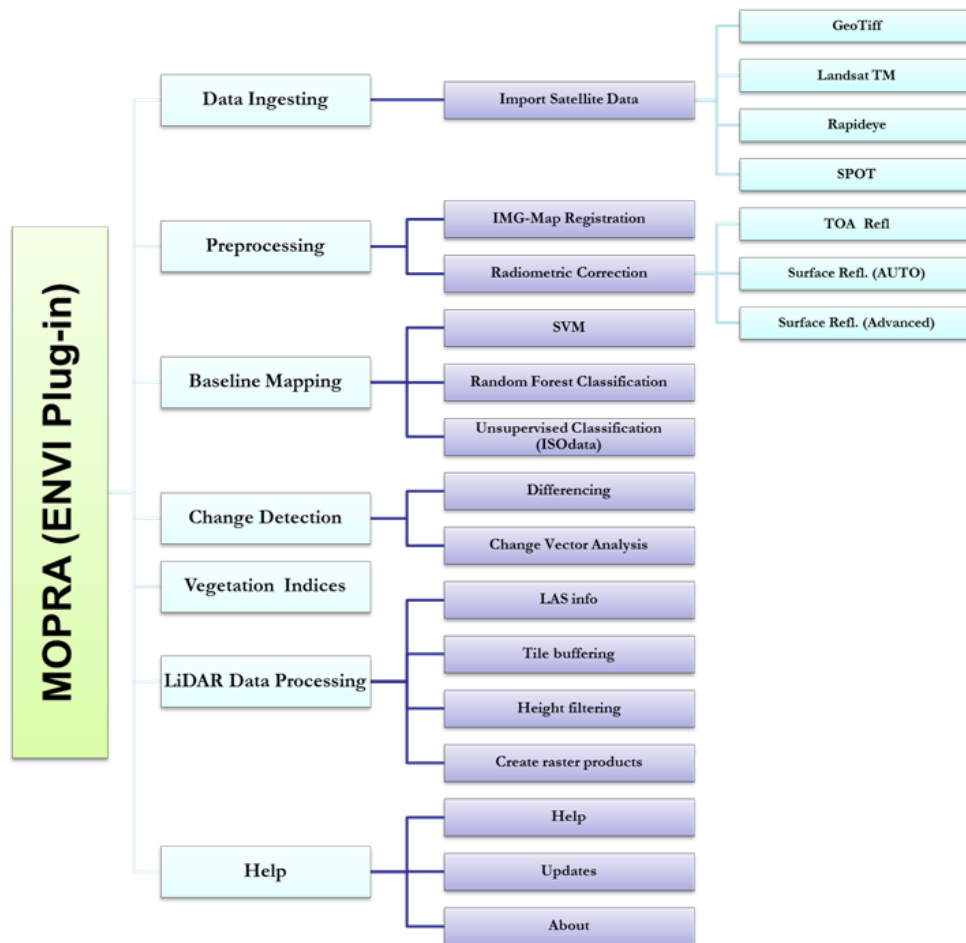


Figure 4: Menu layout for the MOPRA mapping/monitoring toolbox (LAS = LASer, SVM = Support Vector Machine).

The GUIs for the toolbox were implemented in the IDL language, because it is quite flexible and easily interacts with various built-in ENVI functions. Although the ENVI software provides users with a very strong geospatial processing capacity, it does not meet all requirements of the MOPRA mapping/monitoring toolbox. For example, the standard ENVI version cannot directly load RapidEye satellite image data in NTIF format, and the processing capability of LiDAR data is also quite limited. These functions were developed or adapted from open source/free packages, and then linked into the MOPRA mapping/monitoring toolbox through different programming mechanism (Figure 5). If new algorithms are coded in IDL, they can be directly called from the MOPRA toolbox menu. In case where only the executable file is available for certain algorithms, the IDL “spawn” method is used to trigger these tools through the menu. Currently, only two open source packages are used in the toolbox, the GDAL library (for data ingesting) and R language (for the random forestry classification). Other than the aforementioned two packages, all other functions were coded in native IDL code.

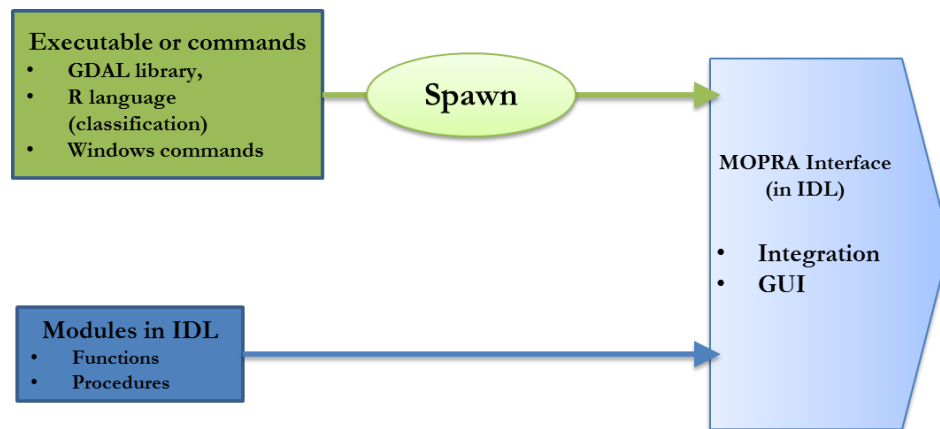


Figure 5: Mechanism to integrate different software tools into the MOPRA mapping/monitoring toolbox (GUI = graphical user interface).

#### 2.1.4 Summary of Major Functions of the MOPRA ENVI Plug-in Toolbox

Major functions of the toolbox are listed in Table 1. When certain functions are not available in the ENVI software, they are adapted from open source/free software or were developed at ATIC.

Table 1: Summary of major functions for the MOPRA project.

Category	Sub_category1	Sub_category2	Newly Developed or Adapted from ENVI	Programming Language
Visualization			Adapted from ENVI	
Data Ingestion	Import Geotiff		Adapted from ENVI	
	Import SPOT		Newly Developed	IDL + ENVI functions
	Import Landsat TM			IDL + ENVI functions
	Import RapidEye			IDL (Using GDAL library)
Baseline Mapping	Supervised classification	SVM	Adapted from ENVI	
		Random Forest	Newly Developed	IDL+R
		ROI Tool	Adapted from ENVI	IDL
	Unsupervised classification	ISODATA	Adapted from ENVI	IDL
Pre-processing	Geometric correction	Image-map	Adapted from ENVI	IDL
	Radiometric correction	Surface reflectance (Auto)	Newly Developed	IDL
		Surface Refl (Advanced)	Newly Developed	IDL
		TOA Reflectance	Newly Developed	IDL
Change Detection	Change vector analysis		Newly Developed	IDL
	Differencing		Newly Developed	IDL
Vegetation Characterization	Vegetation indices	NDVI	Newly Developed	IDL
		EVI	Newly Developed	IDL
		SRI	Newly Developed	IDL
		SAVI	Newly Developed	IDL
		ARVI	Newly Developed	IDL
	LiDAR products	LAS info	Newly Developed	IDL (using BCAL IDL library)
		Tile buffering	Newly Developed	IDL (using BCAL IDL library)
		Height filtering	Newly Developed	IDL (using BCAL IDL library)
		Fractional cover	Newly Developed	IDL (using BCAL IDL library)
		Canopy height	Newly Developed	IDL (using BCAL IDL library)
		Canopy Surface	Newly Developed	IDL (using BCAL IDL library)
		Bare ground surface model	Newly Developed	IDL (using BCAL IDL library)
		Intensity	Newly Developed	IDL (using BCAL IDL library)
		Percentile	Newly Developed	IDL (using BCAL IDL library)

### 3. Workflows

The toolbox supports different product types, which fall into the following three general job types:

1. Baseline mapping about the pre-disturbance condition of the mine and wellsite,
2. Change detection to study the temporal evolution of vegetation condition in reclaimed areas, and
3. Information (maps) about vegetation condition in reclaimed areas (vegetation status, plant health, canopy structure and ground topography).

#### 3.1 Workflow for the Baseline Mapping

The general processing steps for baseline mapping are described in Figure 6. It should be noted that, depending on data characteristics, it is possible that not all steps will be carried out as shown. For example, when the LANDSAT TM data are downloaded from the USGS website, the geometric correction may have already been applied. Accordingly, the processing of the geometric correction step may not be necessary. The Raster-to-vector processing is not necessary if the raster display/analysis is preferred.

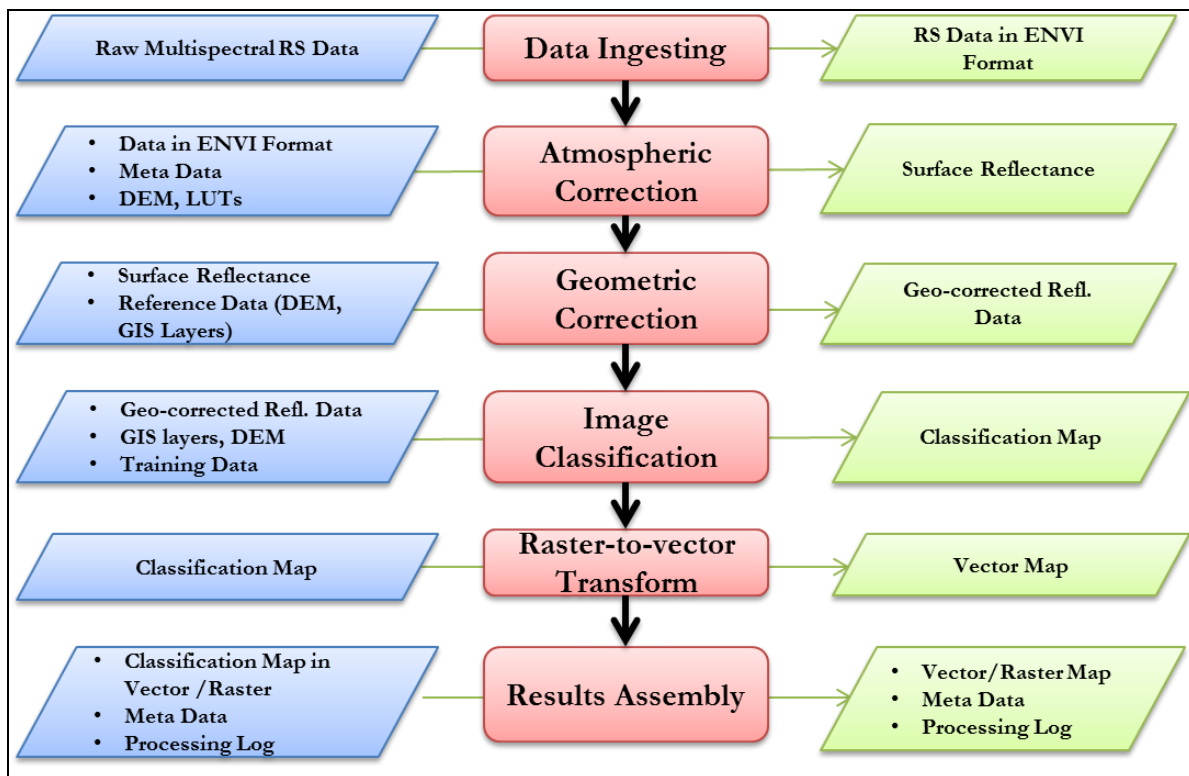


Figure 6: Processing steps for baseline mapping  
(DEM = digital elevation model, LUTs = look-up tables, RS = remote sensing).

### 3.2 Workflow for Monitoring Change Detection

The common way to analyse the temporal evolution of target conditions is to use the change detection approach as illustrated in Figure 7, which lists two change detection procedures, the simple differencing and change vector analysis.

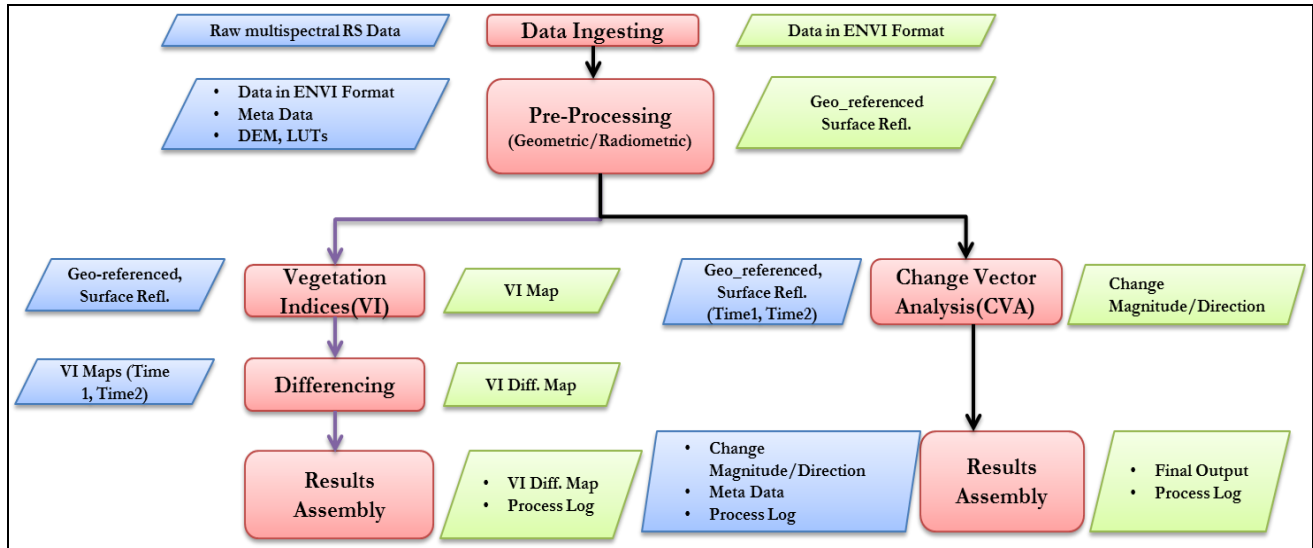


Figure 7: Workflow for the change detection (DEMs = digital elevation models, LUTs = look-up tables, RS = remote sensing, VI = vegetation indices).

### 3.3 Workflow to Derive Indicators Related to Vegetation Conditions

The work flow to derive indicators related to vegetation condition in reclaimed areas (vegetation status, plant health, and canopy structure and ground topography) mainly relies on the airborne LiDAR and multispectral data sets. The general processing steps are listed in Figure 8. Using LiDAR data, some important parameters, such as tree height, fractional cover, and a bare ground surface elevation model, can be directly calculated. Multispectral data provides detailed information on vegetation biophysical/biochemical conditions. The species composition and fractional cover can also be derived from multispectral data using classification or spectral mixture analysis (SMA). The latter is not implemented in the current version of the toolbox.

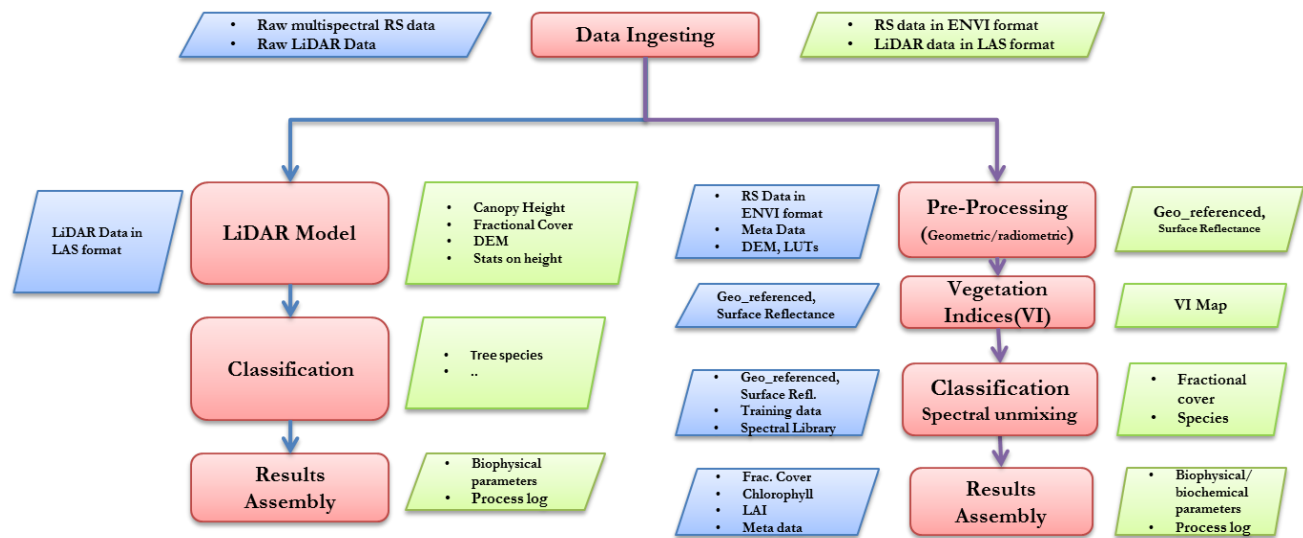


Figure 8: Workflow to derive indicators for vegetation conditions in reclaimed areas (RS = remote sensing LAS =LASer, RS = remote sensing, DEM = digital elevation model, LUTs = look-up tables, LAI = leaf area index, VI = vegetation indices).

## 4. Description of Different Processing Components

### 4.1 Data Ingestion Engine

#### 4.1.1 Purpose

This module is used to fetch the data from the data storage and transfer them to the standard formats (ENVI format) that can be easily handled by the MOPRA toolbox.

#### 4.1.2 Background

Image data may be in different formats, depending on the source from which the raw data are downloaded. For example, the Landsat TM data from the USGS website are recently in GeoTiff format (every individual band will be one Geotiff file). However, SPOT data could be in either Digital Image MAP (DIMAP) (SPOT5) or Centre d'Archivage et de Prétraitement (CAP) format (SPOT 2 and SPOT 4). RapidEye data are usually provided in NTIF format. To make the data processing easier, this module will first be used to convert all data sets to standard formats as listed in Table 2. When the built-in function in ENVI cannot handle the format conversion, the GDAL translator library for raster geospatial data formats (<http://www.gdal.org/>) is used for this purpose.

Another objective of this module is to go through the metadata to collect/calculate parameters that will be used for the future automatic atmospheric correction. The following parameters are collected and stored in the ENVI header file during the data ingesting process:

- Sensor name and number (e.g., SPOT 5),
- Solar azimuth and zenith angles,
- Viewing azimuth and zenith angles,
- Geographical bounding box for the image,
- Radiometric calibration coefficients to convert the digital number (DN) to radiance,
- Imaging time and date,
- Field of view of the sensor, and
- Exo-atmospheric irradiances for each band.

### 4.1.3 Input Data

When importing the raw data from different sensors, different files should be chosen based on Table 2. Currently, only the imagery from SPOT, RapidEye and Landsat TM are supported.

Table 2: Input file data format for different sensors.

Sensor		Examples for the input file	Notes
SPOT	CAP	IMAG_01.DAT	Binary file
	DIMAP	Metadata.dim	The metadata file including various information about the imagery
RapidEye		2013-07-01T193536_RE5_1B-NAC_13174968_164792_metadata.xml	XML file including various information about the imagery
Landsat		LC80400222013222LGN00_MTL.txt	Text file for the metadata associated with the Landsat imagery

### 4.1.4 Output Data

The output data will be the image file in ENVI format with additional information included in the header file. Figure 9 shows one header file for the ENVI format image from the RapidEye sensor.

```

ENVI
description = {
  ENVI File, Created [Fri Feb 14 12:27:45 2014]}
samples = 11781
lines = 10807
bands = 5
header offset = 0
file type = ENVI Standard
data type = 12
interleave = bsq
sensor type = RapidEye
byte order = 0
coordinate system string = {GEOGCS["GCS_WGS_1984", DATUM["D_WGS_1984", SPHEROID["WGS_1984", 6378137.0, 298.257223563]],
  PRIME["Greenwich", 0.0], UNIT["Degree", 0.0174532925199433]]}
wavelength units = Micrometers
geo points = {
  1.0000, 1.0000, 49.93812943, -113.09981537,
  11781.0000, 1.0000, 49.77869034, -112.03966522,
  1.0000, 10807.0000, 49.32918549, -113.34917450,
  11781.0000, 10807.0000, 49.17191315, -112.30172729}
pixel size = {6.50000000e+000, 6.50000000e+000, units=Meters}
wavelength = {
  0.475000, 0.555000, 0.657000, 0.710000, 0.805000}
sun_angle = {
  180.42540, 63.68393}
view_angle = {
  13.00000, 7.48000, -6.28024}
source = {
  RE-5, 2013-07-01, 19:35:36}
physical_unit = equivalent radiance (W.m-2.Sr-1.um-1)
physical_gain = {
  100.00000, 100.00000, 100.00000, 100.00000, 100.00000}
physical_bias = {
  0.00000, 0.00000, 0.00000, 0.00000, 0.00000}
solar_irradiance = {
  1997.80005, 1863.50000, 1560.40002, 1395.00000, 1124.40002}
fov = 13.50000
sensor_str = RapidEye

```

Figure 9: An example of the header file of the imported satellite image. The information highlighted with the red box is new information generated during the importing process.

## 4.2 Atmospheric Correction

### 4.2.1 Purpose

The purpose of this module is to remove the impact of the solar illumination and atmospheric absorption/scattering effects from the reflected electromagnetic signal of the targets in question.

### 4.2.2 Background

This step is critical for the subsequent information extraction and change detection. Whenever possible, the atmospheric radiative transfer code MODTRAN is used in this module due to its superior performance in modeling atmospheric scattering/absorption effects. Two options were implemented in the toolbox: automatic and advanced modes.

The automatic approach is adapted from the ATMOSCOT code developed in previous ATIC projects. If the data were imported using the Data Ingesting in the MOPRA toolbox, all the information required for the correction has been stored in the ENVI header file. In this case, the automatic mode can be used. If the data are from other sources, the advanced mode should be used for the atmospheric correction and all the relevant information needs be manually supplied by the user (Figure 10). However, it is not recommended for most of users due to its complexity.

Figure 10: Interface for the atmospheric correction (advanced mode).

### 4.2.3 Input Data

The following input data will be required for the automatic atmospheric correction:

- Raw images in radiance (user specified), and
- Reference data (embedded in the toolbox)
  - aerosol products from the Moderate Resolution Imaging Spectroradiometer (MODIS),
  - Shuttle Radar Topography Mission (SRTM) DEM, and
  - Look-up tables generated from MODTRAN 4.

#### **4.2.4 Output Data**

The following output data will be generated:

- Images in surface reflectance and
- Processing Log.

### **4.3 *Geometric Rectification Module***

#### **4.3.1 Purpose**

The purpose of this module is to correct the geometric distortions caused by sensor and/or topographic effects. This module geo-rectifies and transfers the imagery to a user-specified map projection to facilitate the generation of GIS ready thematic layers.

#### **4.3.2 Background**

This module mainly relies on the built-in function in the ENVI software.

#### **4.3.3 Input Data**

The following input data will be required:

- The image to be rectified, and
- Reference data
  - Metadata and DEM.

#### **4.3.4 Output Data**

The following output data will be generated:

- Orthorectified images and
- Log files.

### **4.4 *Information Extraction Module – Baseline Mapping***

#### **4.4.1 Purpose**

This module is used to convert the radiometrically and geometrically corrected image data into thematic maps.

#### 4.4.2 Background

Multiple classification and/or target detection algorithms are included. Three algorithms have been considered: support vector machine (SVM), random forest (RF) classification and unsupervised classification (e.g., ISODATA). The SVM and unsupervised classification algorithms are adapted from the ENVI software and the RF classification is based on the RF package in the R language. Figures 11 and 12 show the interfaces for the RF and SVM classification algorithms, respectively. The discussion about the unsupervised classification is omitted here, because it is not commonly used.

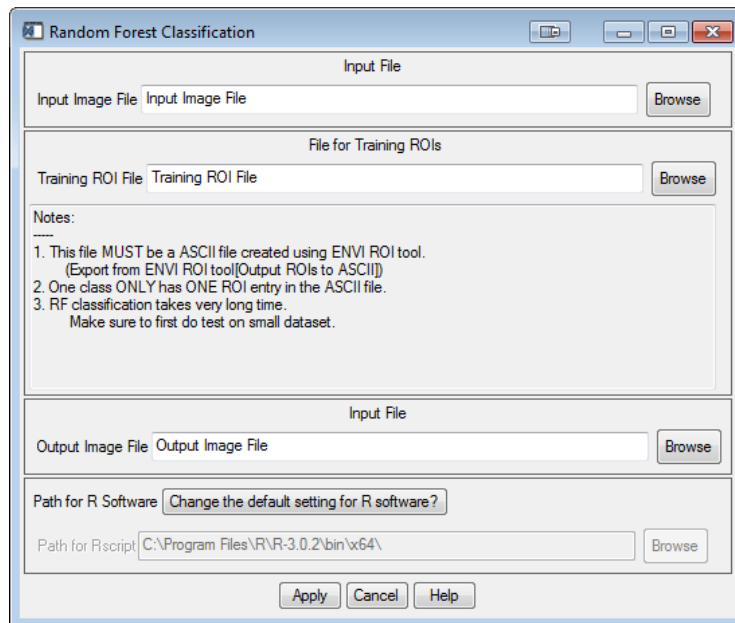


Figure 11: GUI for the random forest (RF) classification.

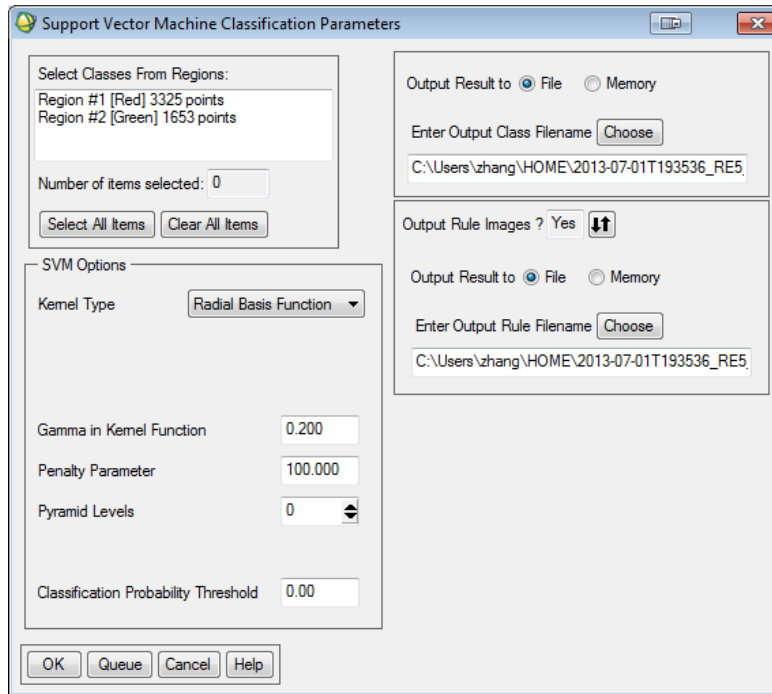


Figure 12: GUI for the support vector machine (SVM) classification.

The classification results from RF and SVM are very similar, but RF performs a bit better than SVM. However, the processing time for the RF is much longer than the one for SVM. When the RF classification was developed, the interface was optimized and simplified to let the user just supply three necessary parameters: input file, training data and output file (Figure 11). The SVM interface was adapted from the ENVI built-in function. Although more options are available to the user, it is recommend keeping these options to default values.

### 4.4.3 Input Data

The following input data will be required:

- Radiometrically and geometrically corrected images, and
- Training data in native ENVI format or ASCII (depending on the algorithm).

### 4.4.4 Output Data

The following output data will be generated:

- Thematic map and
- Log file.

#### **4.5 Information Extraction Module – Vegetation Indices**

The vegetation indices (VI) are important indicators for the vegetation growth conditions. Because the major data sources for this project are SPOT, Landsat and RapidEye, five VIs are considered based on the band information for these sensors:

- Normalized Difference Vegetation Index (NDVI),
- Simple Ratio Index (SRI),
- Enhanced Vegetation Index (EVI),
- Soil Adjusted Vegetation Index (SAVI), and
- Atmosphere Resistant Vegetation Index (ARVI).

Figure 13 shows the GUI for the VI calculation. If the input data have the band information in the associated header file, the software will automatically find the right bands for different VIs. Of course, the user always has the option to choose the correct bands when the band information is not in the header file. Special attention should be paid to the scale factor when the EVI and SAVI are chosen. The user should type in a value that can be multiplied to convert the pixel values to real reflectance values between 0.0 and 1.0.

##### **4.5.1 Input Data**

The following input data will be required:

- Radiometrically corrected multispectral data.

##### **4.5.2 Output Data**

The following output data will be generated:

- Image file in ENVI format and
- Log file.

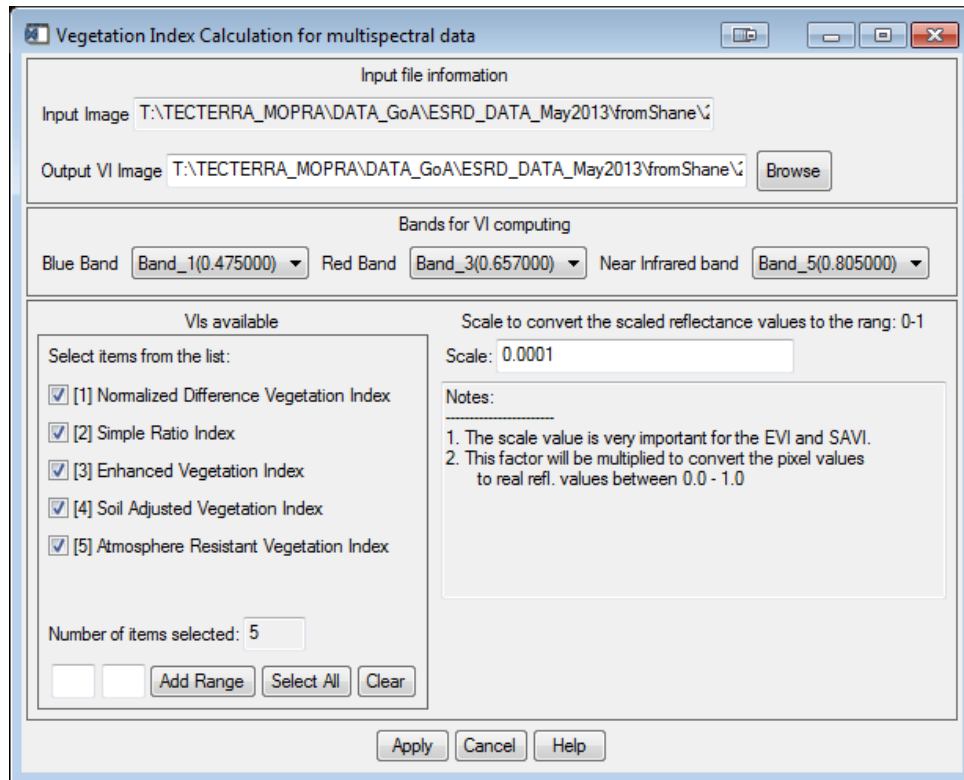


Figure 83: GUI for VI calculation for multispectral data.

## 4.6 Information Extraction Module - Biophysical Parameter Retrieval from LiDAR Data

### 4.6.1 Purpose

The main purpose of this module is to derive specific biophysical parameters from LiDAR data. The following major parameters can be calculated in this module:

- Fractional cover,
- Canopy height,
- Bare ground DEM,
- Canopy surface model,
- Intensity, and
- Percentile of tree height.

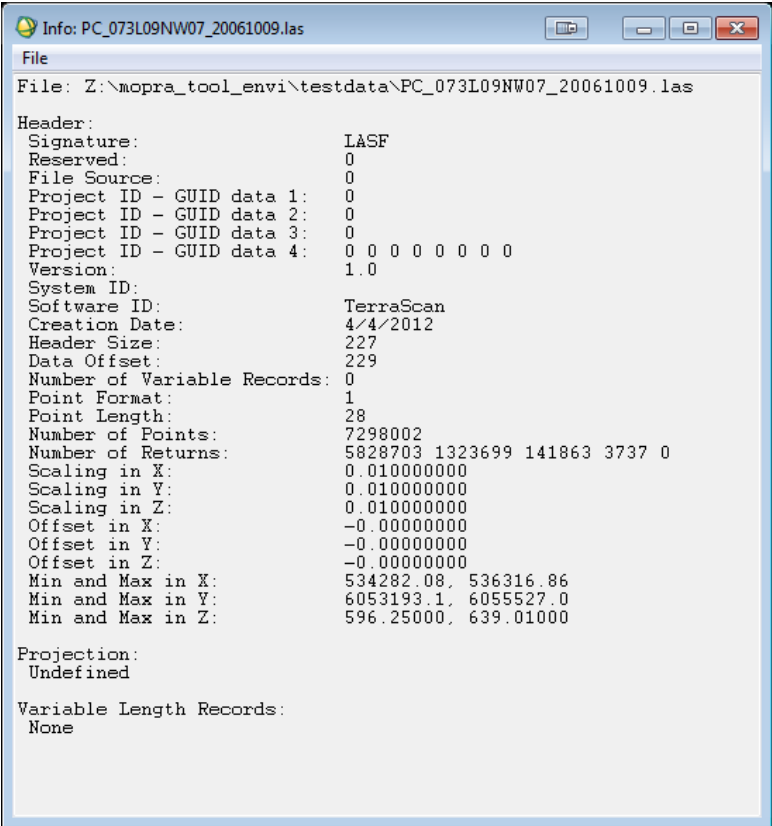
## 4.6.2 Background

This module is for airborne LiDAR data. The related tools/commands were developed in IDL or adapted from BCAL LiDAR tools (<http://bcal.boisestate.edu/blog/2012/12/08/lidar/>). The following functions are currently included in this module:

- View the information of LAS file,
- Buffering of data tiles,
- Height filtering, and
- Creating of various raster products.

### 4.6.2.1 View the Information of LAS files

This tool is used to display information about a LAS file. Once this function is selected, a text window will display information about the selected file. All of the information in the file header is displayed. If the file contains embedded projection information, it is displayed. Figure 14 lists one example.



```
Info: PC_073L09NW07_20061009.las
File
File: Z:\mopra_tool_envi\testdata\PC_073L09NW07_20061009.las
Header:
Signature:          LASF
Reserved:           0
File Source:        0
Project ID - GUID data 1: 0
Project ID - GUID data 2: 0
Project ID - GUID data 3: 0
Project ID - GUID data 4: 0 0 0 0 0 0 0 0
Version:            1.0
System ID:
Software ID:        TerraScan
Creation Date:       4/4/2012
Header Size:        227
Data Offset:        229
Number of Variable Records: 0
Point Format:        1
Point Length:       28
Number of Points:    7298002
Number of Returns:   5828703 1323699 141863 3737 0
Scaling in X:        0.010000000
Scaling in Y:        0.010000000
Scaling in Z:        0.010000000
Offset in X:         -0.000000000
Offset in Y:         -0.000000000
Offset in Z:         -0.000000000
Min and Max in X:    534282.08, 536316.86
Min and Max in Y:    6053193.1, 6055527.0
Min and Max in Z:    596.25000, 639.01000

Projection:
Undefined

Variable Length Records:
None
```

Figure 94: Information of a LAS file.

#### 4.6.2.2 Buffering of Data Tiles

This tool is meant to buffer neighboring LAS files such that they will overlap geographically. The purpose of this tool is to overcome difficulties near tile seams when multiple tiles need to be mosaicked. The user needs to specify the value for the buffer distance that is the amount by which two adjacent tiles will overlap (Figure 15).

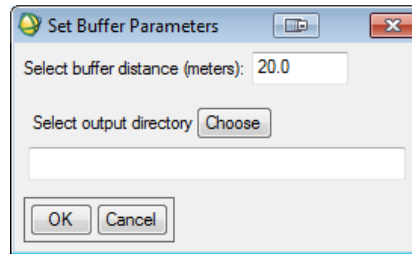


Figure 15: GUI to set buffer parameters.

#### 4.6.2.3 Height Filtering

In nearly all LiDAR applications, ground filtering (or height filtering) is necessary and the first step to determine which LiDAR returns are from the ground surface and which are from non-ground surface features. Distinguishing ground from non-ground can be a significant challenge in regions with high surface variability. There are many approaches for this purpose (Meng et al. 2010). The approach used in this tool is based on the algorithm proposed by Streutker and Glenn (2006). Figure 16 shows a GUI for the parameter setup.

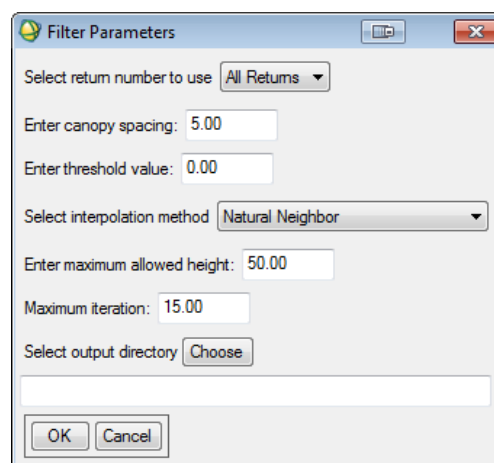


Figure 16: GUI for height filtering.

The following parameters need to be specified for the processing:

- **Return to use.** The 1<sup>st</sup> return, last return, or all returns.
- **Canopy spacing.** This parameter reflects how "open" the canopy is, and is in the units of the horizontal coordinates of the data. Generally, 4 m to 5 m seems to work fairly well.
- **Threshold value.** The default value of 0 is fine for most cases. When more ground returns need to be generated, for example, to preserve features like ridges, or rock outcrops, the threshold value needs to be increased.
- **Interpolation method.** The method chosen may have a significant effect on processing speed, with "Linear" being the fastest. "Natural Neighbor" has also been found to work quite well. The "Natural Neighbor" interpolation is a method of spatial interpolation, developed by Sibson (1981). The method is based on Voronoi tessellation of a discrete set of spatial points. It has advantages over simpler methods of interpolation, such as nearest-neighbor interpolation, in that it provides a more smooth approximation to the underlying "true" function.
- **Maximum allowed height** (in units of the elevation data). Any computed height values greater than this limit will be assumed in error.
- **Maximum iteration value.** By default, height filtering runs for a maximum of 15 iterations, which is fine if the threshold value is 0. If the threshold value is  $> 0$ , the iteration number is also required to be increased. Otherwise, some LiDAR points will remain unclassified.

#### 4.6.2.4 Creating Various Raster Products

This is the major tool to generate different raster products mentioned in Section 4.6.2. The input to this module should be first processed using the "height filtering" tool as discussed before. Figure 17 shows the GUI for this module. It accepts single or multiple LAS files.

A list of products that can be calculated are listed on the right of the GUI layout, including fractional cover, canopy height, DEM, canopy surface model (CSM), intensity, and percentile of tree height. The users can choose the desired products they prefer. By default, 5 products (DEM, CSM, mean intensity, fractional cover and mean-tree height) will be calculated.

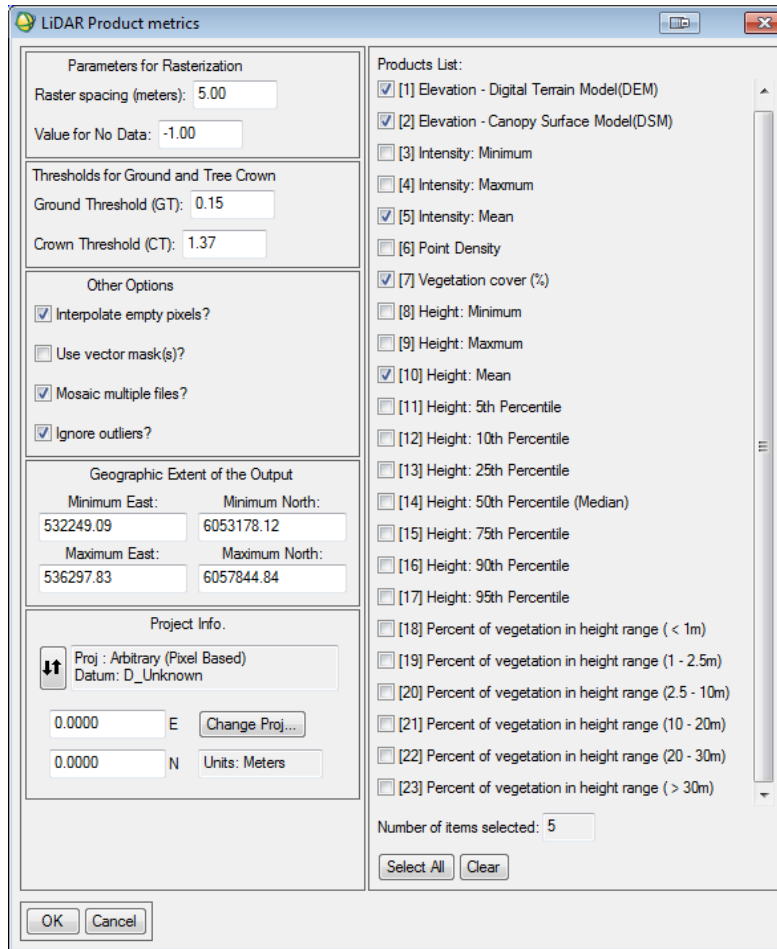


Figure 107: GUI for the LiDAR products.

A lot of options are listed on the left side. The following are some explanations of these options:

- **Raster Spacing:** The raster pixel resolution for the output.
- **Value for no Data:** The value for pixels where no data exists. The default value is -1.
- **Ground threshold (GT):** Any points with the height below this value will be considered as ground returns. The GT is used for calculation of canopy density and height distribution products.
- **Crown threshold (CT):** If a threshold value of 1.37 m is specified, all the points that have an above-ground height greater than 1.37 m will be considered as crown returns. The CT is used for calculation of fractional cover.
- **"Interpolate data?":** If this box is checked, the tool will interpolate missing data within the raster. However, the tool does not extrapolate outside the edges of the data.

- **"Use vector mask(s)?"**: If this box is checked, the tool will prompt the user to select one or more ENVI Vector Format (EVF) files. Pixels within these areas will not be processed.
- **"Mosaic multiple files?"**: If this box is checked, then multiple input files will be combined into a single raster. If this box is not checked, and multiple input files are selected, a raster will be created for each input file.
- **"Ignore outliers?"**: If this box is checked, then LiDAR points whose elevation is five or more standard deviations from the median will be ignored.
- **Geographic Extent of the Output**: Set the desired geographic extent of the output raster. The default values are the overall extents of the selected input file(s).
- **Project Info.:** If necessary, set the projection associated with the data.

#### 4.6.2.5 Normal Data Processing Flow for LiDAR Data

If possible, the following processing order should be always used to ensure the generation of correct products:

LAS info → Height Filtering → Tile buffering → Topographical products and Vegetation metrics

### 4.6.3 Input Data

The following input data will be required:

- LiDAR data in LAS format.

### 4.6.4 Output Data

The following output data will be generated:

- Parameters listed in Section 4.6.1 and
- Log file.

## 4.7 *Change Detection Module*

### 4.7.1 Purpose

The purpose is to assess the temporal change of land condition and its extent.

### 4.7.2 Background

The change detection works on remote sensing data acquired in different years and at different times within the same season. Two methods have been implemented in the toolbox: simple differencing and change vector analysis (CVA) (Figures 18 and 19). When using the simple differencing method (Figure 18), the user should pick the band that will be used in the calculation. Otherwise, the first band will be chosen. For the CVA approach, either the RMSE or spectral angle measure or both can be used. By default, the RMSE will be used.

The screenshot shows a software window titled "Change Detection -- Differencing". It is divided into three main sections for configuring two input images and the output.

- IMAGE FOR TIME 1:**
  - Input Image 1: F:\MOPRA\test\_data\change\_detection\subset\LT50400221998229PAC03\_subset.img
  - Band for the difference: Resize (Blue:LT5040022\_02219980817\_ENVI\_surf\_refl.img)
  - Map Projection: UTM, Pixel\_Size\_X: 30.000000, Pixel\_Size\_Y: 30.000000, Units: Meters
  - Background Value: 0.000000
- IMAGE FOR TIME 2:**
  - Input Image 2: F:\MOPRA\test\_data\change\_detection\subset\LT50400222011217EDC00\_subset.img
  - Band for the difference: Resize (Blue:LT5040022\_02220110805\_ENVI\_surf\_refl.img)
  - Map Projection: UTM, Pixel\_Size\_X: 30.000000, Pixel\_Size\_Y: 30.000000, Units: Meters
  - Background Value: 0.000000
- OUTPUT IMAGE:**
  - Output Image: (empty field) [Browse]
  - Map Projection for the Output: ☒ Same to Image 1, ☐ Same to Image 2
  - Background Value: 0.000000, ☐ Keep both positive and negative values, ☒ Convert negative values to positive

At the bottom of the window are three buttons: "Apply", "Cancel", and "Help".

Figure 18: GUI for the simple differencing change detection approach.

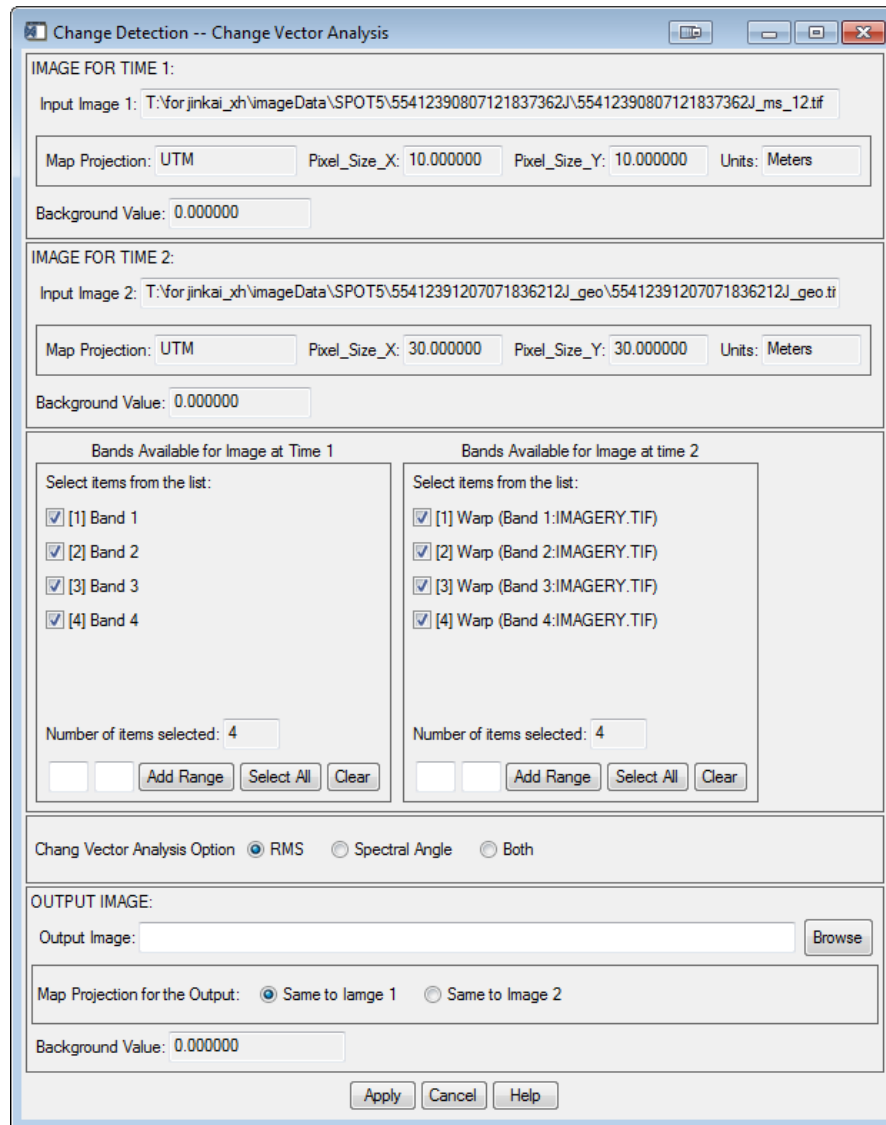


Figure 19: GUI for the CVA change detection approach.

Two datasets used for the change detection are required to be geo-referenced and projected, otherwise an error will rise. Two image data sets could have different map projection and pixel size. The tool will automatically determine the overlapped region where the change detection will be performed. When the two images have different map projections, the user has the option to pick the projection type for the output. The user also has the option to specify the background value for the output related to the areas in one of the two images where no data exist.

It should be pointed out that the images should be geometrically corrected and the atmospheric correction may be required prior to the change detection.

### **4.7.3 Input Data**

The following input data will be required:

- Two radiometrically and geometrically corrected images.

### **4.7.4 Output Data**

The following output data will be generated:

- The difference images and
- Log file.

## **4.8 Results Assembly Module**

### **4.8.1 Purpose**

This final step of the whole processing chain includes three major parts: (1) the results from different scenes will be assembled into a seamless coverage map, (2) the map data will be converted to GIS ready vector format (if required) to allow implementation in existing inventory databases, and (3) all relevant parameters used in the procedure will be formulated into a metadata file for future reference.

### **4.8.2 Background**

This module is mainly based on various tools from the ENVI software package and, therefore, no new GUI was developed for this purpose.

### **4.8.3 Input Data**

The following input data will be required:

- Individual classification/change detection maps and
- Relevant log files.

### **4.8.4 Output Data**

The following output data will be generated:

- Mosaicked thematic map over the whole mapping area,
- GIS layers over the whole mapping area, and
- Metafile in ASCII format.

## 5. Software Setup

### 5.1 Prerequisites

#### 5.1.1 Operating System

The plug-in toolbox has been designed, implemented and tested on the Windows platforms (Windows XP and Windows 7). It runs on both 32-bit and 64-bit systems.

Although most of the functions are made independent of the operating system, the toolbox has never been tested on the Linux platform.

#### 5.1.2 Reliance on Other Software

The toolbox needs ENVI 5.0 or newer version. The IDL is not necessary, but it is preferred for the easy debugging of the programs.

The GDAL library and R language need to be properly installed on the computer where the toolbox will be hosted.

### 5.2 Software Set-up

The software setup should follow the following steps:

**Step 1: Download all folders and files from the ATIC ftp site or shared Dropbox folder.**

The following folder structure is shown in Figure 20.

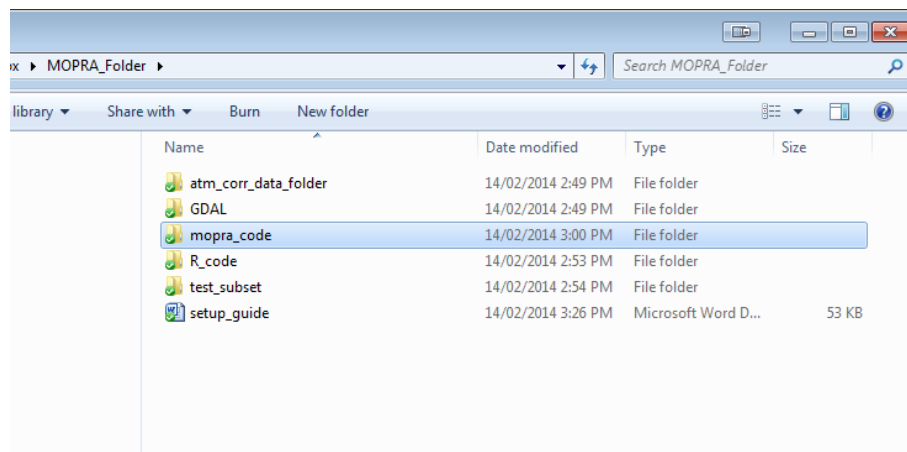


Figure 20: Folder structure for the source code and associated data.

## Step 2: Install R package

- 1) Install R base.
- 2) Install packages: randomForest, rgdal, raster and epitools (the command to install the packages is as follows: `install.packages("randomForest")`).

## Step 3: Make a directory to store the data associated with the toolbox

- 1) Make a new directory: C:\MOPRA
- 2) Copy the following three folders into the folder \C:\MOPRA:

\atm\_corr\_data\_folder,

\GDAL, and

\R\_code.

## Step 4: Copy the source code to the specific folder

Copy the folder\mopra\_code to the following folder: *ENVI install folder*\classic\save\_add.

For example C:\Program Files\Exelis\ENVI50\classic\save\_add

(Everything was tested under ENVI 5.0, and should also work on ENVI 5.1).

## Step 5: Edit the ‘data\_folder.pro’

- 1) Go to the folder: *ENVI install folder*\classic\save\_add \mopra\_code\datafolder,
- 2) Open the file ‘data\_folder.pro’ using any text editor. The text should appear as shown in Figure 21.

```

pro data_folder, at_map=at_map, aod=aod, dem=dem, lut_folder=lut_folder,$
  r_path=r_path, gdal_path=gdal_path,rf_file=rf_file

;at_map='H:\modtran_idl_proj\atm_corr\data\Urban_Buffer3'
;aod='H:\modtran_idl_proj\atm_corr\data\AOT_all12month_2003_to_2007_New_Min_of_Mean.dat'
;dem='H:\modtran_idl_proj\atm_corr\data\SRTM_GTOPO_005degree.img'
;lut_folder='H:\modtran_idl_proj\lut_folder\'

;at_map='S:\atm_corr_data_folder\data\Urban_Buffer3'
;aod='S:\atm_corr_data_folder\data\AOT_all12month_2003_to_2007_New_Min_of_Mean.dat'
;dem='S:\atm_corr_data_folder\data\SRTM_GTOPO_005degree.img'
;lut_folder='S:\atm_corr_data_folder\lut_folder\'

;for mopra -test
at_map='C:\mopra\atm_corr_data_folder\data\Urban_Buffer3'
aod='C:\mopra\atm_corr_data_folder\data\AOT_all12month_2003_to_2007_New_Min_of_Mean.dat'
dem='C:\mopra\atm_corr_data_folder\data\SRTM_GTOPO_005degree.img'
lut_folder='C:\mopra\atm_corr_data_folder\lut_folder\'

;for classification
R_PATH = 'C:\Program Files\R\R-3.0.2\bin\x64\'
rf_file='C:\mopra\R_code\RF.R'

;for data import
GDAL_PATH = 'C:\mopra\GDAL\'

end

```

Figure 21: Example of the data\_folder.pro file.

- 3) Edit the line highlighted in blue, change the directory name to the directory where you installed R (see Step 1). **REMEMBER TO PUT THE ‘\’ AT THE END OF THE STRING.**

## Step 6: Start ENVI+IDL

Start→All program→ENVI5.0→Tools→ENVI Classic + IDL.

The ENVI menu should then appear and the MOPRA button should be in the ENVI menu system (Figure 22).

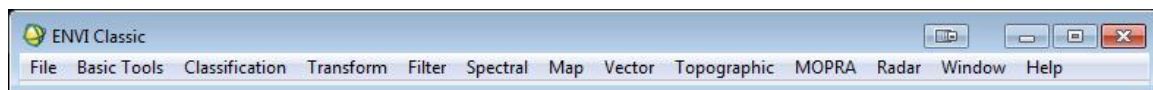


Figure 22: MOPRA menu embedded in ENVI.

## 6. Issues with current release

Several issues have been found during the final debugging stage of the toolbox. They will be fixed in a future release.

- 1) The above instructions only apply to the classical view of the ENVI5.0+IDL. If the user wants to put these into the new ENVI 5.0 interface, please contact Jinkai Zhang ([jinkai.zhang@uleth.ca](mailto:jinkai.zhang@uleth.ca)) for a different setup guideline.
- 2) An error may arise when one or more spaces exist in the folder or file names. Thus, it is best to avoid these spaces in the folder or file names.
- 3) The advanced mode for the atmospheric correction requires more work on the error handling.
- 4) An error may occur as shown in Figure 23: Error message related to the wrong projection information) if the image is not geo-referenced. Just click the **OK** button, the program will continue running and finishing the task.

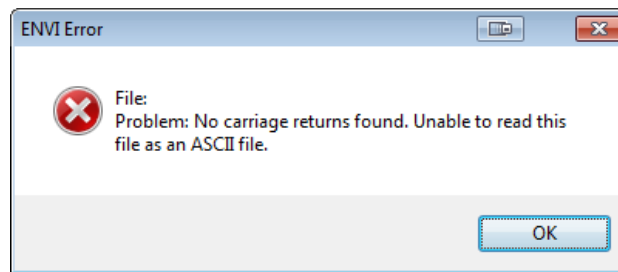


Figure 23: Error message related to the wrong projection information.

- 5) The Progress bar sometimes does not update due to unknown reasons. This does not impact the result.
- 6) The automatic mosaicking function for LiDAR processing is not stable.
- 7) More work is required for LiDAR data with respect to error handling and speed.

## **7. Recommendations**

Based on the successes and failures during the whole software development, the following suggestions are recommended for future work on this toolbox.

### **7.1 Automation**

#### **7.1.1 Automation of Specific Data Processing Task**

Further development in the automation is still required, especially for the preprocessing and classification.

##### **7.1.1.1 Automatic Aerosol Optical Depth (AOD) Estimation**

The current atmospheric correction module does not consider haze contamination and the spatial variation of the AOD.

##### **7.1.1.2 Automatic Definition of Training Samples**

The classification still requires the training data to be manually selected. By incorporating a predefined template map, the selection of training samples could be fully or semi-automated.

##### **7.1.1.3 Automatic Threshold Setup for the Change Detection**

The multivariate alteration detection (MAD) method could be possibly used to set a threshold for identification of change (Canty and Nielsen 2008).

#### **7.1.2 Automation of Specific Work Flow**

This is very useful if the workflow for certain products can be clearly defined. For example, a workflow can be created for the NDVI product from Landsat raw data. The whole procedure can be fully automated so the user does not need to worry about the details of the all processing steps.

### **7.2 Platforms to Run the Toolbox**

Three options can be considered as follows:

1. The toolbox is fully accessible in the current version from the ENVI menu. In this scenario, the software development is easier, but the end user should have the ENVI license installed and be familiar with ENVI.

2. A better way is to implement the toolbox as ARCGIS toolbox through the Python binding. Since most of potential users are familiar with the ARCGIS product, it will be much easier to use this toolbox. In this scenario, the ENVI license is still required.
3. The best way is to implement the whole software using a web-processing service. In this scenario, the user can just use the web browser to submit and view the products. All the data crunching work will be performed on the server side. There is no need to install the ENVI license in the users's computer. But the cost of the development is much higher compared to the other two options.

## 8. Contacts

Jinkai Zhang

Alberta Terrestrial Imaging Centre

University of Lethbridge

Phone: 403-332-4464

[Jinkai.zhang@uleth.ca](mailto:Jinkai.zhang@uleth.ca)

## 9. References

ATIC 2012-007, 2012. Monitoring procedures for site reclamation in Alberta - Temporal monitoring of reclamation success using satellite remote sensing: Algorithm Report. Alberta Terrestrial Imaging Centre, Report ATIC-2012-007, ATIC contract number #120299, Lethbridge, Alberta, 22 pages.

ATIC 2012-009, 2012. Monitoring procedures for site reclamation in Alberta - Temporal monitoring of reclamation success using satellite remote sensing: System Design. Alberta Terrestrial Imaging Centre, Report ATIC-2012-009, ATIC contract number #120299, Lethbridge, Alberta, 23 pages.

Canty, M., and A. Nielsen, 2008. Automatic radiometric normalization of multitemporal satellite imagery with the iteratively re-weighted MAD transformation. *Remote Sensing of Environment*, 112(3): 1025-1036.

Meng, X., N. Currit, and K. Zhao, 2010. Ground filtering algorithms for airborne LiDAR data: a review of critical issues. *Remote Sensing*, 2: 833-860.

Sibson, R., 1981. A brief description of natural neighbor interpolation. IN: Barnett, V. *Interpreting Multivariate Data*. John Wiley, Chichester. Chapter 2, pp. 21-36.

Streutker, D., and N. Glenn, 2006. LiDAR measurement of sagebrush steppe vegetation heights. *Remote Sensing of Environment*, 102: 135-145.

## **APPENDIX 4: Stand-Alone Reclamation Assessment Tool**

### **1. Introduction**

This document describes one of the two components of the MOPRA Reclamation Monitoring System, The Stand-Alone Reclamation Assessment Tool. This package makes use of LiDAR and multi-/hyperspectral optical remote sensing data to extract information about vegetation condition in well/mine lease areas and compare them to reference areas that have no history of mining and or oil and gas activities. This assessment tool includes two automated modules: (1) the reclamation assessment module; and (2) the reclamation temporal trend module. The present tool has been tested in Windows XP and Windows 7 using 34-bit and 64-bit machines. It does not require any software purchase. The only file necessary to run the two executables is a Matlab Compiler Runtime (MCRInstaller.exe) that is delivered together with the tool. The reclamation assessment and temporal trend modules, which are two executables that were developed using the Matlab language, are addressed in the next sections.

### **2. Reclamation Assessment Tool Installation**

The Stand Alone Reclamation Assessment tool is delivered in a single folder, which includes the following set of files/folder:

- REC\_TREND.exe,
- REC\_ASSESS\_v8.exe,
- REC\_ASSESS\_Help.html,
- REC\_ASSESS\_Help folder,
- Readme.txt, and
- MCRInstaller.exe.

Before running the reclamation assessment software, all the files/folder listed above need first to be copied to the same location. The MCRInstaller.exe then needs to be run. A set of installation steps, which need to be followed until the installation is complete, will be displayed.

### **3. Reclamation Assessment Module**

The Reclamation Assessment Module is an executable called REC\_ASSESS\_v8.exe, which analyzes information related to multi-year vegetation index data, land cover, disturbance, species composition, leaf area index, and canopy structural attributes and assigns a flag to those reclaimed areas that are not in agreement with control areas following a pre-defined assessment criteria. The REC\_ASSESS\_v8.exe user interface is illustrated in Figure 1.

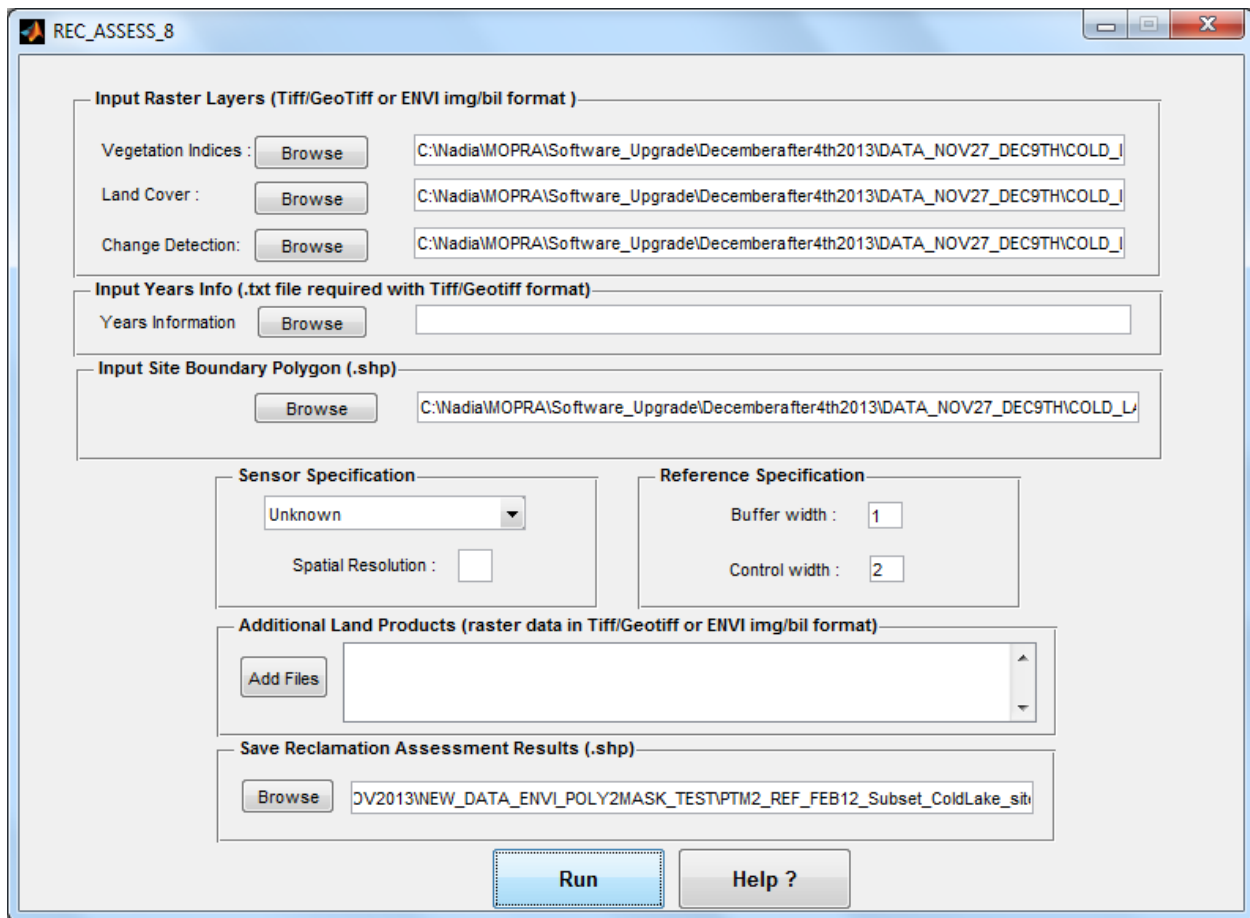


Figure 1: The REC\_ASSESS\_v8.exe User Interface.

The User Interface is made of nine main sections as follows:

1. Input Raster Layers,
2. Input Years Info,
3. Input Site Boundary Polygons,
4. Sensor Specification,
5. Reference Specification,
6. Additional Land Products,
7. Save Reclamation Assessment Results,
8. Run Pushbutton, and
9. Help Pushbutton.

### 3.1. Input Raster Layers

In this section, three data inputs, related to multi-year vegetation index, land-cover and change detection products, are defined. These products are geospatial maps used in the agreement flag analysis that need to have the same spatial resolution and the same map projection. These data inputs can be loaded by pushing the “*Browse*” push button or writing the path to the desired file in the corresponding textbox (Figure 2). If this information is not available, the land-cover and disturbance maps can be skipped as they are optional, although it is preferred to take into account this information to make a meaningful assessment. In such a case, an arbitrary text needs to be written and immediately erased in the textbox, corresponding to the input data layer to be skipped. This step is necessary to the proper execution of this program. The tool can handle input data layers in “*Geotiff*” as well as in “*img*” and “*bil*” ENVI formats.

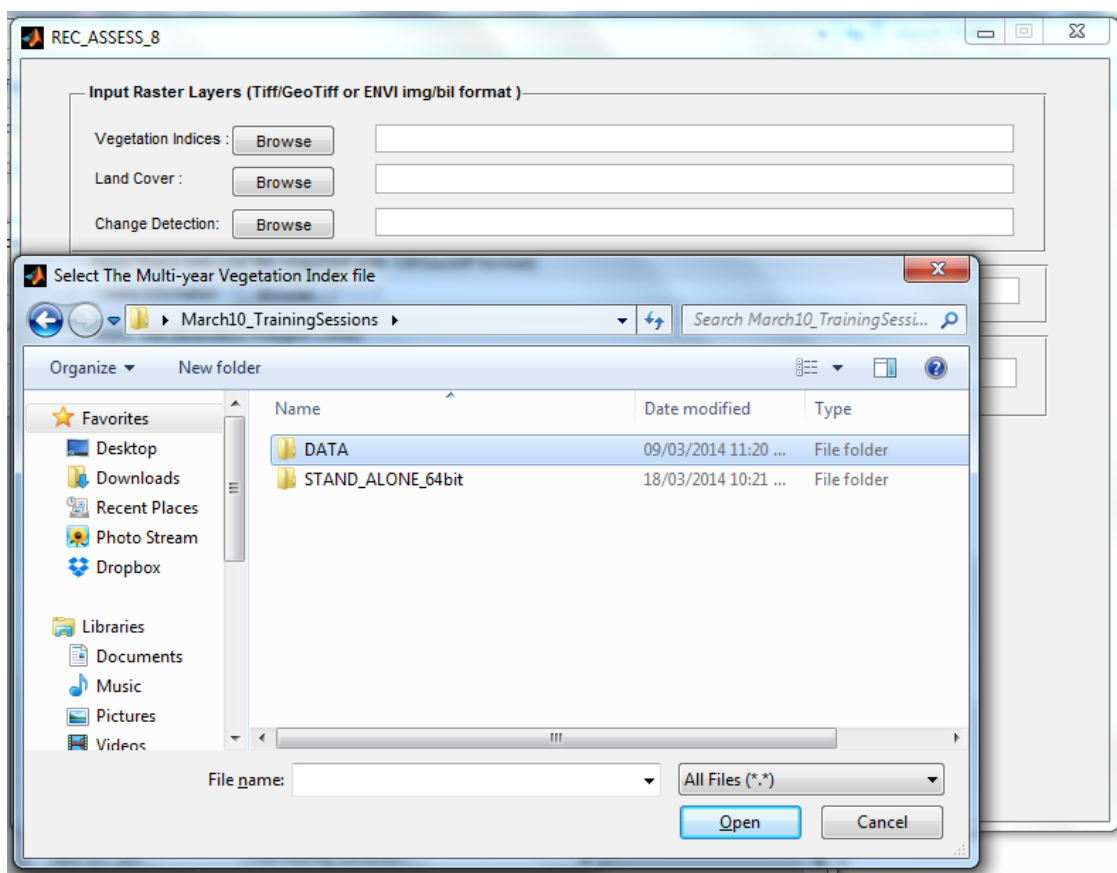


Figure 2: Load the Input Raster Layers by pushing each of the three “*Browse*” pushbuttons or typing in the associated path in each of the corresponding textboxes.

### 3.2 Input Years Info

In this section, a text file summarizing the years for which vegetation index data are available needs to be loaded when the vegetation index input data are in Geotiff format. The file can be loaded by pushing the “*Browse*” push button or writing the path to the desired file in the

corresponding textbox (Figure 3). In the text file, each year must be written in a separate line as the following example illustrates:

1998

2001

2003

2009

2011

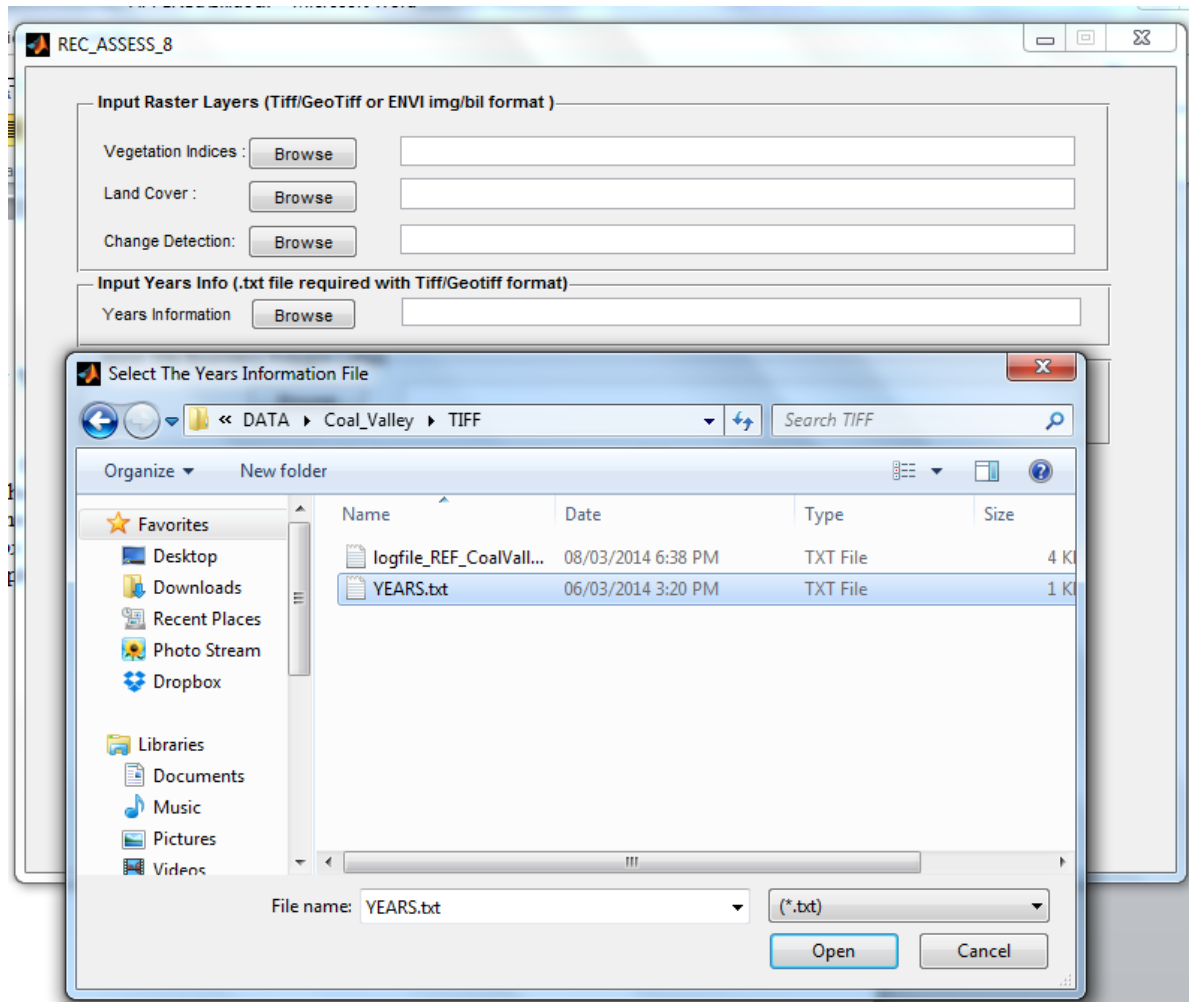


Figure 3: Load the Years Info text file by using the “Browse” pushbutton or text in the associated link in the corresponding textbox.

If using a “Vegetation Index” input data layer in ENVI data format, some arbitrary text needs to be written and immediately erased in the textbox corresponding to the “Year Information”. This is necessary to the proper execution of this program.

### 3.3 Input Site Boundary Polygons

In this section, a shapefile summarizing a set of polygons, corresponding to the lease areas of interest, needs to be loaded by pressing the “*Browse*” pushbutton or writing the link to the desired file in the corresponding textbox (Figure 4). The attribute table associated with this file will be copied in the output shapefile produced with the REC\_ASSESS\_v8.exe at the end of the process. This file has to be in the same map projection as the input data layers defined in section 2.1.

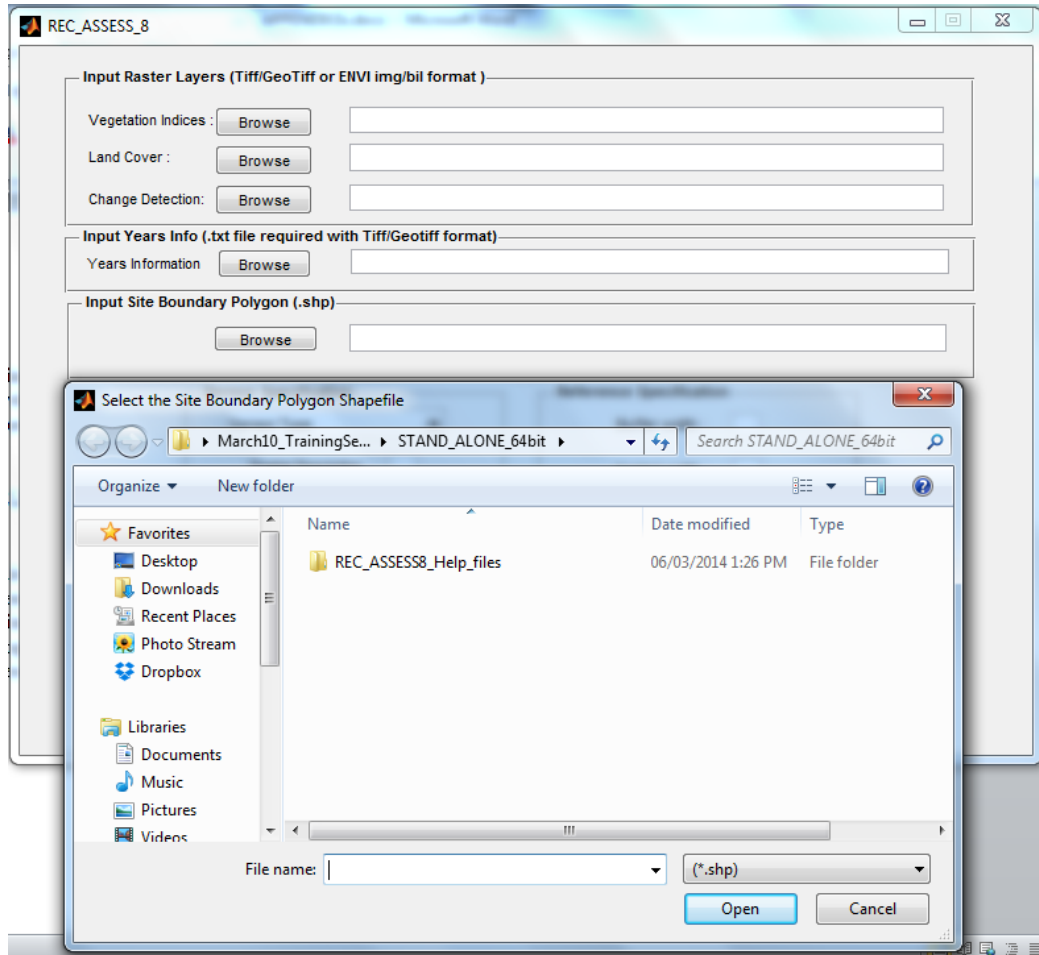


Figure 4: Load the “*site boundary polygons*” shapefile by using the “*Browse*” pushbutton or text in the associated link in the corresponding textbox.

### 3.4 Sensor Specification

In this section, information about the type of sensor that has been used to produce the input data layers needs to be specified. A number of options are provided in the dropdown list as shown in Figure 5. There are three possibilities as follows:

- The input data layers have been produced using the same sensor. In such a case, the type of sensor can be selected from the dropdown list.
- The spatial resolution of the input layers is known to the user. In this case the option “*others*” can be selected from the dropdown list and the spatial resolution can be specified in the textbox as shown in Figure 6.
- The spatial resolution is unknown. The option “*unknown*” must be selected from the dropdown list. In such a case, the spatial resolution will be derived automatically from the input data layer files specified in section 2.1.

The screenshot displays the REC\_ASSESS\_8 application window. It features several input sections: 'Input Raster Layers' with fields for Vegetation Indices, Land Cover, and Change Detection; 'Input Years Info' with a Years Information field; and 'Input Site Boundary Polygon' with a field for the .shp file. The 'Sensor Specification' section contains a dropdown menu that is open, showing options: Sensor Type, SPOT-5, SPOT-4, SPOT-6, RAPIDEYE, Landsat-TM, Landsat-ETM, Landsat-8, Others, and Unknown. To the right, the 'Reference Specification' section includes fields for Buffer width and Control width. Below the sensor dropdown, there are fields for 'data in Tiff/Geotiff or ENVI img/bil format' and 'results (.shp)'. At the bottom, there are 'Run' and 'Help ?' buttons.

Figure 5: Selection of the appropriate sensor option from the dropdown list that will be used to define the input raster data spatial resolution.

The screenshot shows the REC\_ASSESS\_8 application window. It contains several input sections:

- Input Raster Layers (Tiff/GeoTiff or ENVI img/bil format):** Includes three rows for "Vegetation Indices", "Land Cover", and "Change Detection", each with a "Browse" button and a text input field.
- Input Years Info (.txt file required with Tiff/Geotiff format):** Includes a "Years Information" label, a "Browse" button, and a text input field.
- Input Site Boundary Polygon (.shp):** Includes a "Browse" button and a text input field.
- Sensor Specification:** Includes a dropdown menu currently showing "Unknown" and a "Spatial Resolution" input field with the value "30".
- Reference Specification:** Includes "Buffer width" and "Control width" labels, each followed by an empty input field.
- Additional Land Products (raster data in Tiff/Geotiff or ENVI img/bil format):** Includes an "Add Files" button and a large text area.
- Save Reclamation Assessment Results (.shp):** Includes a "Browse" button and a text input field.

At the bottom of the window are two buttons: "Run" and "Help ?".

Figure 6: Selection of the option “Others” from the dropdown list and write in the textbox the spatial resolution associated with the “Input Raster Layers” files.

### 3.5 Reference Specification

In this section, information about the width of the buffer and control areas need to be specified in the corresponding text boxes (Figure 7). The width is defined in pixels. These parameters are used to delineate the buffer and control areas around the site boundary polygon specified in section 2.3 of the final report. The delineation approach is illustrated in Figure 8 using a wellsite-lease area. This approach applies to all types of site boundary polygons.

REC\_ASSESS\_8

**Input Raster Layers (Tiff/GeoTiff or ENVI img/bil format)**

Vegetation Indices :

Land Cover :

Change Detection:

**Input Years Info (.txt file required with Tiff/Geotiff format)**

Years Information

**Input Site Boundary Polygon (.shp)**

**Sensor Specification**

Sensor Type

Spatial Resolution :

**Reference Specification**

Buffer width :

Control width :

**Additional Land Products (raster data in Tiff/Geotiff or ENVI img/bil format)**

**Save Reclamation Assessment Results (.shp)**

Figure 7: Provide the desired buffer and control widths in the Reference Specification section. In this example the buffer and control areas are chosen equal to one pixel and two pixels, respectively.

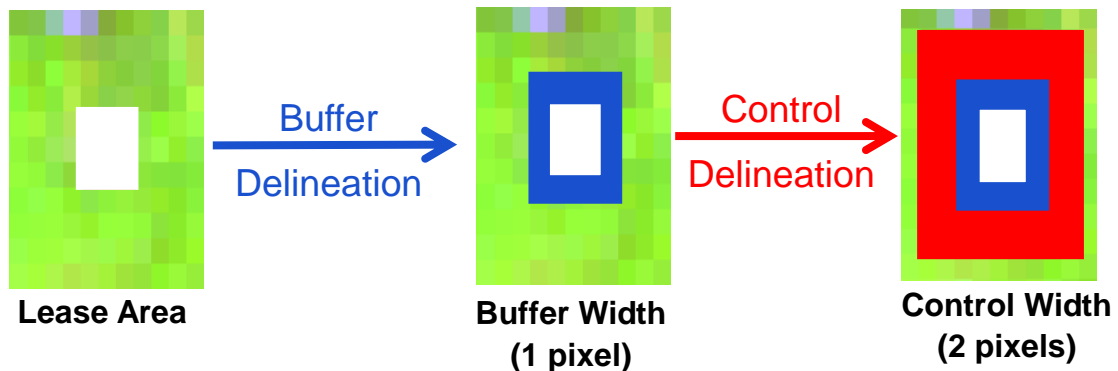


Figure 8: Illustration of the buffer and control areas delineation around a well lease using a width of one pixel and two pixels, respectively.

### 3.6 Additional Land Products

Additional land products that are available can be loaded as described in this section. This information will be extracted for each of the pixels in the lease, buffer and control areas and compiled in the attribute table associated with the output shapefile produced with REC\_ASSESS\_v8.exe at the end of the process. Examples of these additional land products include species composition, leaf area index, canopy height or canopy fractional cover. In this step, it is required to push the “*add button*” file, which will display a new window (Figure 9).

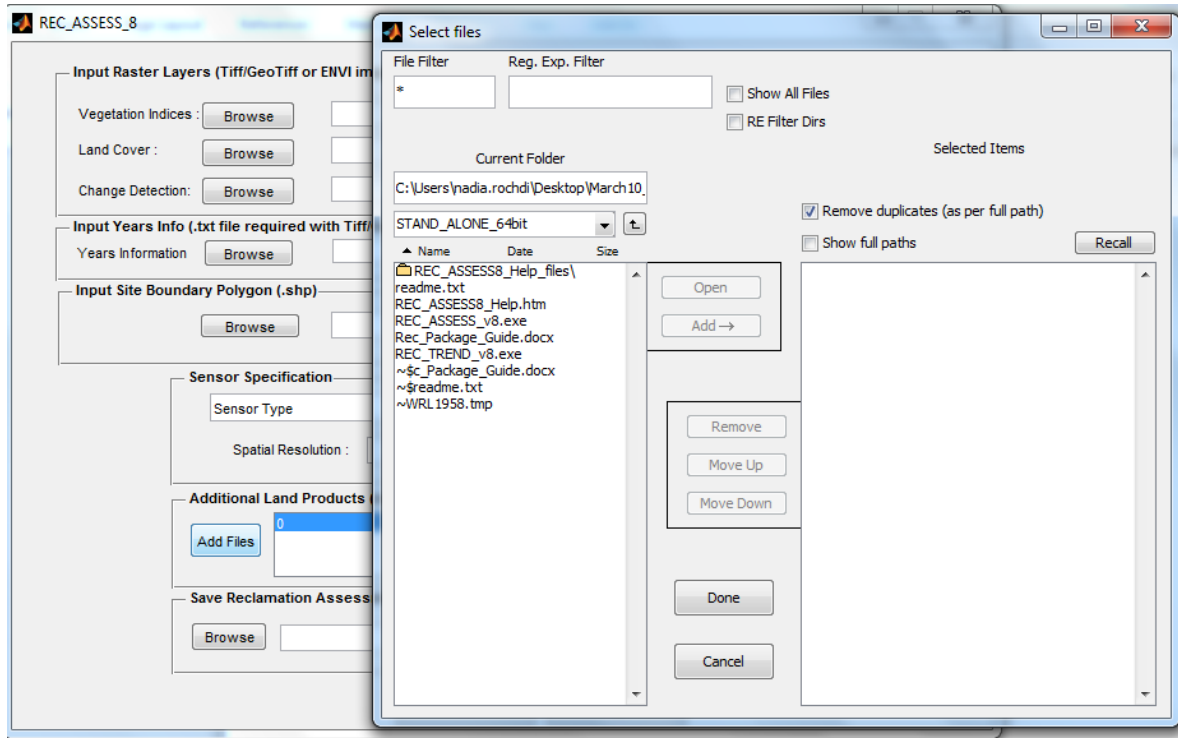


Figure 9: Selection of Additional Land Products using the “*Add Files*” pushbutton.

If no additional land products are available, the new window need to be closed by pushing the “*Done*” pushbutton. Otherwise, the location of the files of interest can be specified by pushing the arrow button on the left side or texting the link to the file location into the “*Current Folder*” textbox. A list of files will appear in the left big box from which the files of interest can be selected and moved to the right big box by pushing the “*Add→*” pushbutton. Once this step is completed, this window can be closed by pushing the “*Done*” pushbutton.

### 3.7 Save Reclamation Assessment Results

In this section, a file name for the output shapefile needs to be specified by pushing the “*Browse*” pushbutton or writing the path to the output file into the corresponding textbox (Figure 10). An

attribute table is then generated, where all data inputs provided in previous sections in addition to the agreement flag are compiled for each pixel in the lease, buffer and control areas.

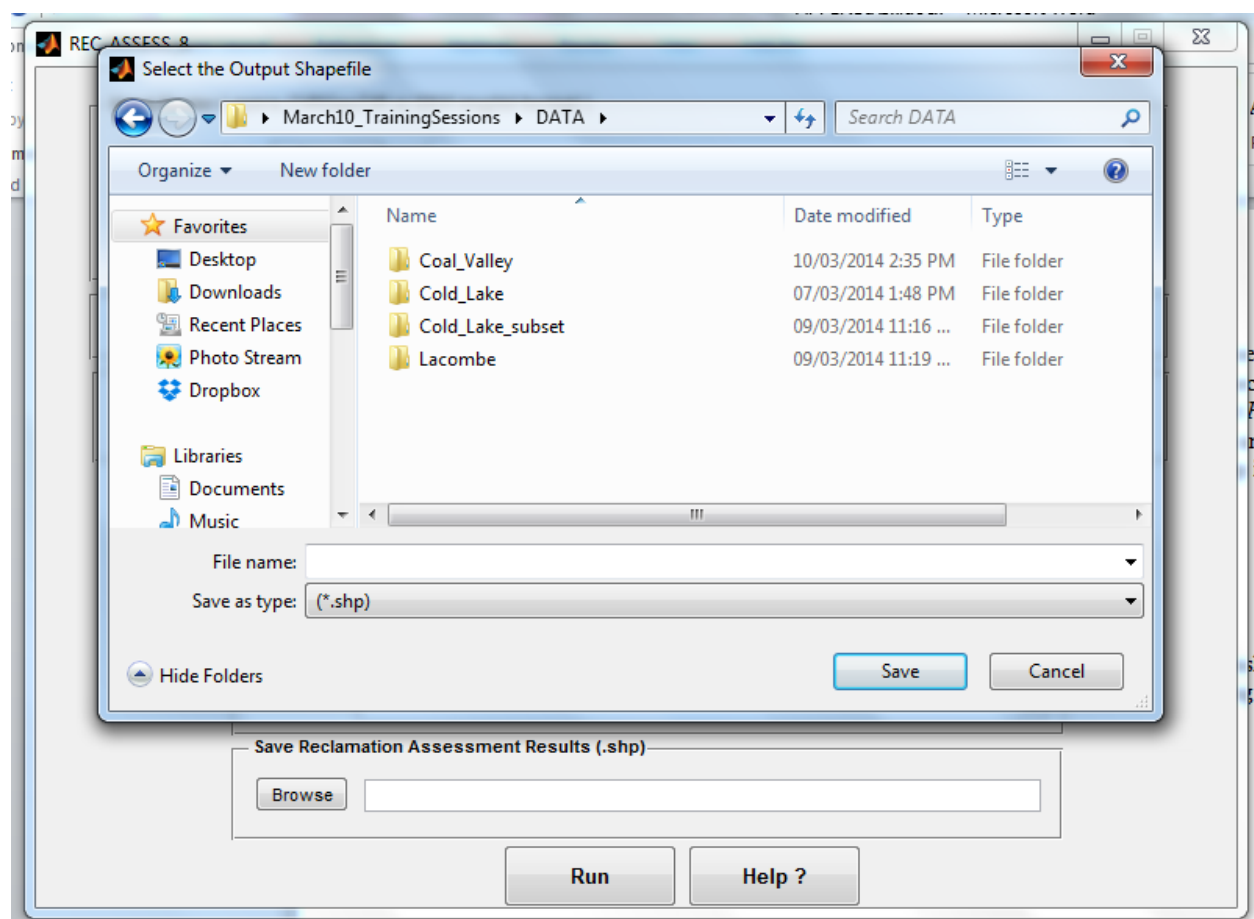


Figure 10: Selection of the output shapefile name, where the reclamation assessment results will be saved.

### 3.8 Run Pushbutton

To run the REC\_ASSESS\_v8.exe, the “Run” pushbutton needs to be pressed. Progress tables are successively displayed during the data processing to indicate the three following processing stages (Figure 11): (1) Reclamation Assessment; (2) Output Shapefile Writing; and (3) Reclamation Assessment Completion. In addition, a log text file summarizing a series of information, such as the geospatial information for each input raster file, the attributes of the site boundary polygon shapefile, the sensor and reference specification parameters, paths to input and output files locations, and processing time is produced and saved in the output shapefile location. An example of this log file is provided later in this Appendix. The log file name format is as following: *logfile\_OutputShapefileName.txt*.

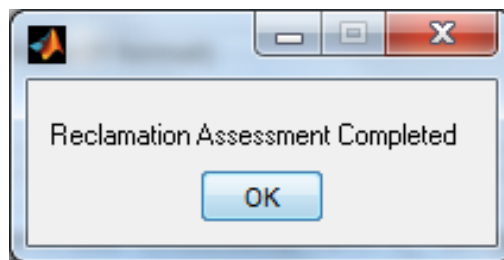
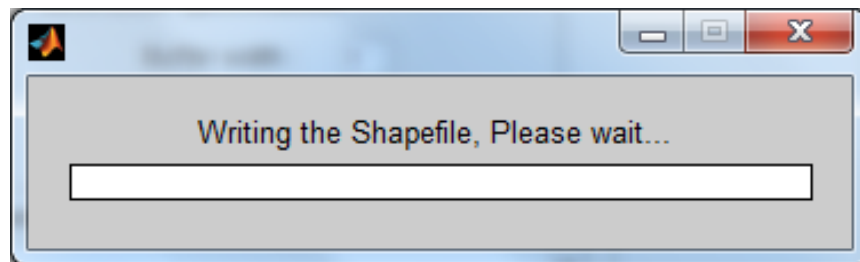
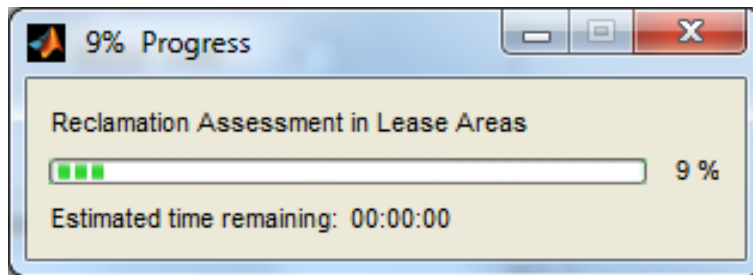


Figure 11: Progress tables indicating the process stages.

### 3.9 Help Pushbutton

The “*Help?*” pushbutton provides access to an html file that explains how the REC\_ASSESS\_v8.exe can be used (Figure 12). This help is provided later in this Appendix.

## REC\_ASSESS\_8.exe HELP GUIDE

Nadia Rochdi  
Alberta Terrestrial Imaging Centre, University of Lethbridge, Lethbridge Alberta

February 3<sup>rd</sup>, 2014

The REC\_ASSESS\_8.exe automated tool is an executable that process a set of remote sensing data products to provide information about reclamation condition in well and mine lease areas.

The tool requires as input variables both raster and shapefile data format. The tool supports the Tiff and Geotiff format as well as both .img and .bil ENVI format. The input data must have the same type of map projection. In addition the raster data must have the same spatial resolution and spatial coverage. The operator needs to assure that these conditions are verified before running the tool.

The three major raster inputs required are: i) a multi-year vegetation index file, ii) a land cover map file; and iii) a change detection map file. Additional raster data information if available can also be processed by the tool. In addition, the tool requires a shapefile summarizing the well/mine lease boundaries.

The REC\_ASSESS\_8 interface (Figure 1) is composed of seven major sections: 1) Input Raster Layers; 2) Input Years Info; 3) Input Site Boundary Polygon; 4) Sensor Specification; 5) Reference Specification; 6) Additional Land Products; 7) Save reclamation Assessment Results. In addition, it also contains two pushbuttons to run the tool and display the associated help.

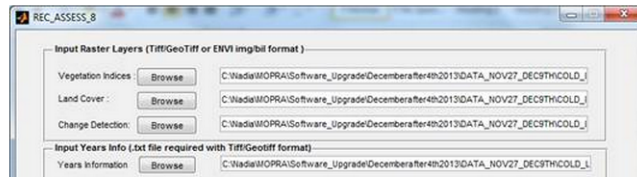


Figure 12: A screen capture of the html help file.

### 3.10 Reclamation Assessment Results

The output shapefile produced with the REC\_ASSESS\_v8.exe is made of a set of polygons where each polygon corresponds to one pixel (Figure 13). The map projection of this output shapefile is similar to the input file map projection. All the attributes provided in the input boundary polygon file are first copied to the output attributes table. Additional attributes (Table 1) are added to this output table (Figures 14 to 16). The land-cover and change-detection information are incorporated in the attribute table only if they are part of the reclamation assessment process. Similarly, if additional land products as specified in section 3.6 of this Appendix were used to run the REC\_ASSESS\_v8.exe, the corresponding attributes will be added to the output table in the order they were loaded immediately before the “*REC\_Trend*” attribute.

Table 1: Examples of the attributes provided in the output shapefile attribute table.

Area	<i>Control, Buffer or Lease</i>
Grid_id	Pixel label for each area (e.g., <i>L1, B2, C10</i> )
Nb_years	Number of years for which vegetation index (VI) data are available
AVAI_VI_Yea	Years for which vegetation index data are available (e.g., NDVI_1998)
VI_YEAR	Vegetation index value at a given year
Total_Grid	Total number of pixels in each of <i>Control, Buffer and Lease</i> areas
MIN_VIYEAR	Minimum VI value for a given area, year, and land cover
MAX_VIYEAR	Maximum VI value for a given area, year, and land cover
AVG_VIYEAR	Average VI value for a given area, year, and land cover
STD_VIYEAR	Standard deviation VI value for a given area, year, and land cover
FLAG_VIYEAR	Agreement/No-Agreement flag for a given lease pixel in a given year
CONT_STAT	Land-cover similarity with control areas for each lease pixel
Land_Cover	Land-cover type
Land_Manage_U	A blank space to be used by the user to input information about land cover based on their personal assessment
Change_Detec	Presence of disturbance
Rec_Trend	Link to the location of reclamation trend plots



Figure 13: A screen capture of the output shapefile produced with REC\_ASSESS\_v8.exe as displayed in ESRI/Arcmap.

Lease, buffer and controls areas are displayed in green, red and yellow, respectively.

L_D_ABAND	L_D_REVEG	L_D_RECLAIMC	L_D_REC_CERC	L_D_REC_INSC	L_RECCERT_NC	L_DISPO_TYPC	L_D_SPUD	Area
20000313			20120221				20000309	Buffer
20000313			20120221				20000309	Control
20000313			20120221				20000309	Control
20000313			20120221				20000309	Control
20000313			20120221				20000309	Control
20000313			20120221				20000309	Buffer
20000313			20120221				20000309	Lease
20000313			20120221				20000309	Lease
20000313			20120221				20000309	Buffer
20000313			20120221				20000309	Buffer
20000313			20120221				20000309	Control
20000313			20120221				20000309	Control
20000313			20120221				20000309	Control
20000313			20120221				20000309	Control
20000313			20120221				20000309	Buffer
20000313			20120221				20000309	Lease
20000313			20120221				20000309	Lease
20000313			20120221				20000309	Lease
20000313			20120221				20000309	Buffer
20000313			20120221				20000309	Control

Figure 14: A screen capture of the attribute table associated with the output shapefile produced with the REC\_ASSESS\_v8.exe. The attributes provided in the input boundary polygon file (e.g., reclamation certification date, well abandon date) are copied for each pixel in addition to an “Area” attribute, which is included to specify if the pixel belongs to a lease, buffer or control area.

MIN_VI2001	MAX_VI2001	AVG_VI2001	STD_VI2001	FLAG_VI2001N
0.70127	0.83015	0.76244	0.03276	0
0.70127	0.83015	0.76244	0.03276	0
0.70127	0.83015	0.76244	0.03276	0
0.70127	0.83015	0.76244	0.03276	0
0.70127	0.83015	0.76244	0.03276	0
0.70127	0.83015	0.76244	0.03276	0
0.70127	0.83015	0.76244	0.03276	0
0.70127	0.83015	0.76244	0.03276	0
0.70127	0.83015	0.76244	0.03276	0
0.70127	0.83015	0.76244	0.03276	0
0.70127	0.83015	0.76244	0.03276	0
0.70127	0.83015	0.76244	0.03276	0
0.70127	0.83015	0.76244	0.03276	0
0.70127	0.83015	0.76244	0.03276	0
0.70127	0.83015	0.76244	0.03276	0
0.70127	0.83015	0.76244	0.03276	0
0.76781	0.82317	0.79656	0.020405	0
0.76781	0.82317	0.79656	0.020405	0
0.76781	0.82317	0.79656	0.020405	0
0.70127	0.83015	0.76244	0.03276	0

Figure 15: A screen capture of the attribute table associated with the output shapefile produced with the REC\_ASSESS\_v8.exe. Minimum, maximum, average, and standard deviation values of the vegetation index for each of the years available as well as an agreement flag for each year are provided for each pixel.

CONT_STAT	Land_Cover	Land_Mana_UC	Chang_DetectN
UNDEF	Coniferous_forest		0
UNDEF	Coniferous_forest		0
UNDEF	Mixed_forest		0
UNDEF	Wetland		0
UNDEF	Wetland		0
UNDEF	Wetland		0
AVAI	Wetland		0
AVAI	Mixed_forest		0
UNDEF	Wetland		0
UNDEF	Coniferous_forest		0
UNDEF	Mixed_forest		0
UNDEF	Wetland		0
UNDEF	Wetland		0
UNDEF	Wetland		0
AVAI	Mixed_forest		0
NON_AVAI	Shrub_Herbaceous		1
AVAI	Mixed_forest		1

Figure 16: A screen capture of the attribute table associated with the output shapefile produced with the REC\_ASSESS\_v8.exe. Examples of attributes include land cover and change for each pixel. In addition, a “CONT\_STAT” attribute was included to indicate if the lease land-cover type is present in the control area. For a lease pixel, this attribute is labeled either as available “AVAI” or unavailable “NON\_AVAI”. For control and buffer pixels, this attribute is labeled as undefined “UNDEF”.

#### 4. Reclamation Trend Module

The reclamation trend module is an executable called REC\_TREND.exe that produces a temporal trend of a vegetation index for the lease and control areas. The module user interface is provided in Figure 17. It requires as input the output shapefile produced with the REC\_ASSESS\_v8.exe. This file can be loaded either by pressing the “Rec\_Assessment Shapefile” pushbutton or by writing its associated path into the corresponding textbox. In addition, a license number of the well/mine area of interest for which the temporal trend will be plotted needs to be specified. This module can be run by pressing the “Generate Trend Plot” pushbutton. Three progress bars are successively displayed indicating the progress of the following three steps: (1) information extraction for the license number of interest; (2) temporal trend plots for the license number of interest; and (3) reclamation trend completion.

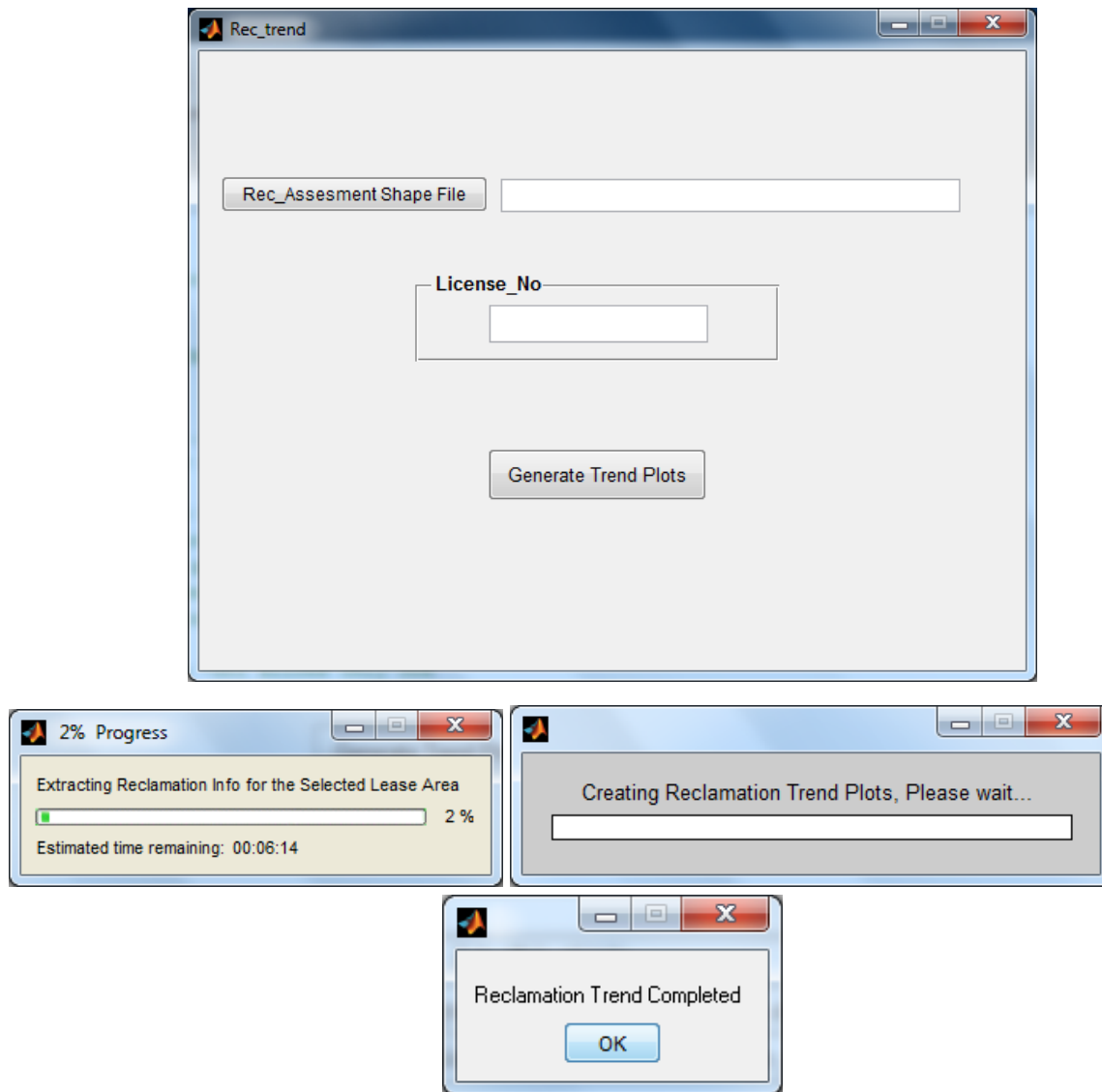


Figure 17: User interface of the Reclamation Trend tool.

A temporal trend plot will be produced for each of the land-cover types present in the lease area (Figure 18). On each plot, information about the lease license number, date of abandonment, date of reclamation certification and the type of land cover are provided. The average VI for each of the lease and reference areas are provided together with their associated error bars which correspond to 2 VI standard deviations. These plots are saved in a bitmap format in a folder in the same location as the output shapefile produced with the REC\_ASSES\_v8.exe. The folder name format is PLOTS\_License\_Nb\_XXX (e.g., PLOTS\_License\_Nb\_48358).

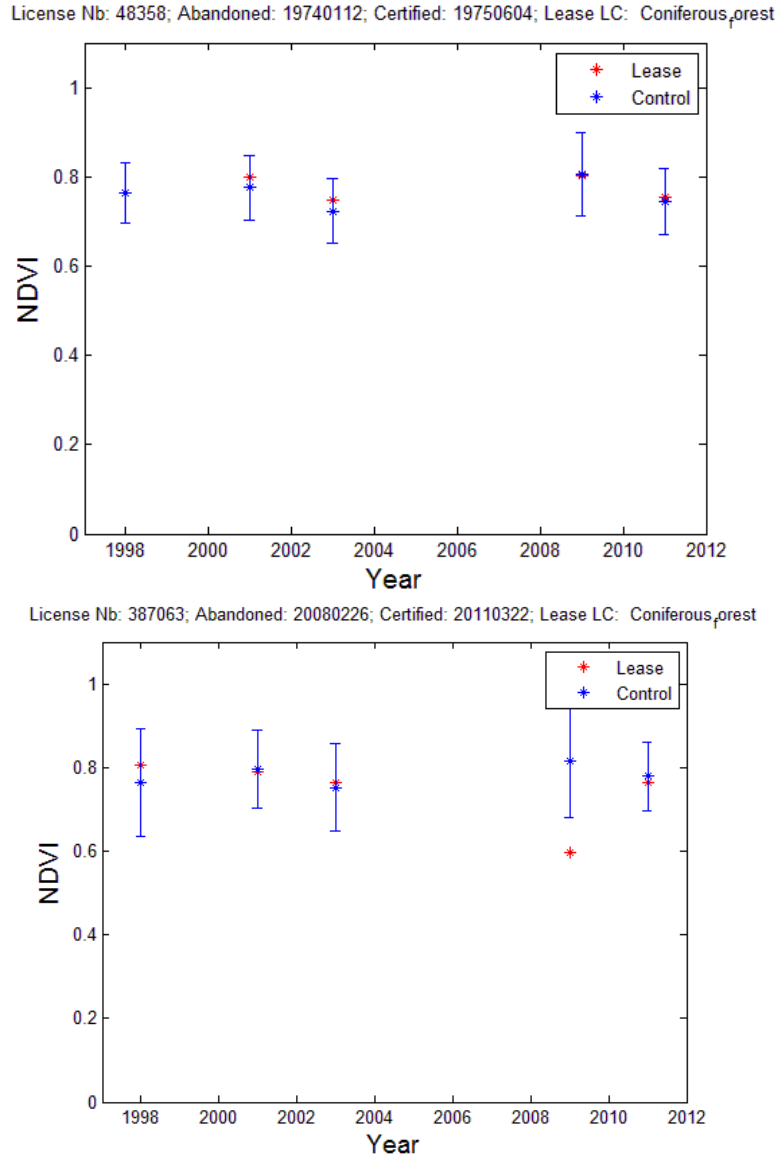


Figure 18: Temporal trend profile examples using NDVI for two different wellsites.

## 5. Conclusions

The present document summarizes the Stand-Alone Reclamation Assessment tool that has been developed within MOPRA as a part of its remote sensing-based monitoring system. The tool is made of reclamation assessment and temporal trend modules that analyze information related to vegetation condition in well/mine lease areas as well as reference areas. A comparison of the vegetation index temporal profiles of these two areas determines the agreement between these areas using statistical parameters.

These modules make use of different types of remote sensing data at different spatial resolution. During the MOPRA project, they have been tested on both multispectral 30 m Landsat and 20 m

SPOT data. The modules have been validated using wellsites as well as mine areas in agricultural and forested landscapes.

Although these modules have been developed within the context of land-reclamation monitoring in mine and oil-and-gas well areas, it is expected that they can be applied to areas affected by other source of disturbance as well as undisturbed areas.

## **6. Contact**

Nadia Rochdi

Alberta Terrestrial Imaging Centre

University of Lethbridge

Phone: 403-332-4447

nadia.rochdi@uleth.ca

## Logfile Example

---

### PROCESSING SUMMARY

---

PROCESSING DATE:

08-Mar-2014 18:40:49

---

### %% VEGETATION INDICES FILE METADATA

---

%% File Path

C:\Users\nadia.rochdi\Desktop\March10\_TrainingSessions\DATA\Cold\_Lake\ENVI\NDVI\_LA  
NDSAT\_CL.bil

%% ENVI File Description

Image\_Columns\_Number: 900

Image\_Lines\_Number: 1041

Image\_Layers\_Nb: 5

Image\_Layers\_Name: [1x55 char]

Map\_Projection: 'UTM,'

Zone: 12

Hemi: 'North,'

Datum: 'WGS-84,'

Units: 'Metres'

Spatial\_Resolution: 30

-----  
%%LANDCOVER FILE METADATA  
-----

%%File Path

C:\Users\nadia.rochdi\Desktop\March10\_TrainingSessions\DATA\Cold\_Lake\ENVI\LC\_LAND  
SAT\_2011\_CL.bil

%%ENVI File Description

Image\_Columns\_Number: 900

Image\_Lines\_Number: 1041

Image\_Layers\_Nb: 1

Image\_Layers\_Name: '{Landsat\_Landcover\_2011}'

Map\_Projection: 'UTM,'

Zone: 12

Hemi: 'North,'

Datum: 'WGS-84,'

Units: 'Metres'

Spatial\_Resolution: 30

%%CHANGE DETECTION FILE METADATA

%%File Path

C:\Users\nadia.rochdi\Desktop\March10\_TrainingSessions\DATA\Cold\_Lake\ENVI\CHANGE  
\_Disturbed.bil

%%ENVI File Description

Image\_Columns\_Number: 900  
Image\_Lines\_Number: 1041  
Image\_Layers\_Nb: 1  
Image\_Layers\_Name: '{Disturbed}'  
Map\_Projection: 'UTM,'  
    Zone: 12  
    Hemi: 'North,'  
    Datum: 'WGS-84,'  
    Units: 'Metres'  
Spatial\_Resolution: 30

-----  
%%OTHER PRODUCTS METADATA  
-----

-----  
%%LEASE AREAS INFO  
-----

%%Directory Path

C:\Users\nadia.rochdi\Desktop\March10\_TrainingSessions\DATA\Cold\_Lake\ENVI\ColdLake\_  
Reclaimed\_Wells.shp

%%Number of Polygons

%%Attributes

11x1 struct array with fields:

Geometry  
BoundingBox  
X  
Y  
OBJECTID  
LICENSE\_NO  
UTM\_ZONE  
UTM\_DATUM  
STATUS  
MERIDIAN  
RANGE  
TOWNSHIP  
SECTION  
SPUD\_DATE  
SHAPE\_Leng  
SHAPE\_Area  
APPROV\_NO  
OPER\_NAME  
FACIL\_TYPE  
FACIL\_ID  
FACIL\_NAME  
UTM\_NORTH  
UTM\_EAST  
D\_SURVEY  
D\_CONSTR  
D\_ABAND

D\_REVEG  
D\_RECLAIM  
D\_REC\_CERT  
D\_REC\_INSP  
RECCERT\_NO  
DISPO\_TYPE  
D\_SPUD

-----  
%%SENSOR TYPE  
-----

Unknown

-----  
%%SPATIAL RESOLUTION(Pixel Size) in METRE  
-----

30

-----  
%%BUFFER WIDTH IN PIXELS  
-----

1

-----  
%%CONTROL WIDTH IN PIXELS  
-----

2

-----

%%OUTPUT SHAPEFILE INFO

-----

%%Directory Path

C:\Users\nadia.rochdi\Desktop\March10\_TrainingSessions\DATA\Cold\_Lake\ENVI\REF\_Cold  
Lake\_Reclaimed\_Wells.shp

-----

PROCESSING TIME IN MINUTES

-----

1

-----

END OF RECLAMATION ASSESSMENT

-----

## **REC\_ASSESS\_8.exe HELP GUIDE**

Nadia Rochdi

Alberta Terrestrial Imaging Centre, University of Lethbridge, Lethbridge Alberta

**February 3<sup>rd</sup>, 2014**

The REC\_ASSESS\_8.exe automated tool is an executable that process a set of remote sensing data products to provide information about reclamation condition in well and mine lease areas.

The tool requires as input variables in both raster and shapefile data format. The tool supports the Tiff and Geotiff format as well as both .img and .bil ENVI format. The input data must have the same type of map projection. In addition, the raster data must have the same spatial resolution and spatial coverage. The operator needs to assure that these conditions are verified before running the tool.

The three major raster inputs required are: (1) a multi-year vegetation index file, (2) a land-cover map file; and (3) a change detection map file. Additional raster data information, if available, can also be processed by the tool. In addition, the tool requires a shapefile summarizing the well/mine lease boundaries.

The REC\_ASSESS\_8 interface (Figure 1) is composed of seven major sections: (1) Input Raster Layers; (2) Input Years Info; (3) Input Site Boundary Polygon; (4) Sensor Specification; (5) Reference Specification; (6) Additional Land Products; and (7) Save Reclamation Assessment Results. In addition, it also contains two pushbuttons to run the tool and display the associated help.

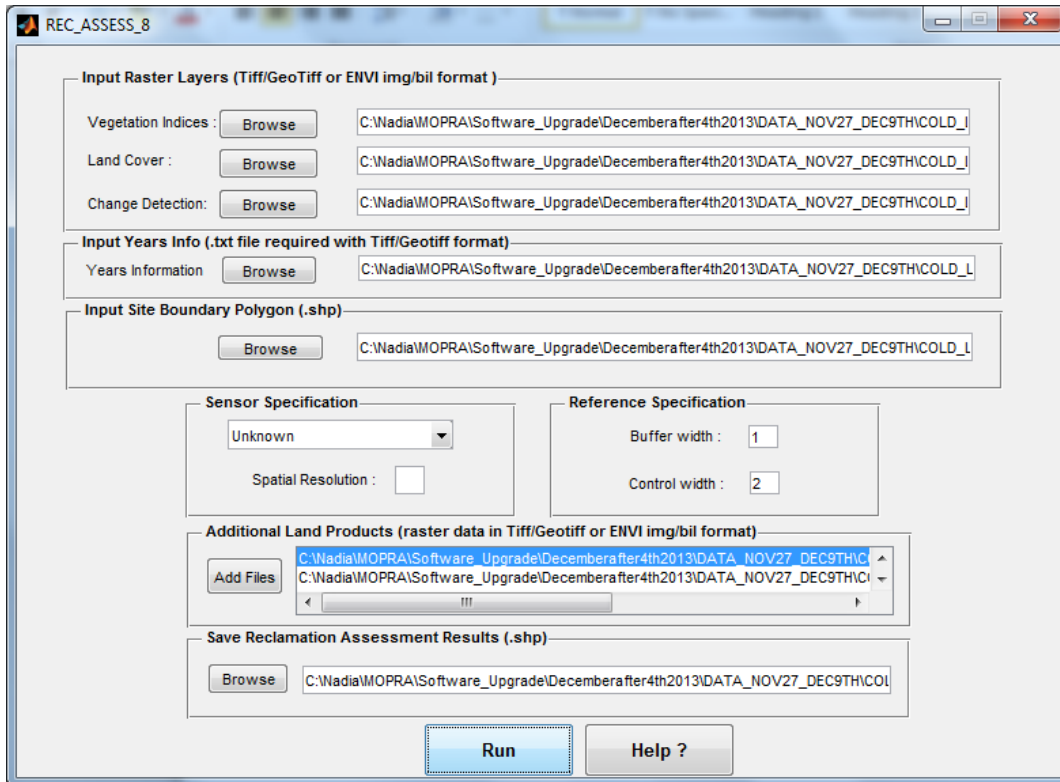


Figure 1: The Rec\_ASSESS\_8 User Interface.

Running the REC\_ASSESS\_8.exe requires the user to follow the steps outlined here.

### Step1: Input Raster Layers Section

1. Select first the multi-year Vegetation Index raster file by pushing the browse button and navigating to the folder where the file is located.
2. Then select the land cover map raster file using the corresponding browse button.
3. Finally, in the same way select the change detection raster file.

*Note:*

- *Raster data format must be in Tiff/Geotiff or ENVI format (bil or img).*
- *Raster files must have the same spatial coverage and the same spatial resolution.*
- *The change detection file is optional and can be skipped if this information is not available. If the user decides to do so, he/she still needs to write in the corresponding textbox an arbitrary text and delete it so the tool can properly run.*
- *The above input files are used in the assessment of reclamation within lease areas.*

- *The multi-year Vegetation index raster file should be named as following: “VI\_XXX.\*” (e.g., NDVI\_ColdLake.bil).*
- *The layers in the multi-year Vegetation index raster file should be named as follows: “VI\_Year” (e.g., NDVI\_1998).*

## **Step2: Input Years Info Section**

1. If the multi-year Vegetation Index raster file is in Tiff/Geotiff format, the user needs to load a .txt file that summarizes the years for which vegetation index data are available. The number of years will be equivalent to the number of layers available in the multi-year Vegetation index raster file.
2. The .txt file must list the years as shown in the example below:
  - 1998
  - 2001
  - 2003
  - 2009
  - 2011

### *Note:*

- *This step can be skipped if the multi-year vegetation index raster file is in the ENVI .img or .bil format.*
- *If the user decides to skip this step he still needs to write in the corresponding textbox an arbitrary text and delete it so the tool can properly run.*
- *In addition to NDVI the tool can handle different types of vegetation indices such as Simple Ratio (SR), Infrared Simple Ratio (ISR), Enhanced Vegetation Index (EVI), and Atmospherically Resistant Vegetation Index (ARVI).*

## **Step 3: Input Site Boundary Polygon Section**

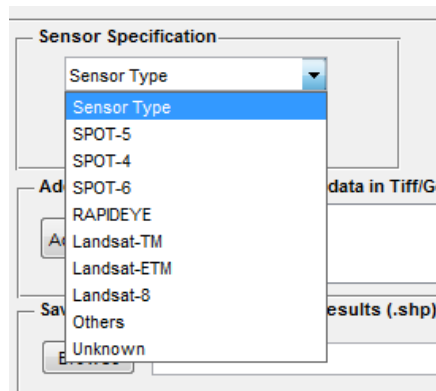
1. Select the shapefile that contains the well/mine lease polygons by pushing the browse button and navigating to the folder where the file is located.
2. The tool is set up so it can process the attributes format provided by ESRD. The following attributes need to have the following format:
  - LICENSE\_NO (lease license number),

- D\_ABAND (abandonment date), and
- D\_REC\_CERT (reclamation certification date).

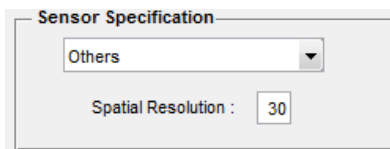
*Note: All the attributes associated with the lease polygons will be saved in the output shapefile.*

#### Step 4: Sensor Specification Section:

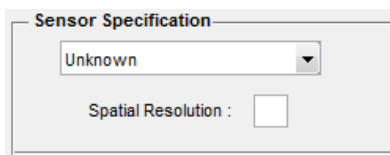
1. This step is required to determine the spatial resolution of the multi-year Vegetation Index raster file. The user can use the following three options to provide this information:
  - a. If the user knows which sensor has been used to derive the above mentioned file, a sensor type can be selected from the sensor list provided by pushing the following top-down list.



- a. If the user knows the spatial resolution of the multi-year Vegetation Index raster file, he can select “others” from the top-down list and write the spatial resolution value in the “spatial resolution” textbox:

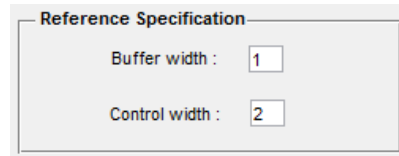


- a. If the spatial resolution of the multi-year Vegetation Index raster file and the sensor type is unknown to the user, he can select “unknown” from the top-down list as shown below. The spatial resolution will be automatically extracted.



### Step 5: Reference Specification Section

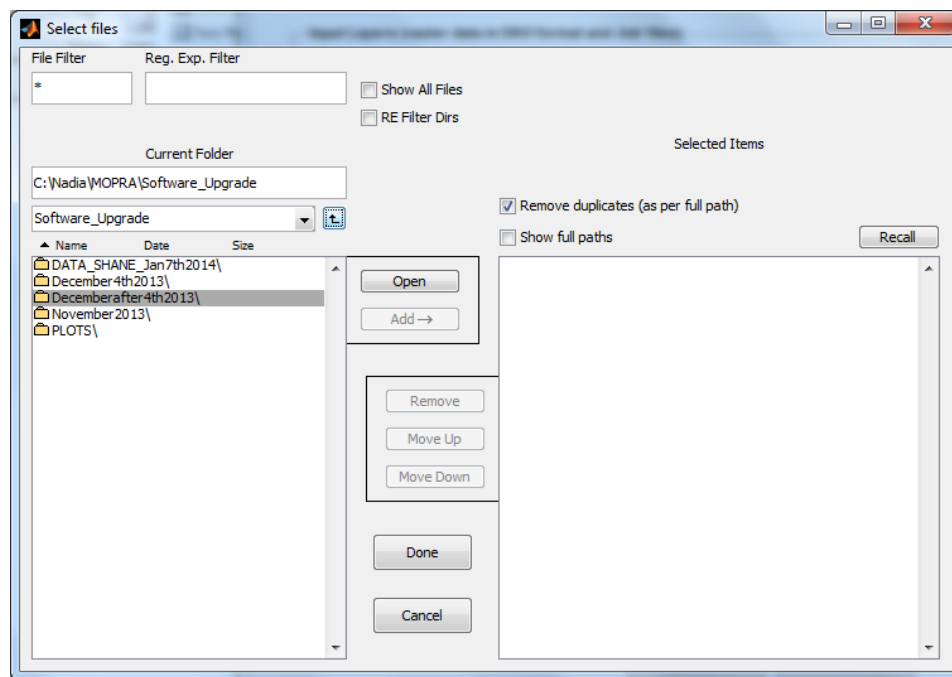
1. The user needs to define the buffer and control widths. These parameters are used to delineate the reference areas to be used as control for assessing the condition of vegetation within the reclaimed lease area.
2. The buffer and control widths are defined in pixels. In the following example one and two pixels were used for buffer and reference widths, respectively.



A dialog box titled "Reference Specification" with two input fields. The first field is labeled "Buffer width :" and contains the value "1". The second field is labeled "Control width :" and contains the value "2".

### Step 6: Additional Land Products Section

1. *This step is optional.* In this section other land products such as canopy structural attributes, leaf area index, or species composition that might be available to the user can be loaded by pushing the add file button and selecting the following files of interest.



*Note: The products provided in this section are not used in the assessment process. However, they are extracted for lease, buffer and control areas and added as attributes in the output shapefile.*

## Step 7: Save Reclamation Assessment Results

1. Select the output shapefile name where the assessment results will be summarised.

*Note:*

- *The output shapefile summarizes all the pixels belonging to lease, buffer and control areas that are delineated by the tool.*
- *In addition to the attributes provided in the Site Boundary Polygon file (section3), a new set of attributes is added including:*

<i>Area</i>	<i>Control, buffer or lease</i>
<i>Grid_id</i>	<i>Pixel label for each area (e.g., L1, B2, C10)</i>
<i>Nb_years</i>	<i>Number of years for which vegetation index (VI) data are available</i>
<i>AVAI_VI_Yea</i>	<i>Years for which vegetation index data are available (e.g., NDVI_1998)</i>
<i>VI_YEAR</i>	<i>Vegetation index value at a given year</i>
<i>Total_Grid</i>	<i>Total number of pixels in each of control, buffer and lease areas</i>
<i>MIN_VIYEAR</i>	<i>Minimum VI value for a given area, year, and land cover</i>
<i>MAX_VIYEAR</i>	<i>Maximum VI value for a given area, year, and land cover</i>
<i>AVG_VIYEAR</i>	<i>Average VI value for a given area, year, and land cover</i>
<i>STD_VIYEAR</i>	<i>Standard deviation VI value for a given area, year, and land cover</i>
<i>FLAG_VIYEAR</i>	<i>Problem/No-problem flag for a given lease pixel in a given year</i>
<i>CONT_STAT</i>	<i>Land-cover similarity with control areas for each lease pixel</i>
<i>Land_Cover</i>	<i>Land-cover type</i>
<i>Land_Manage_U</i>	<i>A blank space to be used by the user to input info about land cover based on their personal assessment</i>
<i>Change_Detec</i>	<i>Presence of disturbance</i>
<i>Rec_Trend</i>	<i>Link to the location of reclamation trend plots</i>

## Step 8: Run REC\_ASSESS\_8

1. After the above steps have been completed the user can push the run pushbutton to execute the reclamation assessment process.
2. A .txt log file will be generated and saved in the output shapefile location. The log file name format is as following: *logfile\_OutputShapefileName.txt*

## APPENDIX 5: Assessment of Reclaimed Areas near Cold Lake Using Hyperspectral Data

Interim Report

December 2014

### 1. Introduction

The present work explores the use of remote sensing data for mapping the condition in reclaimed well sites. The original study area planned for this work was the Long Lake area. However due to a delay in the hyperspectral and ground data availability, the Cold lake area was selected instead. Within this context, the AISA airborne hyperspectral and ground-reference data collected in the Cold Lake study area (Figure 1) within the framework of the MOPRA project (discussed in the main body of this report) were used. Three objectives were defined as follows:

- Mapping of forest species composition using AISA data,
- Simulation of Sentinel-2 VNIR data for species composition mapping, and
- Assessment of reclaimed areas with regard to the reclamation age.

This short report summarizes the findings related to mapping tree species composition using hyperspectral data.



Figure 1. Locations of the Cold Lake study area adopted in the MOPRA project.

## 2. AISA Airborne Hyperspectral and LiDAR Data

AISA and LiDAR data acquired by Terra Remote Sensing Inc. over the Cold Lake study area in July 2012 were delivered to ATIC by the University of Victoria in summer 2013. AISA hyperspectral data were orthorectified based on the LiDAR digital elevation model and atmospherically corrected using the atmosphere radiative transfer model (MODTRAN4) to derive surface reflectance data. LiDAR data were acquired with an average point density of 1 point/m<sup>2</sup> per flight line. However, with most flight lines overlapping, the average density was close to 2 points/m<sup>2</sup>. The study area was flown using the Eagle AISA system at an altitude of 1,150 m, resulting in a spatial resolution of 1.3 m and 138 spectral bands located in the Visible/Near-InfraRed (VNIR) spectral domain (Figure 2). Data were acquired using a total of 26 flight lines covering an area of ~270 km<sup>2</sup> (Figure 3).

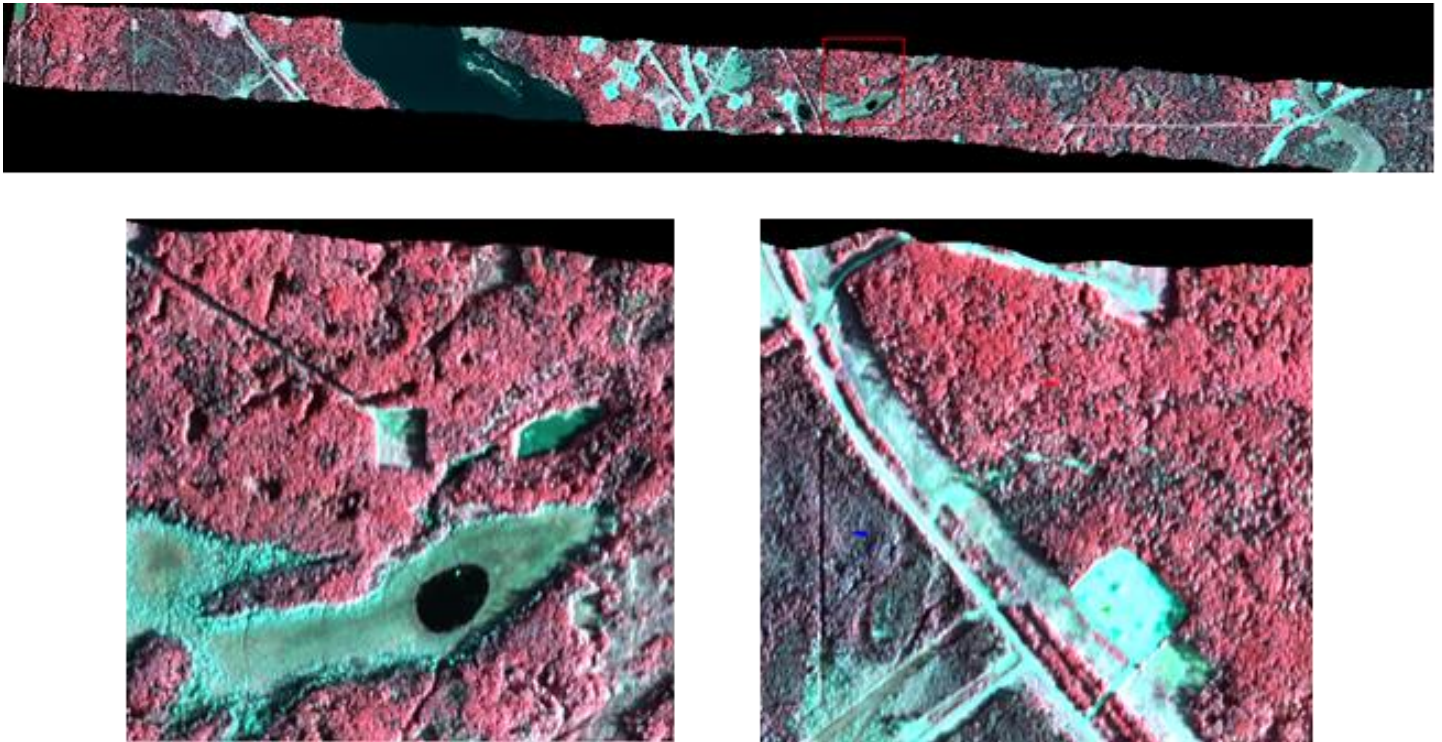


Figure 2. Example of AISA flight lines acquired over the Cold Lake area and zoomed-in subsets.



Figure 3. The 2012 AISA/LiDAR coverage (white boxes) over the Cold Lake study area. The red boxes represent the planned coverage.

### 3. Cold Lake Field Data

The study site, mostly dominated by forest and wetland areas, was characterized on the ground from July 20 to July 30th, 2012. The sampling scheme was governed by the location of certified reclaimed wells and the difficulty of access to these areas. To sample the spatial variability of vegetation regrowth in wellsites, the well's reclamation certificate issue date and the temporal NDVI derived from LANDSAT TM/ETM+ between 1998 and 2011 were used in the site selection procedure. The Alberta Vegetation Inventory data were used to sample wellsites that had different forest characteristics (e.g., species, crown closure). Test plots were selected for each site following the guidelines established by Canada's National Forest Inventory (NFI). For each test plot, geographic coordinates were collected using a GPS, and land-cover type and tree species as well as tree diameter at breast height (DBH) and height were recorded.

## 4. Material and Methods

### 4.1. AISA Hyperspectral and LiDAR Data Processing

The processing of the AISA data was conducted using the ENVI software (Research Systems, Inc. Boulder, Colorado). Sixteen AISA flight lines covering the south part of the study area were processed using the ENVI Effort Polishing module to remove the presence of spikes in the spectral profile. The flight lines were then mosaicked as shown in Figure 4. The Minimum Noise fraction (MNF) transformation was applied to the AISA mosaic to reduce the spectral dimensionality and innate spectral noise. MNF is based on two cascaded principal component analysis (PCA) transformations. The first PCA is applied to decorrelate and rescale the noise in the data and is then followed by the second transformation, which is applied to the noise-whitened data. The resulting MNF transformed bands are organized so that the first MNF bands contain most of the spectral information and the noise progressively increases as function of the increasing MNF components. The first nine MNF components were selected as they were found to represent most of the information embedded in the original spectral data with a minimum of noise. An inverse MNF transformation was then applied to the nine selected MNF bands data to reproduce a noise-reduced hyperspectral data set. Finally both the nine MNF and the noise-reduced hyperspectral data were resampled from 2 m to 5 m by pixel averaging to be consistent with the RapidEye data processing conducted in MOPRA when assessing the performance of both sensors.

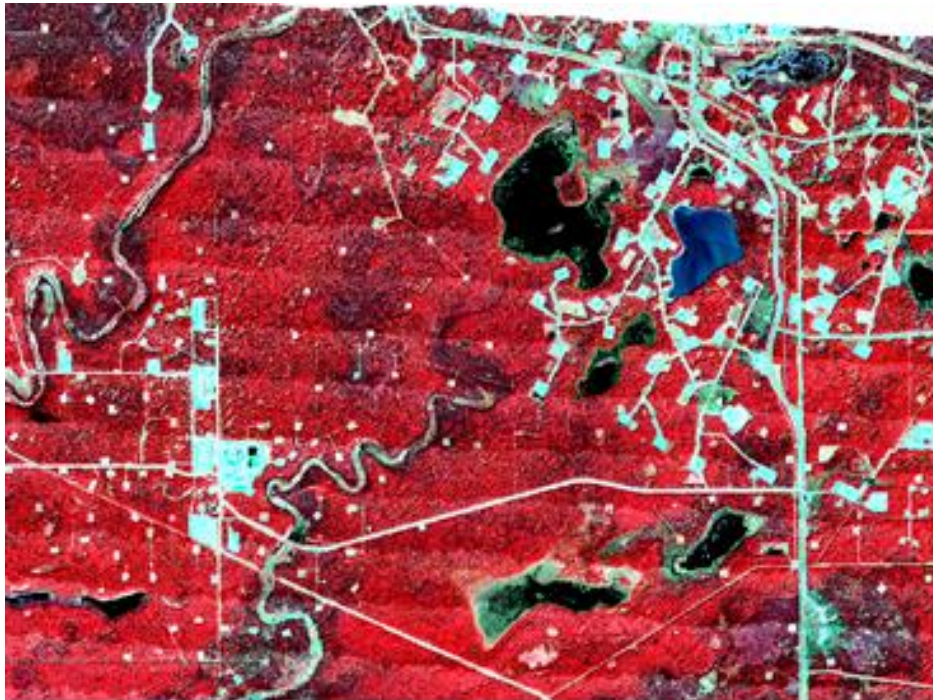


Figure 4. AISA mosaic over the southern part of the Cold Lake study area.

The 2012 LiDAR data acquired over Cold Lake were processed using the FUSION/LDV software (McGaughey 2014). LiDAR point cloud data were filtered to extract the ground returns and generate a 5-m Digital Elevation Model (DEM), which is consistent with the RapidEye spatial resolution. The canopy height model and the percentile heights were derived for all points within a 5-m cell including 50 percentile, 75 percentile, 80 percentile and 95 percentile. Using all LiDAR returns, the percentages of returns above a predefined set of height-break values ranging from 1.4 m to 21.4 m using a 2-m step were calculated within a 5-m cell to stratify the canopy structure profile. In addition, average intensity, terrain slope and aspect were also derived at 5-m resolution.

#### **4.2. *Reference Data***

Reference samples were selected from the 2012 field data and the Alberta Vegetation Inventory Database (AVI) to be used for training and validation of the data classification. Six tree species were considered including trembling aspen, balsam poplar, white spruce, black spruce, tamarack, and jack pine. The reference samples were selected in AVI polygons where the forest cover is above 50% and the percentage cover of the dominant species is above 80%. The 2012 field data collected including tree species, height, and diameter at breast (DBH) were also used. Plots where dominant species have more than 80% volume were selected as a reference set for tree species classification. In total, 169 reference samples were selected; 70% was used for training and 30% was saved for validation purposes.

#### **4.3. *Tree-Species Classification Using the Random Forest Technique***

Non-forested areas were removed from the analysis using a LiDAR-based mask with areas where the canopy height exceeds 1 m. The Random Forest decision tree (RF) classifier was selected due to the good performances it showed in MOPRA when compared to the support vector machine technique. Using the R-project software (<http://www.r-project.org/>), RF was applied to the nine MNF and noise-reduced hyperspectral data alone and in combination with LiDAR data. An accuracy assessment was conducted to characterize the performance using the following accuracy measures:

- Overall accuracy: the probability that pixels in the land-cover map have been correctly classified,
- User accuracy: the probability that pixels for a given class of the land-cover map have been correctly classified, and
- Producer accuracy: the probability that a given land-cover class on the ground was correctly represented in the land-cover map.

### **5. *Preliminary Results***

Visual inspection of each of the four tree species maps produced showed a “salt and pepper” appearance in the classification of the noise-reduced hyperspectral data (Figure 5). This effect tends to be reduced in the classification map produced based on the nine MNF components.

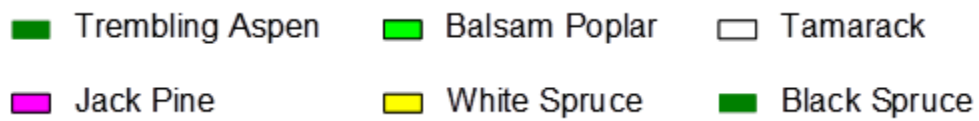
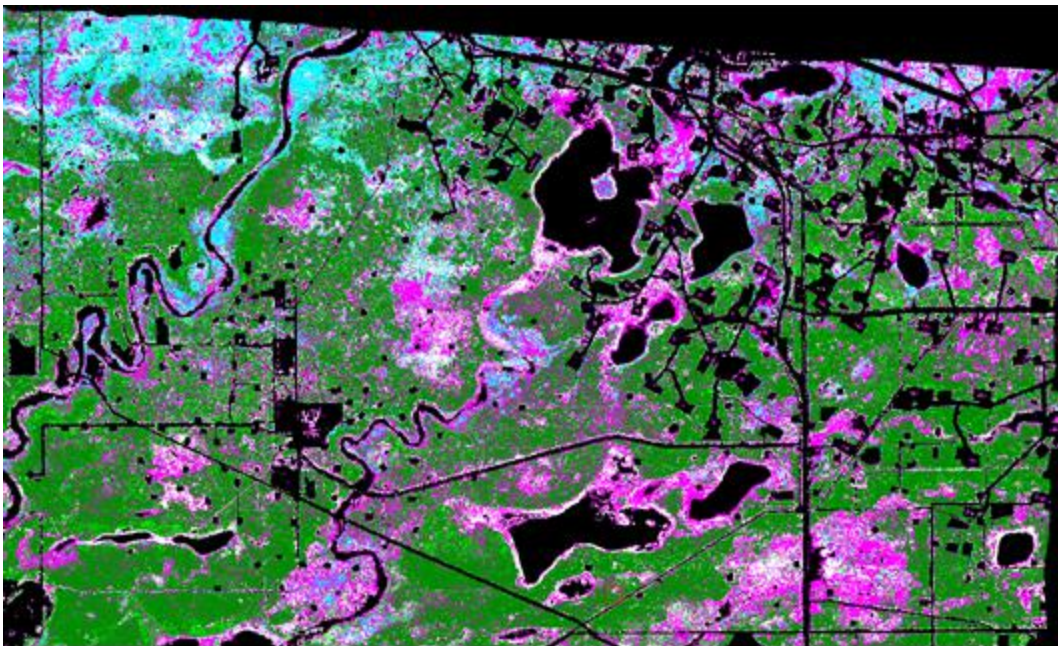
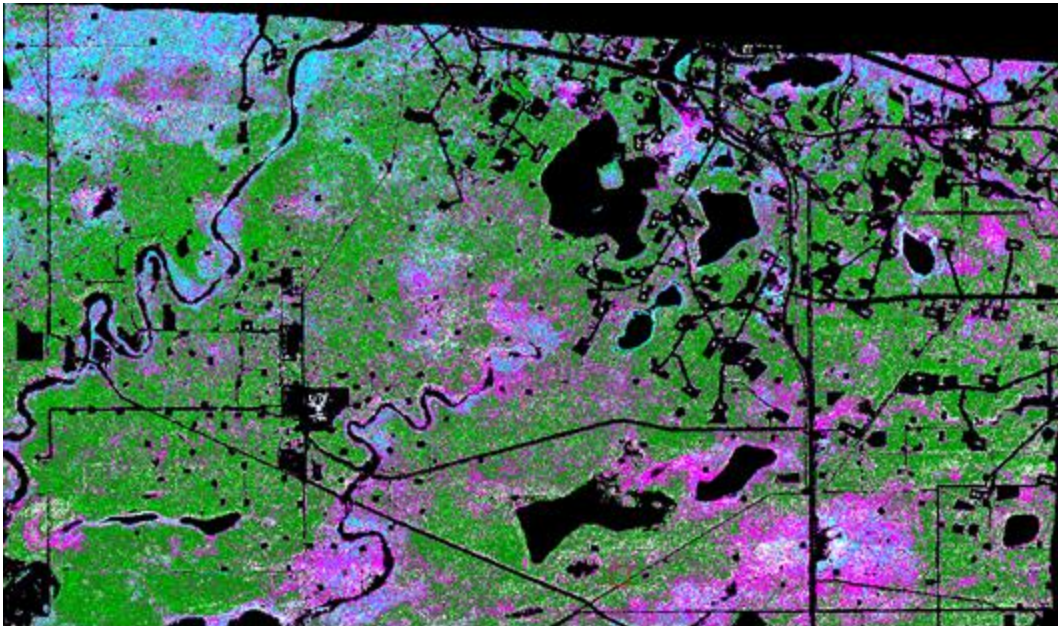


Figure 5. Tree species map produced using the noise-reduced AISA data (top) and the LiDAR/nine MNF data (bottom).

In general, the classification maps based on hyperspectral data lacked well-defined spatial patterns associated with the type of tree species. Introducing the structural information derived from the LiDAR data reduced considerably the “salt and pepper” appearance in the hyperspectral-based classification maps and introduced spatial patterns where tree species tends to be grouped into distinct clusters. This improvement was visually more pronounced when combining LiDAR with the nine MNF components (Figure 5).

A similar trend was observed when assessing the accuracy measures for each type of dataset used (Table 1). Overall accuracy was low to moderate ranging between 41% and 63% with the highest values observed for the LiDAR-based datasets. As much as 18% to 19% improvement in overall accuracy was obtained when adding LiDAR data. Producer’s accuracies were generally low when using noise-reduced hyperspectral data, ranging from ~20% to ~54% with the exception of trembling aspen, which has an accuracy of 70%. However, user accuracies were found low not exceeding 56% for all tree species. Using the nine MNF components showed higher producer’s and user’s accuracy values with an improvement between 1% and ~13% compared to the noise-reduced data. The variation range was from 29% to 70% for producer’s accuracy and from 29% to 60% for user’s accuracy. The positive effect of LiDAR was also observed for user’s and producer’s accuracies. Accordingly, producer’s accuracies for the LiDAR/noise-reduced data range from ~43% to ~70%, while user’s accuracies were between ~37% and 63%. For the LiDAR/nine MNF data, the producer’s accuracies range from ~33% to ~79% and the user’s accuracies vary between ~56% and 71%. Overall, producer’s and user’s accuracies have the highest values when using the LiDAR/nine MNF data except for trembling aspen and tamarack.

## **6. Conclusion**

Assessment of the AISA hyperspectral data for mapping tree species was not successful as accuracies are low to moderate for both the noise-reduced and the nine MNF data. Although improvement was observed when adding the LiDAR-based information, accuracy values overall remain moderate. This is not consistent with the results observed when assessing the spaceborne CHRIS/PROBA hyperspectral data in MOPRA, where high accuracies were obtained for all species. These differences could be attributed to various reasons including:

- The CHRIS PROBA data is a one-time acquisition, which makes the acquisition geometry consistent for each pixel. This is not the case for the AISA data as it involves a series of flight lines that required more than two hours to acquire. This resulted not only in a changing solar geometry, but also in variation of the viewing angle that will introduce changes in the signal of areas with similar characteristics. This would have a major impact on the training process as a large variability will be introduced in the spectral signature for a given class type.
- The CHRIS/PROBA data were assessed using a different approach and involving different training samples. The quality of the training areas used in this work might have contributed to the low accuracy obtained.

Table 1. Summary of the accuracy assessment results obtained for each of the four datasets.

Tree Species	Accuracy Measures (%)	Noise-Reduced	Nine MNF Bands	LIDAR & Nine MNF Bands	LIDAR & Noise-Reduced
	Overall Accuracy	41.00	45.00	63.00	60.00
<b>Trembling Aspen</b>	Producer Accuracy	70.10	67.20	79.10	85.00
	User Accuracy	51.10	59.20	63.10	70.40
<b>Tamarck</b>	Producer Accuracy	31.70	35.40	65.90	58.50
	User Accuracy	54.20	59.20	58.10	67.60
<b>Balsam Poplar</b>	Producer Accuracy	25.40	28.60	33.30	36.50
	User Accuracy	28.60	41.90	75.00	43.40
<b>Jack Pine</b>	Producer Accuracy	54.20	59.70	62.50	62.50
	User Accuracy	30.00	36.40	56.30	49.50
<b>Black Spruce</b>	Producer Accuracy	47.70	47.70	69.40	60.40
	User Accuracy	55.80	60.20	70.60	66.30
<b>White Spruce</b>	Producer Accuracy	22.30	35.00	62.10	57.30
	User Accuracy	29.90	29.00	61.50	62.80

Addressing the first reason would require correcting the data for the effect of the bidirectional reflectance distribution function. Due to the considerable time this would require, the BRDF effect correction is not achievable within the framework of this work due to the limited timeline. However, to identify if this is a reasonable cause, the next step of this work will focus on one flight line, although the number of species might be reduced as it will depend on the flight-line coverage. Accordingly, the effect of the acquisition geometry would be minimized and higher accuracies in tree species mapping would be expected.

In addition, further refinement of the training areas will be investigated to improve the results accuracies. The effect of the spectral band selection and data reduction will be also further examined to improve the classification accuracy.

## **7. References**

McGaughey, R.J. 2014. FUSION/LDV: Software for LiDAR Data Analysis and Visualization. Version 3.42. Pacific Northwest Research Station, US Forest Service, Portland, Oregon.

## LIST OF OSRIN REPORTS

OSRIN reports are available on the University of Alberta's Education & Research Archive at <http://hdl.handle.net/10402/era.17209>. The Technical Report (TR) series documents results of OSRIN funded projects. The Staff Reports (SR) series represent work done by OSRIN staff.

### **OSRIN Technical Reports – <http://hdl.handle.net/10402/era.17507>**

BGC Engineering Inc., 2010. Oil Sands Tailings Technology Review. OSRIN Report No. TR-1. 136 pp. <http://hdl.handle.net/10402/era.17555>

BGC Engineering Inc., 2010. Review of Reclamation Options for Oil Sands Tailings Substrates. OSRIN Report No. TR-2. 59 pp. <http://hdl.handle.net/10402/era.17547>

Chapman, K.J. and S.B. Das, 2010. Survey of Albertans' Value Drivers Regarding Oil Sands Development and Reclamation. OSRIN Report TR-3. 13 pp. <http://hdl.handle.net/10402/era.17584>

Jones, R.K. and D. Forrest, 2010. Oil Sands Mining Reclamation Challenge Dialogue – Report and Appendices. OSRIN Report No. TR-4. 258 pp. <http://hdl.handle.net/10402/era.19092>

Jones, R.K. and D. Forrest, 2010. Oil Sands Mining Reclamation Challenge Dialogue – Report. OSRIN Report No. TR-4A. 18 pp. <http://hdl.handle.net/10402/era.19091>

James, D.R. and T. Vold, 2010. Establishing a World Class Public Information and Reporting System for Ecosystems in the Oil Sands Region – Report and Appendices. OSRIN Report No. TR-5. 189 pp. <http://hdl.handle.net/10402/era.19093>

James, D.R. and T. Vold, 2010. Establishing a World Class Public Information and Reporting System for Ecosystems in the Oil Sands Region – Report. OSRIN Report No. TR-5A. 31 pp. <http://hdl.handle.net/10402/era.19094>

Lott, E.O. and R.K. Jones, 2010. Review of Four Major Environmental Effects Monitoring Programs in the Oil Sands Region. OSRIN Report No. TR-6. 114 pp. <http://hdl.handle.net/10402/65.20287>

Godwalt, C., P. Kotecha and C. Aumann, 2010. Oil Sands Tailings Management Project. OSRIN Report No. TR-7. 64 pp. <http://hdl.handle.net/10402/era.22536>

Welham, C., 2010. Oil Sands Terrestrial Habitat and Risk Modeling for Disturbance and Reclamation – Phase I Report. OSRIN Report No. TR-8. 109 pp. <http://hdl.handle.net/10402/era.22567>

Schneider, T., 2011. Accounting for Environmental Liabilities under International Financial Reporting Standards. OSRIN Report TR-9. 16 pp. <http://hdl.handle.net/10402/era.22741>

Davies, J. and B. Eaton, 2011. Community Level Physiological Profiling for Monitoring Oil Sands Impacts. OSRIN Report No. TR-10. 44 pp. <http://hdl.handle.net/10402/era.22781>

Hurndall, B.J., N.R. Morgenstern, A. Kupper and J. Sobkowicz, 2011. Report and Recommendations of the Task Force on Tree and Shrub Planting on Active Oil Sands Tailings Dams. OSRIN Report No. TR-11. 15 pp. <http://hdl.handle.net/10402/era.22782>

Gibson, J.J., S.J. Birks, M. Moncur, Y. Yi, K. Tatttrie, S. Jasechko, K. Richardson, and P. Eby, 2011. Isotopic and Geochemical Tracers for Fingerprinting Process-Affected Waters in the Oil Sands Industry: A Pilot Study. OSRIN Report No. TR-12. 109 pp. <http://hdl.handle.net/10402/era.23000>

Oil Sands Research and Information Network, 2011. Equivalent Land Capability Workshop Summary Notes. OSRIN Report TR-13. 83 pp. <http://hdl.handle.net/10402/era.23385>

Kindzierski, W., J. Jin and M. Gamal El-Din, 2011. Plain Language Explanation of Human Health Risk Assessment. OSRIN Report TR-14. 37 pp. <http://hdl.handle.net/10402/era.23487>

Welham, C. and B. Seely, 2011. Oil Sands Terrestrial Habitat and Risk Modelling for Disturbance and Reclamation – Phase II Report. OSRIN Report No. TR-15. 93 pp. <http://hdl.handle.net/10402/era.24547>

Morton Sr., M., A. Mullick, J. Nelson and W. Thornton, 2011. Factors to Consider in Estimating Oil Sands Plant Decommissioning Costs. OSRIN Report No. TR-16. 62 pp. <http://hdl.handle.net/10402/era.24630>

Paskey, J. and G. Steward, 2012. The Alberta Oil Sands, Journalists, and Their Sources. OSRIN Report No. TR-17. 33 pp. <http://hdl.handle.net/10402/era.25266>

Cruz-Martinez, L. and J.E.G. Smits, 2012. Potential to Use Animals as Monitors of Ecosystem Health in the Oil Sands Region – July 2013 Update. OSRIN Report No. TR-18. 59 pp. <http://hdl.handle.net/10402/era.25417>

Hashisho, Z., C.C. Small and G. Morshed, 2012. Review of Technologies for the Characterization and Monitoring of VOCs, Reduced Sulphur Compounds and CH<sub>4</sub>. OSRIN Report No. TR-19. 93 pp. <http://hdl.handle.net/10402/era.25522>

Kindzierski, W., J. Jin and M. Gamal El-Din, 2012. Review of Health Effects of Naphthenic Acids: Data Gaps and Implications for Understanding Human Health Risk. OSRIN Report No. TR-20. 43 pp. <http://hdl.handle.net/10402/era.26060>

Zhao, B., R. Currie and H. Mian, 2012. Catalogue of Analytical Methods for Naphthenic Acids Related to Oil Sands Operations. OSRIN Report No. TR-21. 65 pp. <http://hdl.handle.net/10402/era.26792>

Oil Sands Research and Information Network and Canadian Environmental Assessment Agency, 2012. Summary of the Oil Sands Groundwater – Surface Water Interactions Workshop. OSRIN Report No. TR-22. 125 pp. <http://hdl.handle.net/10402/era.26831>

Valera, E. and C.B. Powter, 2012. Implications of Changing Environmental Requirements on Oil Sands Royalties. OSRIN Report No. TR-23. 21 pp. <http://hdl.handle.net/10402/era.27344>

Dixon, R., M. Maier, A. Sandilya and T. Schneider, 2012. Qualifying Environmental Trusts as Financial Security for Oil Sands Reclamation Liabilities. OSRIN Report No. TR-24. 32 pp. <http://hdl.handle.net/10402/era.28305>

Creasey, R., 2012. Professional Judgment in Mineable Oil Sands Reclamation Certification: Workshop Summary. OSRIN Report No. TR-25. 52 pp. <http://hdl.handle.net/10402/era.28331>

Alberta Innovates – Technology Futures, 2012. Investigating a Knowledge Exchange Network for the Reclamation Community. OSRIN Report No. TR-26. 42 pp. <http://hdl.handle.net/10402/era.28407>

Dixon, R.J., J. Kenney and A.C. Sandilya, 2012. Audit Protocol for the Mine Financial Security Program. OSRIN Report No. TR-27. 27 pp. <http://hdl.handle.net/10402/era.28514>

Davies, J., B. Eaton and D. Humphries, 2012. Microcosm Evaluation of Community Level Physiological Profiling in Oil Sands Process Affected Water. OSRIN Report No. TR-28. 33 pp. <http://hdl.handle.net/10402/era.29322>

Thibault, B., 2012. Assessing Corporate Certification as Impetus for Accurate Reporting in Self-Reported Financial Estimates Underlying Alberta’s Mine Financial Security Program. OSRIN Report No. TR-29. 37 pp. <http://hdl.handle.net/10402/era.29361>

Pyper, M.P., C.B. Powter and T. Vinge, 2013. Summary of Resiliency of Reclaimed Boreal Forest Landscapes Seminar. OSRIN Report No. TR-30. 131 pp. <http://hdl.handle.net/10402/era.30360>

Pyper, M. and T. Vinge, 2013. A Visual Guide to Handling Woody Materials for Forested Land Reclamation. OSRIN Report No. TR-31. 10 pp. <http://hdl.handle.net/10402/era.30381>

Mian, H., N. Fassina, A. Mukherjee, A. Fair and C.B. Powter, 2013. Summary of 2013 Tailings Technology Development and Commercialization Workshop. OSRIN Report No. TR-32. 69 pp. <http://hdl.handle.net/10402/era.31012>

Howlett, M. and J. Craft, 2013. Application of Federal Legislation to Alberta’s Mineable Oil Sands. OSRIN Report No. TR-33. 94 pp. <http://hdl.handle.net/10402/era.31627>

Welham, C., 2013. Factors Affecting Ecological Resilience of Reclaimed Oil Sands Uplands. OSRIN Report No. TR-34. 44 pp. <http://hdl.handle.net/10402/era.31714>

Naeth, M.A., S.R. Wilkinson, D.D. Mackenzie, H.A. Archibald and C.B. Powter, 2013. Potential of LFH Mineral Soil Mixes for Land Reclamation in Alberta. OSRIN Report No. TR-35. 64 pp. <http://hdl.handle.net/10402/era.31855>

Welham, C. and B. Seely, 2013. Oil Sands Terrestrial Habitat and Risk Modelling for Disturbance and Reclamation: The Impact of Climate Change on Tree Regeneration and Productivity – Phase III Report. OSRIN Report No. TR-36. 65 pp. <http://hdl.handle.net/10402/era.31900>

- Eaton, B., T. Muhly, J. Fisher and S-L. Chai, 2013. Potential Impacts of Beaver on Oil Sands Reclamation Success – an Analysis of Available Literature. OSRIN Report No. TR-37. 65 pp. <http://hdl.handle.net/10402/era.32764>
- Paskey, J., G. Steward and A. Williams, 2013. The Alberta Oil Sands Then and Now: An Investigation of the Economic, Environmental and Social Discourses Across Four Decades. OSRIN Report No. TR-38. 108 pp. <http://hdl.handle.net/10402/era.32845>
- Watson, B.M. and G. Putz, 2013. Preliminary Watershed Hydrology Model for Reclaimed Oil Sands Sites. OSRIN Report No. TR-39. 193 pp. <http://hdl.handle.net/10402/era.34250>
- Birks, S.J., Y. Yi, S. Cho, J.J. Gibson and R. Hazewinkel, 2013. Characterizing the Organic Composition of Snow and Surface Water in the Athabasca Region. OSRIN Report No. TR-40. 62 pp. <http://hdl.handle.net/10402/era.36643>
- De Corby, R.G., 2013. Development of Silicon-Based Optofluidic Sensors for Oil Sands Environmental Monitoring. OSRIN Report No. TR-41. 19 pp. <http://hdl.handle.net/10402/era.36936>
- Iqbal, M., T.K. Purkait, J.G.C. Veinot and G.G. Goss, 2013. Benign-by-Design: Synthesis of Engineered Silicon Nanoparticles and their Application to Oil Sands Water Contaminant Remediation. OSRIN Report No. TR-42. 30 pp. <http://hdl.handle.net/10402/era.37308>
- Oil Sands Research and Information Network, 2013. Future of Shrubs in Oil Sands Reclamation Workshop. OSRIN Report No. TR-43. 71 pp. <http://hdl.handle.net/10402/era.37440>
- Smreciu, A., K. Gould and S. Wood, 2013. Boreal Plant Species for Reclamation of Athabasca Oil Sands Disturbances. OSRIN Report No. TR-44. 23 pp. plus appendices. <http://hdl.handle.net/10402/era.37533>
- Pereira, A.S. and J.W. Martin, 2014. On-Line Solid Phase Extraction – HPLC – Orbitrap Mass Spectrometry for Screening and Quantifying Targeted and Non-Targeted Analytes in Oil Sands Process-Affected Water and Natural Waters in the Athabasca Oil Sands Region. OSRIN Report No. TR-45. 33 pp. <http://hdl.handle.net/10402/era.37793>
- Liang, J., F. Tumpa, L.P. Estrada, M. Gamal El-Din and Y. Liu, 2014. Ozone-Assisted Settling of Diluted Oil Sands Mature Fine Tailings: A Mechanistic Study. OSRIN Report No. TR-46. 43 pp. <http://hdl.handle.net/10402/era.38226>
- Rochdi, N., J. Zhang, K. Staenz, X. Yang, D. Rolfson, J. Banting, C. King and R. Doherty, 2014. Monitoring Procedures for Wellsite, In-Situ Oil Sands and Coal Mine Reclamation in Alberta. OSRIN Report No. TR-47. 156 pp. <http://hdl.handle.net/10402/era.38742>
- Taheriazad, L., C. Portillo-Quintero and G.A. Sanchez-Azofeifa, 2014. Application of Wireless Sensor Networks (WSNs) to Oil Sands Environmental Monitoring. OSRIN Report No. TR-48. 51 pp. <http://hdl.handle.net/10402/era.38858>
- Marey, H.S., Z. Hashisho and L. Fu, 2014. Satellite Remote Sensing of Air Quality in the Oil Sands Region. OSRIN Report No. TR-49. 104 pp. <http://hdl.handle.net/10402/era.38882>

- Li, C., A. Singh, N. Klammerth, K. McPhedran, P. Chelme-Ayala, M. Belosevic and M. Gamal El-Din, 2014. Synthesis of Toxicological Behavior of Oil Sands Process-Affected Water Constituents. OSRIN Report No. TR-50. 101 pp. <http://hdl.handle.net/10402/era.39659>
- Jiang, Y. and Y. Liu, 2014. Application of Forward Osmosis Membrane Technology for Oil Sands Process-Affected Water Desalination. OSRIN Report No. TR-51. 27 pp. <http://hdl.handle.net/10402/era.39855>
- Zhu, L., M. Yu, L. Delgado Chávez, A. Ulrich and T. Yu, 2014. Review of Bioreactor Designs Applicable to Oil Sands Process-Affected Water Treatment. OSRIN Report No. TR-52. 39 pp. <http://hdl.handle.net/10402/era.39903>
- Oil Sands Research and Information Network, 2014. Oil Sands Rules, Tools and Capacity: Are we Ready for Upcoming Challenges? OSRIN Report No. TR-53. 120 pp. <http://hdl.handle.net/10402/era.39985>
- Iqbal, M., T.K. Purkait, M. Aghajamali, L. Hadidi, J.G.C. Veinot, G.G. Goss and M. Gamal El-Din, 2014. Hybrid Aerogel SiNP Membranes for Photocatalytic Remediation of Oil Sands Process Water. OSRIN Report No. TR-54. 29 pp. <http://hdl.handle.net/10402/era.40004>
- Schoonmaker, A., J-M. Sobze, E. Fraser, E. Marenholtz, A. Smreciu, C.B. Powter and M. Mckenzie, 2014. Alternative Native Boreal Seed and Plant Delivery Systems for Oil Sands Reclamation. OSRIN Report No. TR-55. 61 pp. <http://hdl.handle.net/10402/era.40099>
- Aguilar, M., E. Glücksman, D. Bass and J.B. Dacks, 2014. Next Generation Sequencing of Protists as a Measure of Microbial Community in Oil Sands Tailings Ponds: Amplicon Versus Metagenomic Approaches. OSRIN Report No. TR-56. 24 pp. <http://hdl.handle.net/10402/era.40100>
- Alessi, D.S., M.S. Alam and M.C. Kohler, 2014. Designer Biochar-Coke Mixtures to Remove Naphthenic Acids from Oil Sands Process-Affected Water (OSPW). OSRIN Report No. TR-57. 38 pp. <http://hdl.handle.net/10402/era.40122>
- Oil Sands Research and Information Network, 2014. Survey of Oil Sands Environmental Management Research and Information Needs. OSRIN Report No. TR-58. 67 pp. <http://hdl.handle.net/10402/era.40128>
- Huang, Q., H. Wang and M.A. Lewis, 2014. Development of a Toxin-Mediated Predator-Prey Model Applicable to Aquatic Environments in the Athabasca Oil Sands Region. OSRIN Report No. TR-59. 59 pp. <http://hdl.handle.net/10402/era.40140>
- Currie, R., S. Bansal, I. Khan and H. Mian, 2014. An Investigation of the Methylene Blue Titration Method for Clay Activity of Oil Sands Samples. OSRIN Report No. TR-60. 50 pp. <http://hdl.handle.net/10402/era.40164>
- Welham, C., 2014. Risk and Uncertainty in Oil Sands Upland Reclamation: Best Management Practices within the Context of Climate Change. OSRIN Report No. TR-61. 26 pp. <http://hdl.handle.net/10402/era.40171>

- Mahdavi, H., H. Mian, S. Hepperle and Z. Burkus, 2014. Standard Operating Procedures for Analysis of Naphthenic Acids from Oil Sands Process-Affected Water. OSRIN Report No. TR-62. 67 pp. <http://hdl.handle.net/10402/era.40181>
- McPhedran, K., M.S. Islam and M. Gamal El-Din, 2014. Development of a Novel Engineered Bioprocess for Oil Sands Process-Affected Water and Tailings Fines/Bitumen/Water Separation. OSRIN Report No. TR-63. 28 pp. <http://hdl.handle.net/10402/era.40190>
- Birks, J., Y. Yi, S. Cho, E. Taylor and J. Gibson, 2014. Characterizing the Organic Composition of Snow and Surface Water Across the Athabasca Region: Phase 2. OSRIN Report No. TR-64. 47 pp. <http://hdl.handle.net/10402/era.40243>
- Alberta Centre for Reclamation and Restoration Ecology and Oil Sands Research and Information Network, 2014. Creating a Knowledge Platform for the Reclamation and Restoration Ecology Community: Expanding the OSRIN Model Beyond the Oil Sands. OSRIN Report No. TR-65. 19 pp. <http://hdl.handle.net/10402/era.40323>
- Liang, J., Z. Guo, L. Deng and Y. Liu, 2014. MFT Consolidation Through Microbial Induced Calcium Carbonate Precipitation. OSRIN Report No. TR-66. 31 pp. <http://hdl.handle.net/10402/era.40330>
- Eaton, B.R., J.T. Fisher, G.T. McKenna, and J. Pollard. 2014. An Ecological Framework for Wildlife Habitat Design for Oil Sands Mine Reclamation. OSRIN Report No. TR-67. 83 pp. <http://hdl.handle.net/10402/era.40338>
- Hopkins, D, K. Wall and C. Wilson, 2014. Measured Concentrations of Metals and Polycyclic Aromatic Hydrocarbons in Plants, Berries and Soil Located North of Fort McMurray, Alberta. OSRIN Report No. TR-68. 134 pp. <http://hdl.handle.net/10402/era.40339>
- Richardson, E., G. Walker, G. MacIntyre, S. Quideau, J.B. Dacks and S. Adl, 2014. Next-Generation Sequencing of Protists as a Measure of the Microbial Community in Oil Sand-Associated Soils. OSRIN Report No. TR-69. 26 pp. <http://hdl.handle.net/10402/era.40343>
- Christensen-Dalsgaard, K.K., R.N. Sinnatamby and M. Poesch, 2014. Metrics for Assessing Fisheries Productivity and Offsetting Strategies under Canada's New *Fisheries Act*. OSRIN Report No. TR-70. 58 pp. <http://hdl.handle.net/10402/era.40345>
- Mackenzie, M.D., S. Hofstetter, I. Hatam and B. Lanoil, 2014. Carbon and Nitrogen Mineralization and Microbial Succession in Oil Sands Reclamation Soils Amended with Pyrogenic Carbon. OSRIN Report No. TR-71. 29 pp. <http://hdl.handle.net/10402/era.40354>

**OSRIN Videos –** <http://hdl.handle.net/10402/era.29304>

Rooney Productions, 2012. [Assessment Methods for Oil Sands Reclamation Marshes](#). OSRIN Video No. V-1. 20 minutes. Also available on the [University of Alberta You Tube Channel](#) (recommended approach).

Rooney Productions, 2012. [Assessment Methods for Oil Sands Reclamation Marshes](#). OSRIN Video No. V-1. Nine-part mobile device version. Also available on the University of Alberta You Tube Channel ([link to Part 1](#) - recommended approach).

**OSRIN Staff Reports – <http://hdl.handle.net/10402/era.19095>**

OSRIN, 2010. Glossary of Terms and Acronyms used in Oil Sands Mining, Processing and Environmental Management – December 2014 Update. OSRIN Report No. SR-1. 125 pp. <http://hdl.handle.net/10402/era.17544>

OSRIN, 2010. OSRIN Writer's Style Guide – November 2013 Update. OSRIN Report No. SR-2. 29 pp. <http://hdl.handle.net/10402/era.17545>

OSRIN, 2010. OSRIN Annual Report: 2009/2010. OSRIN Report No. SR-3. 27 pp. <http://hdl.handle.net/10402/era.17546>

OSRIN, 2010. Guide to OSRIN Research Grants and Services Agreements - June 2011 Update. OSRIN Report No. SR-4. 21 pp. <http://hdl.handle.net/10402/era.17558>

OSRIN, 2011. Summary of OSRIN Projects – October 2014 Update. OSRIN Report No. SR-5. 113 pp. <http://hdl.handle.net/10402/era.20529>

OSRIN, 2011. OSRIN Annual Report: 2010/11. OSRIN Report No. SR-6. 34 pp. <http://hdl.handle.net/10402/era.23032>

OSRIN, 2011. OSRIN's Design and Implementation Strategy. OSRIN Report No. SR-7. 10 pp. <http://hdl.handle.net/10402/era.23574>

OSRIN, 2012. OSRIN Annual Report: 2011/12. OSRIN Report No. SR-8. 25 pp. <http://hdl.handle.net/10402/era.26715>

OSRIN, 2013. OSRIN Annual Report: 2012/13. OSRIN Report No. SR-9. 56 pp. <http://hdl.handle.net/10402/era.31211>

OSRIN, 2014. OSRIN Annual Report: 2013/14. OSRIN Report No. SR-10. 66 pp. <http://hdl.handle.net/10402/era.38508>

OSRIN, 2014. OSRIN's Did You Know Series: The Collected Works. OSRIN Report No. SR-11. 163 pp. <http://hdl.handle.net/10402/era.40220>

OSRIN, 2014. Media Coverage of Oil Sands Pipelines: A Chronological Record of Headlines from 2010 to 2014. OSRIN Report No. SR-12. 140 pp. <http://hdl.handle.net/10402/era.40331>